UNIVERSITY OF CALIFORNIA

Los Angeles

Elucidating the mechanism of synergy in actin assembly by Spire and Cappuccino

A dissertation submitted in partial satisfaction of the requirements for the degree Doctor of Philosophy in Biochemistry, Molecular and Structural Biology

by

Alexander Odysseus Bradley

2019

ABSTRACT OF THE DISSERTATION

Elucidating the mechanism of synergy
in actin assembly by Spire and Cappuccino

by

Alexander Odysseus Bradley
Doctor of Philosophy in Biochemistry, Molecular and Structural Biology
University of California, Los Angeles, 2019
Professor Margot E. Quinlan, Chair

Two actin nucleators, Spire and Cappuccino, collaborate to build a network of actin filaments that connect vesicles and the cortex in the fruit fly oocyte. This actin mesh is built by a conserved mechanism and by homologous proteins (Spire-1/2 and Fmn-2) in mouse oocytes. In each animal, proper regulation of mesh is necessary to establish cell polarity. A direct interaction between Spire and Cappuccino is required to regulate the actin mesh and for in vitro synergistic actin assembly; however, we understand little about why the interaction is necessary. To mimic the geometry of Spire and Cappuccino in vivo, Spire was immobilized on beads and observed by TIRF microscopy. These experiments revealed that increased nucleation is a major part of synergy with Cappuccino and that Spire alone binds both barbed- and pointed-ends of actin filaments. We identified Spire's barbed-end binding domain (WH2-A) and observed partial rescue of fertility by a loss-of-function mutant, indicating that barbed-end binding is not necessary for Spire's in vivo function, but that it may play a role under normal circumstances.

In addition, we found that Spire's four WH2 domains variably participate in nucleation and other functions (e.g. sequestration) and that mutants of each WH2 domain can be modularly combined to tune Spire activities. We also identified new value in an existing, nucleation-incompetent Cappuccino mutant as a tool to reciprocally explore its own contributions to synergy with Spire. We found that this mutant does not nucleate actin but processively protects barbed ends from capping protein, and allows – but does not accelerate – the elongation of filaments in the presence of profilin. Furthermore, preliminary data suggest that this mutant synergizes with Spire – both in pyrene assembly assays and on beads – through a mechanism other than the dimerization of Spire. Finally, we demonstrate that Spire's amino acids 490-520 – recently identified as containing a MyoV binding site – have an inhibitory effect on nucleation by Spire, resolving some discrepancies in reported actin assembly rates.

Taken together, these insights emphasize the complexity of Spire—Cappuccino synergy, mesh production, and regulation of polarity in the fruit fly oocyte. Our improved understanding of the components of synergy studied herein should permit the development of a more sophisticated, biomimetic mesh assembly system, and a more precise interrogation of actin assembly activities by Spire and Cappuccino.

The dissertation of Alexander Odysseus Bradley is approved.

Alvaro Sagasti

Emil Reisler

Margot Elizabeth Quinlan, Committee Chair

University of California, Los Angeles

2019

I dedicate this dissertation to my loving and untiringly supportive wife, Suzanna – without whom, love would have often been labor – and to my beautiful daughter, Cora, whose wonderment and innate hypothesis testing remind me daily of the romance in science.

TABLE OF CONTENTS

List of figures

List of tables

Acknowledgements

Thank you to each member of my committee for offering their valuable insights and attentive support of my personal and scientific growth, and for posing keen questions which focused my thoughts and methods. This includes Dr. Albert Courey who was not a certifying member of the committee and is therefore not listed on page “iv.” I extend particular gratitude to my committee chair and principal investigator, Dr. Margot Quinlan. Margot, you wore every hat one could expect to find on the head of a boss, friend, colleague, and even therapist. Your guidance and sincere care were essential in this journey and I cannot envision a better mentor. “What’s the question? Slow down. Step back.” Though you may not remember uttering some or all of these words, I will cherish them throughout my career.

Thanks to Christina Vizcarra, whose attentive mentorship and guidance in establishing the bead experiment methodology were integral to my success. Thanks to Eric Torres for being the truly selfless, empathetic human being he is, in addition to “up-lifting” buddy, cynical commiserator, conspirator, and best friend. Thanks to Aanand Patel for myriad, emotional support sessions and countless, valuable scientific insights; and for being as sincere a friend as they come. Thanks to Will Silkworth for conversations of very unscientific nature, and for the scientific sort, as well. Without either, my mental health would have certainly suffered. Thanks to Cliff Boldridge and Jonelle White for their patient friendship, collegiate support, and for providing many welcome and humorous respites from the bench. Thanks to Kathryn Bremer for being a dependable support, in and outside of the lab, and for normalizing my PhD experience by being as strange as me. Possibly stranger. Thanks to Michelle Panzica for daily comedic relief and constant offers of support in the final stage of this work, and to the rest of the Quinlan lab for much more of the same. Without question, you all have been the most intelligent, caring, helpful, and inspiring humans I have had the privilege to call colleagues.

The reader should note that Chapter 2 (Spire stimulates nucleation by Cappuccino and binds both ends of actin filaments) is a manuscript in submission (BioRxiv pre-print doi: 10.1101/773812). Some minimal pyrene-actin data and the Spir(A*) fly data included in this manuscript were obtained by Christina Vizcarra and Hannah Bailey, respectively. Much of the pyrene data shown in Chapter 3 (Unique domain functions in Spire—Cappuccino synergy) were obtained and/or repeated by two undergraduate mentees of mine: Joe Rich and Jamel Simpson. Another undergraduate mentee, Ruchi Desai, assisted in the purification and FRET testing of several of the Spir-GFP fusions listed in **Table 4-1** in Chapter 4 (Development of a Spire—Cappuccino FRET system). Margot E. Quinlan was the principal investigator for all projects.

Special thanks to the Kovar lab for providing the purified mDia1 protein used in Chapter 2 (**Fig. 2-2C**) and to the Reisler lab for always volunteering their time and reagents to assist mine and other Quinlan lab experiments. Finally, tremendous thanks to Jon Lowenson and Steve Clarke for their tireless and often thankless supervision of trainees and their thoughtful presentations of ethical issues in science throughout my tenure on the CMB Training Grant. Additional thanks are due to the NIH for providing this opportunity for funding which I benefited from for three years of my graduate school journey.

Vita

Education
B.S., Biochemistry — June 2014
Arizona State University

Research Experience
Graduate Student Researcher — March 2015 – September 2019
Laboratory of Dr. Margot E. Quinlan
Department of Chemistry and Biochemistry
University of California, Los Angeles

Undergraduate Researcher — December 2012 – December 2013
Laboratory of Dr. Edward Skibo
Department of Chemistry
Arizona State University

Publications
Bradley AO, Vizcarra CL, Bailey HM, Quinlan ME. Spire stimulates nucleation by Cappuccino and binds both ends of actin filaments. J. Cell. Biol., Manuscript under review. BioRxiv pre-print doi: 10.1101/773812

Abstracts and Speaking Engagements
Bradley, AO, A meshy synergy: Spire stimulates Cappuccino and forms filament bridges to build a dynamic network of actin. Technical talk, Dissertation Seminar. UCLA, Los Angeles, CA, 2019

Bradley, AO, Pointed- and barbed-end filament binding by Spire bridges networks of filaments in vitro. Technical talk, American Society for Cell Biology Annual Meeting. San Diego, CA, 2018.

Bradley, AO, Elucidating the Collaborative Mechanism of Spire and Capu in Creating the Actin Mesh. Technical talk, CMB/NIH Trainee Seminar. UCLA, Los Angeles, CA, 2018.

Bradley, AO, Science and Politics. Seminar, CMB/NIH Training Grant cohort. UCLA, Los Angeles, CA, 2018.

Bradley, AO. 314 Action Panel; From Lab to the Ballot (Bringing STEM to Politics). Discussion panelist. UCLA, Los Angeles, CA 2018.

Bradley, AO, Science and Politics: Two Species of the Same Genus. Non-technical talk, ASBMB Science Communication Capstone. Online, 2017.

Bradley, AO, Elucidating the Collaborative Mechanism of Spire and Capu in Creating the Actin Mesh. Technical talk, Department of Chemistry and Biochemistry Seminar Series. UCLA, Los Angeles, CA, 2017.

Bradley, AO, The Necessity of Science in Government. Live speech, March for Science Los Angeles. City Hall, Los Angeles, CA, 2017.

Bradley, AO, Thousands Will March for Science. Live interview, KPFA/KPFK; Rising Up with Sonali. Online, 2017.

Bradley, AO, Symbols in a Movement. Live interview, KCRW/NPR; DnA: Design and Architecture. Online, 2017.

Bradley, AO, A Biomimetic System for the in vitro Study of Actin Network Assembly by Spire-Cappuccino Complexes. Poster, UCLA MBI Retreat. Arrowhead Conference Center, Lake Arrowhead, CA, 2016.

Awards

Dean's Scholar Award (2014 – 2015)
University Fellowship Award (2014 – 2015)
Cellular and Molecular Biology Training Grant (2015 – 2018)
Hanson-Dow Excellence in Teaching Award (2017)
American Society for Cell Biology travel award (2018)

Mentorship

Joe Rich — August 2018 – October 2019
Undergraduate student in MCDB; Biomedical research minor

Jamel Simpson — March 2018 – October 2019
Undergraduate student in Chemistry and Biochemistry; CARE Scholar (NIH)

Luis Sanchez — May 2017 – October 2018
Graduate student in Chemistry and Biochemistry; PEERS Student

Alex McQuown — Summer 2015
Undergraduate student; visiting Amgen Scholar

Ruchi Desai — January 2016 – June 2017
Undergraduate student in Biochemistry; Biomedical research minor

Teaching

TA – CHEM156 (Physical Biochemistry) — Spring 2019
TA – CHEM156 (Physical Biochemistry) — Spring 2015
TA – CHEM153L (Biochemistry Lab) — Winter 2014

Service

Organizing Chair — 2016 – 2019
Equity, Inclusion, and Diversity Day, at UCLA

Founder, Executive Director — January 2017 – July 2018
March for Science, Los Angeles

Vice President of Outreach and Communications — January 2018 – October 2019
Advanced Degree Consulting Club (ADCC), at UCLA

Chapter 1: Introduction

The actin cytoskeleton

Actin is a ubiquitous protein and an essential component of cellular cytoskeletons. Actin serves critical roles in a cell's division, exploration of its environment, morphology, motility, vesicle trafficking, and more. The highly conserved, globular actin (G-actin) monomer (≥ 93% sequence identity between all human isoforms (Perrin and Ervasti 2010)) must polymerize into dynamic filaments (F-actin) to accomplish these functions. These filaments scaffold structures to resist forces and provide structural rigidity; grow and push other structures, like membranes; and operate as molecular highways along which motor proteins travel and transport various cargoes.

Despite serving in such essential and varied roles, actin's ability to form filaments and accomplish these dynamic tasks is hindered from the onset, due to the kinetically disfavored nucleation step (Pollard 1986; Pollard and Cooper 1986). This initial, spontaneous assembly of actin filaments occurs slowly due to the instability of actin dimers. Actin trimers or tetramers (nuclei) are stable enough to template the growth of a filament but the kinetic hurdles of the species preceding this complex prohibit the spatiotemporal precision required for actin's various, dynamic roles in the cell.

There are myriad actin-binding proteins (ABP's) which even further discourage actin polymerization. ABP's which sever and halt the growth of filaments (e.g. ADF/cofilin and capping protein, respectively (Edwards et al. 2014; Maciver and Hussey 2002)) or bind and sequester G-actin (e.g. profilin and β-thymosin (Huff et al. 2001; Theriot and Mitchison 1993)) further disfavor the assembly of various actin structures. However, within the entourage of known ABP's lies an astonishing diversity of regulation, including three protein classes which accelerate the rate of elongation and/or nucleation of filaments: Arp2/3 complex, formins, and tandem actin-binding domain proteins (**Fig. 1-1**) (Goode and Eck 2007). Members of these ABP families are typically observed to assemble structures with distinct morphologies and functions.

However, two ABP's of particular interest – Cappuccino (Capu, a formin) and Spire (Spir, a tandem actin-binding domain protein) – have been demonstrated to collaborate to build a single structure: the actin mesh.

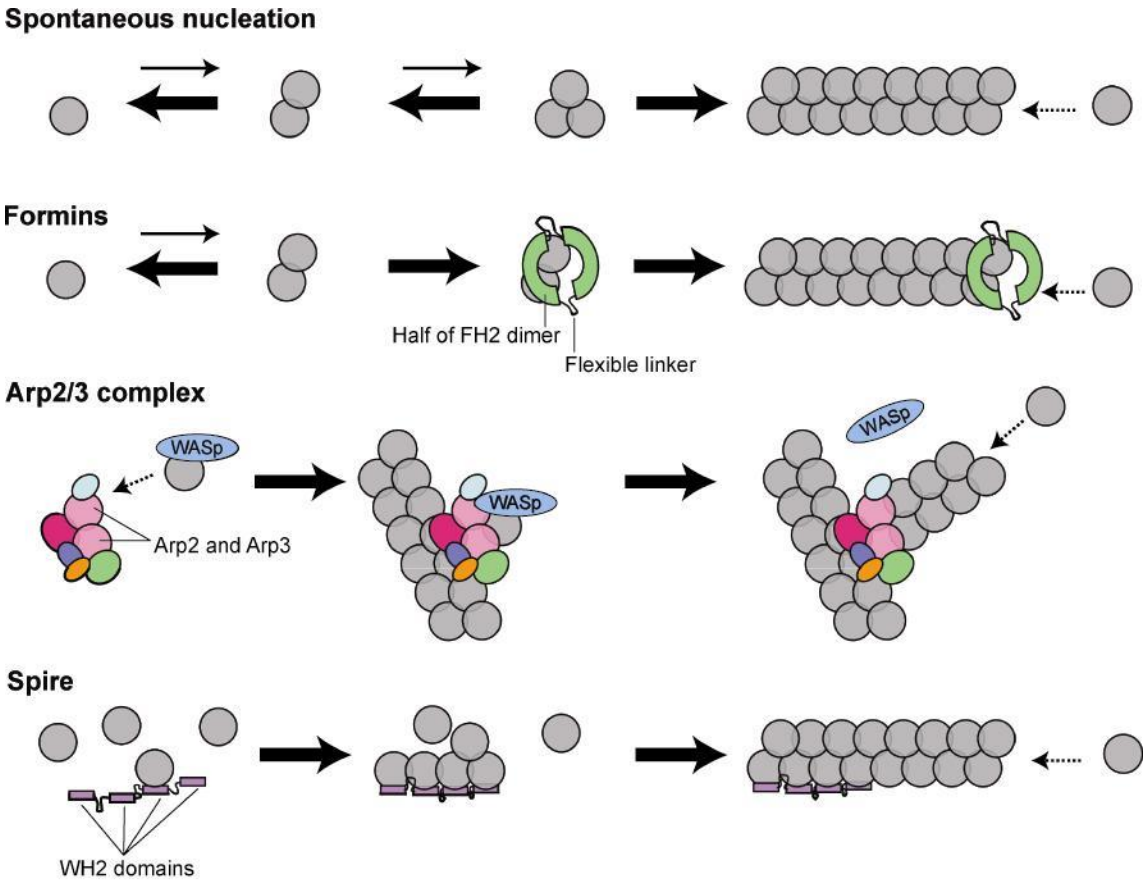

Figure 1-1 – *Comparison of the mechanisms by which formins, the Arp2/3 complex, and Spire nucleate actin polymerization*

From Goode & Eck (2007). (*From top*) Spontaneous actin assembly. Actin dimers and trimers are unstable and rapidly dissociate. Formins (*green dimer*) stabilize intermediate structures, like the actin dimer. The Arp2/3 complex (*multi-colored*) is thought to mimic an actin trimer, forming a branch off of an existing filament. Spire (*purple WH2 domains*) binds and organizes up to four actin monomers into stable, rod-like complexes.

Formins and Cappuccino

Capu and other formins assemble into donut-shaped homodimers which can bind and nucleate actin (Xu et al. 2004). Their formin homology 2 (FH2) domain is required for dimerization and

nucleation, via stabilization of the kinetically disfavored actin homo-dimers and –trimers. Once a filament has been nucleated, it can elongate at either end, but each end interacts with a different complement of proteins and grows at a different rate. The slower growing of these is called the pointed end, while the barbed end elongates ~10-fold faster (Pollard 1986).
Like other proteins in the formin family, Capu can processively track and enhance the elongation of the already faster-growing, barbed end of an actin filament (Paul and Pollard 2009). Capu acquires G-actin to accomplish this function by binding the aforementioned, ubiquitous ABP, profilin. With nearly all G-actin predicted to be profilin-bound in the typical cell, the two proline-rich, profilin-binding FH1 (formin homology 1) domains of the Capu homodimer are aptly suited to rapidly acquire and add actin monomers to a filament (Courtemanche and Pollard 2012).

Capu accelerates the polymerization of actin filaments ~6-fold (to ~35 actin subunits/s), utilizing profilin-actin (PA) (Vizcarra, Bor, and Quinlan 2014). Its processivity permits Capu to accelerate the addition of over 300,000 PA subunits in this manner before falling off of a filament; all the while, protecting the barbed end from becoming bound by other ubiquitous ABP's like capping protein, which can arrest its growth (Bor et al. 2012; Vizcarra et al. 2011). The combination of these activities typically results in the production of long bundles of filaments by formins. However, to build mesh, Capu collaborates with another nucleator: Spir.

WH2-domains and Spire

Another common class of actin nucleator contains tandem, actin-binding domains. The most common of these domains is the Wiskott-Aldrich syndrome protein (WASp) homology 2 (WH2) domain. The WH2 is a ubiquitous, ~20 amino acid-long domain found in activators of the Arp2/3 complex (e.g. N-WASp, WAVE2) and in formins (e.g. INF2, mDia1), in addition to proteins containing tandem stretches of WH2 domains (e.g. Spir, CobL, VopL, Sca2) (Dominguez 2016).

Spir is the founding member of the tandem WH2 domain-containing protein class. Identified by Dr. Quinlan in 2005 to be a novel, pointed-end nucleator of actin filaments, Spir contains four closely spaced, central WH2 domains (See **Fig. 2-1A**) (Quinlan et al. 2005). Electron microscopy (EM) data suggest that Spir binds a single actin monomer to each WH2 domain and arranges them into a rod-like shape (Quinlan et al. 2005). These Spir—actin rods may be structurally similar to the long-pitch of the two-start actin filament helix. However, it is unclear if this species templates the growth of a filament or if nucleation by Spir occurs by a different mechanism.

Many tandem WH2 nucleators contain dimerization domains (e.g. VopL/F, Sca2) or can dimerize through interactions with other dimers (e.g. Cobl and BAR proteins) (Dominguez 2016). Without such a domain or partner, a single Spir—actin rod structure, as seen by EM, may be better equipped for involvement in the polymerization-inhibiting functions of Spir (i.e. forming a so-called SA_4 complex (Bosch et al. 2007)). In addition to its nucleation activity, Spir has been shown to sequester actin monomers and sever actin filaments and dimerization may be necessary for nucleation to prevail over these other activities. Indeed, when Spir is dimerized via fusion to VopL's dimerization domain or GST, its nucleation activity is impressively augmented (Namgoong et al. 2011; Vizcarra et al. 2011; Vizcarra and Quinlan 2017). Therefore, an interaction with a dimeric protein such as Capu is likely to be favorable for actin assembly by Spir. In fact, genetic evidence of such an interaction was found as early as 1989.

Ooplasmic streaming

Shüpbach and Manseau identified the *cappuccino* and *spire* loci as essential for proper embryonic axial patterning (affecting the development of both the anterior/posterior and dorsal/ventral axes) in *Drosophila melanogaster* (Manseau and Schupbach 1989). Five years

later, they were implicated in the proper temporal control of ooplasmic streaming – a fascinating and still incompletely understood process by which the *Drosophila* oocyte mixes its contents in a concerted and rapid manner (Theurkauf 1994). The initiation of ooplasmic streaming requires precise regulation. Loss of function of either the *cappuccino* or *spire* gene results in the premature onset of this phenomenon and a catastrophic lack of polarity establishment in the fly embryo (Manseau and Schupbach 1989; Theurkauf 1994).

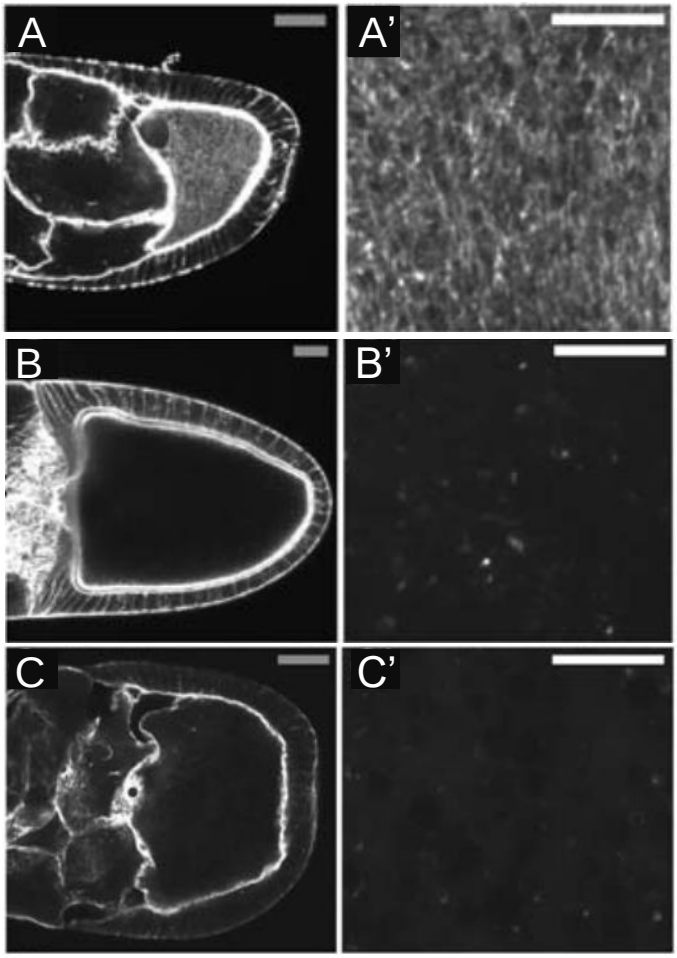

Figure 1-2 – *The actin mesh is prematurely absent in capu or spir-deficient oocytes*

Modified from Dahlgaard, et al. (2007). *(A)* The actin mesh is clearly present in a Stage 9 fly oocyte. *(B)* The actin mesh is absent in Stage 10b (shown), when fast streaming begins. *(C)* The mesh is prematurely absent in a *capu*-deficient, Stage 9 oocyte. The result is the same for *spir*-deficient flies. *(A'-C')* Images on right are blown up regions of the oocyte shown on the left. Scale bars = 30μm (*gray*) and 10μm (*white*).

Shüpbach and Manseau suggested that the phenotypes observed in mutant embryos might be due to defects in actin-based transport systems. Subsequent to these studies, an explosion of literature on actin nucleators, discussed above in brief, showed that formins are both nucleators and processive elongators of actin filaments, while Dr. Quinlan's seminal work on Spir showed it to be a novel type of pointed end actin nucleator. These insights suggested a link between fast ooplasmic streaming and actin regulation by Spir/Capu. In fact, concomitant with the onset of fast streaming in Stage 10b and later oocytes, an actin mesh within the fly egg conspicuously disappears (**Fig. 1-2A,B**) (Dahlgaard et al. 2007).

Actin mesh

A dense, interdigitated network of filaments, the actin mesh is a conserved structure found to serve roles in polarity establishment in multiple animals. In the fly, F-actin depolymerizing agents phenocopy *capu* and *spir* mutants (Manseau, Calley, and Phan 1996), which suggested that the process of fast streaming within the oocyte is temporally controlled by the Spir/Capu-mediated mesh. In fact, it was subsequently shown that both Capu and Spir are necessary to build the mesh (**Fig. 1-2C**) (Dahlgaard et al. 2007). In the absence of mesh, premature fast streaming of fly ooplasm results in disturbed microtubule (MT) organization and the mislocalization of MT-dependent, essential polarity factors, such as *bicoid*, *oskar*, and *nanos* (Dahlgaard et al. 2007; Johnstone and Lasko 2001; Theurkauf 1994; Theurkauf et al. 1992). However, late onset of streaming is also detrimental. Oocytes with constitutively active Spir or Capu have denser meshes which disassemble too late in the egg's development, thus delaying streaming and again interfering with proper polarity establishment (Bor, Bois, and Quinlan 2015; Dahlgaard et al. 2007; Quinlan 2013).

While mesh is necessary for the regulation of streaming and the localization of mRNAs in the fly, analogous structures exist in plants and the oocytes of frogs, mice and starfish. In the eggs of mice and starfish, mesh is required for asymmetric positioning of the meiotic spindle and condensation of chromosomes, respectively (Azoury et al. 2008; Bun et al. 2018; Field and Lénárt 2011; Montaville et al. 2015). In fact, the mammalian homologues of Spir and Capu – Spir-1/2 and Fmn-2 – produce mesh in the mouse oocyte and in the absence of either, mesh is not created and the spindle fails to be properly positioned (Pfender et al. 2011).

Spire and Cappuccino synergy

The discovery that both Spir and Capu are actin nucleators led to the question of why both would be needed to build a single structure (Quinlan et al. 2005). This question is made even

more compelling by the observation that Fmn-2 and Spir-1 demonstrate a conserved function of regulating mesh and polarity within mammalian oocytes (Leader et al. 2002; Pfender et al. 2011).

We now know that a direct interaction between Spir and Capu is required for mesh assembly (Quinlan 2013). Work in the Quinlan lab showed that Capu's C-terminal tail tightly binds (~100 nM affinity) Spir's conserved kinase noncatalytic C-lobe domain (KIND) (Bor et al. 2012). Binding of recombinant KIND domain inhibits Capu's actin assembly. However; conversely, Capu-binding enhances actin assembly by Spir (Pechlivanis, Samol, and Kerkhoff 2009; Quinlan et al. 2007; Vizcarra et al. 2011; Zeth et al. 2011). Further, when Capu is overexpressed, it can weakly rescue *spir* mutants. However, Spir overexpression cannot rescue *capu* mutants (Quinlan 2013). The puzzling nature of the Spir and Capu interaction, by which they simultaneously seem to cooperate with and antagonize one another, has been best described by two differing models: so-called "Hand-off" and "Ping-pong."

"Ping-pong"

The Ping-pong model suggests that a Spir-bound (capped) actin filament enhances Capu (Fmn-2 in the published model) recruitment (i.e. increases the formin's "on" rate). This recruitment occurs via the transient formation of a trimeric complex at the barbed end of a filament, followed by Spir's displacement from the filament by Capu (**Fig. 1-3**) (Montaville et al. 2014). A Capu-bound filament can rapidly polymerize due to the processive formin's elongation activity, until Spir again binds/caps the barbed end, evicting Capu. The recruitment of Capu to a barbed end is in agreement with the synergy observed in actin assembly assays. However, the inhibition of Capu's processivity by subsequent and rapid Spir interference – as seen in a collaborator's unpublished single-molecule data – conflicts with the oocyte's requirement of both proteins to produce mesh. Furthermore, the authors of this model proposed that a protein like ADF/cofilin

must be present to sever Capu-bound filaments and increase the local concentration of barbed ends (**Fig 1-3, step "4"**). However, synergy is consistently observed in the absence of ADF/cofilin (Montaville et al. 2015). Finally, Ping-pong's presumption that synergy occurs through Spir's interaction with filament barbed ends excludes consideration of Dr. Quinlan's paper on Spir, which showed evidence of pointed end binding (**Fig. 1-4**) (Quinlan et al. 2005).

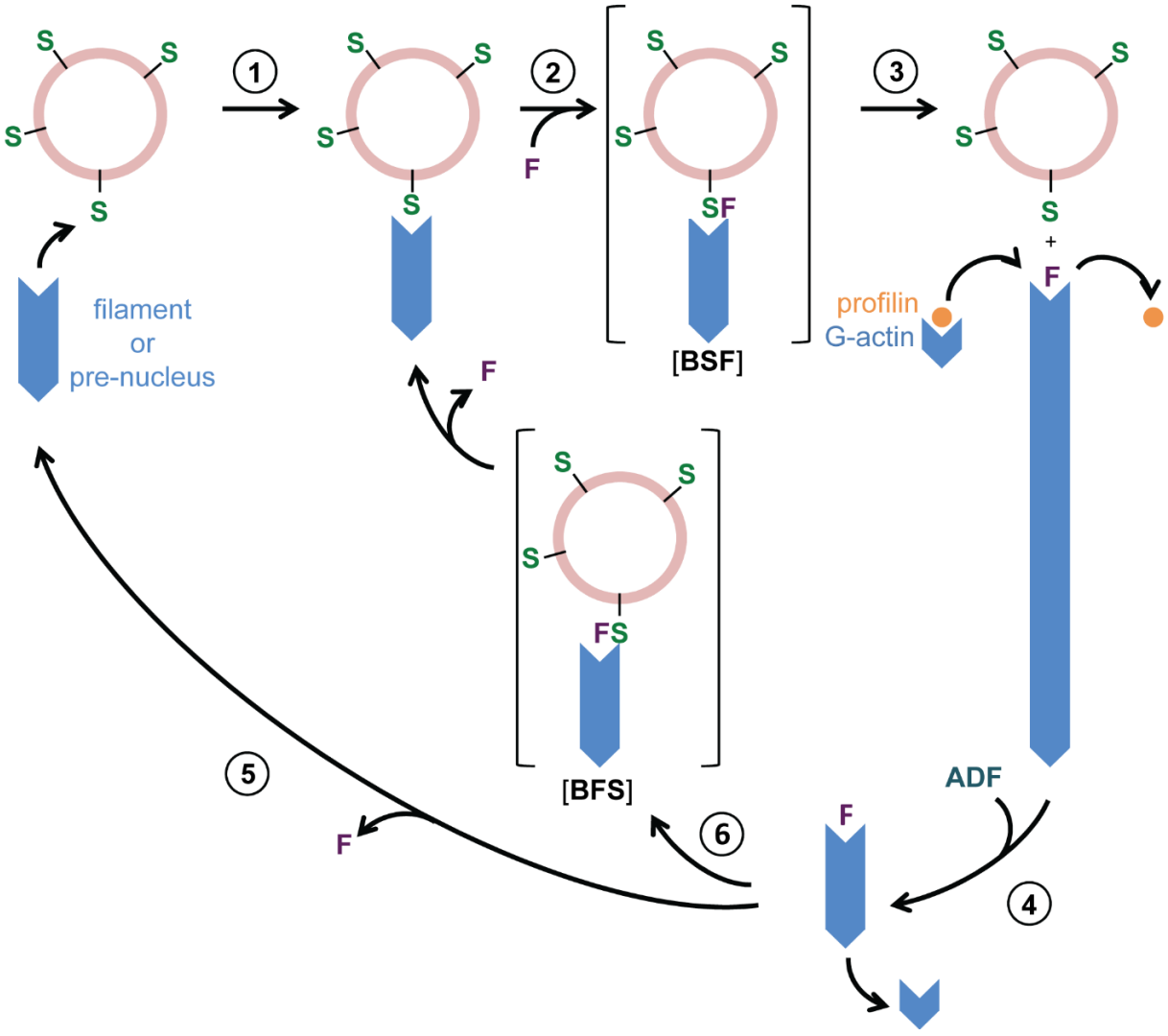

Figure 1-3 – *The "Ping-pong" model*

From Montaville, et al. (2014). Spir is depicted as being anchored to vesicles, consistent with localization data. (*1*) The barbed end of a filament is capped by Spir. (*2*) Spir recruits formin to the barbed end. (*3*) The formin separates from Spir and accelerates the elongation of the barbed end. (*4*) ADF/cofilin severs filaments, creating a pool of barbed ends which are recaptured by Spir with (*6*) or without (*5*) formin bound.

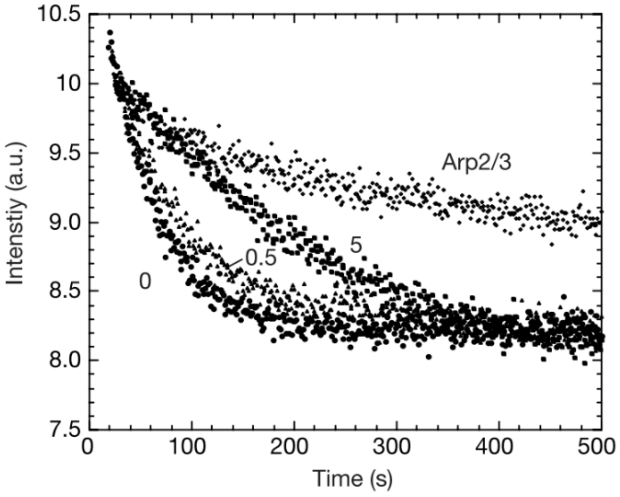

Figure 1-4 – *SpirNT weakly caps the pointed ends of filaments*

From Quinlan (2005). The addition of 0.5 or 5 μM SpirNT inhibits the rate of depolymerization of gelsolin-capped actin filaments. This is a weak interaction (μM affinity), as illustrated by the addition of only 100 nM Arp2/3.

"Hand-off"

The Hand-off model emphasizes Spir's known function as a nucleator, and oppositely describes its synergy with Capu as occurring at the pointed end of a filament. In this model, Spir is first made a better nucleator by dimerization through its interaction with the Capu homodimer (**Fig. 1-5B**) (Quinlan 2013). Through use of its eight WH2 domains, the Spir dimer can then assemble each strand of the two-start actin filament helix (**Fig. 1-5C**). In the final step, Spir and Capu would likely separate so that the former can nucleate again and the latter can accelerate the elongation of the nascent filament (**Fig. 1-5D**).

This model excludes consideration of Spir's interaction with filament barbed ends and does not consider the role of Spire's geometry in synergy (Montaville et al. 2014; Pylypenko et al. 2016). That is, the vesicular anchoring of Spir depicted in the Ping-pong model aligns with localization data and may contribute to the activity of Spir/Capu in vivo.

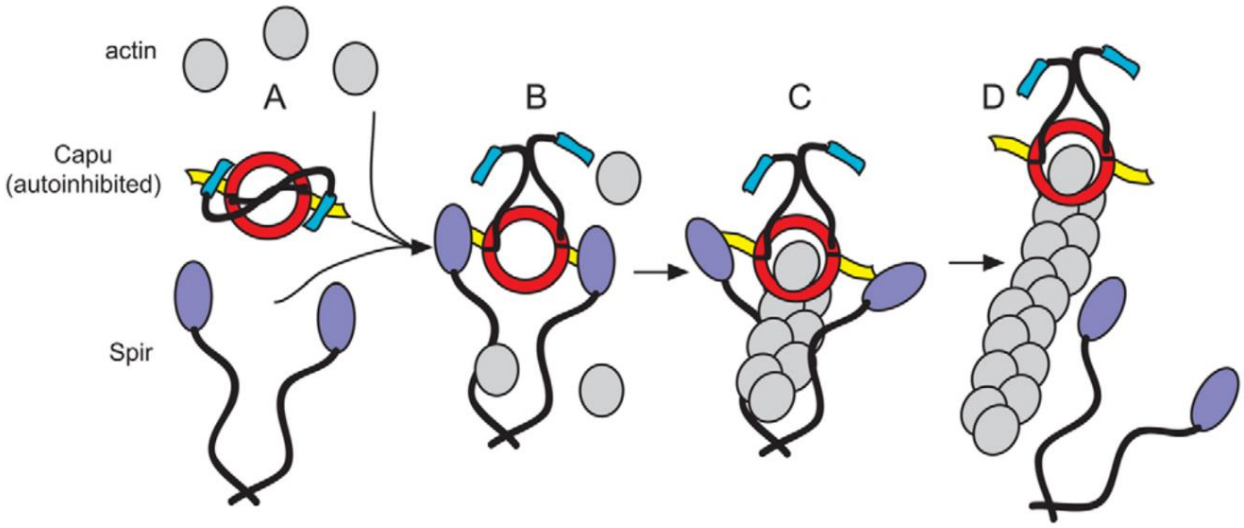

Figure 1-5 – *The "Hand-off" model*

From Quinlan (2013). *(A)* Auto-inhibition of Capu is relieved and Spir is dimerized through interaction with one another *(B). (C)* Spire assembles G-actin into a pre-nucleation complex. *(D)* Capu separates from Spir to elongate the barbed end of the nascent filament.

The bridging hypothesis

In unity with both Ping-pong and Hand-off, I hypothesized that a "bridging" event takes place between concentrated regions of Spir. In this amended model, I proposed that Spir could serve as a paddle and Capu, as the ball. That is, Spir should aid in the initial nucleation of filaments and remain bound at, or localized near, their pointed ends. The relegation of Spir to specific regions of a cell would allow Capu to processively elongate filaments without much chance of eviction until another congregation of Spir were encountered. Localization data are consistent with such a model. GFP-Capu is diffuse in the fly oocyte and Spir (both GFP-tagged and endogenous protein) is enriched at the cortex (Quinlan 2013; Quinlan et al. 2007). Spir is driven to membranes by its C-terminal, modified FYVE (mFYVE) domain which binds negatively charged phospholipids (Blatner et al. 2004; Misra and Hurley 1999; Tittel et al. 2015). In the mouse oocyte, Spir has been shown to localize to vesicles and new, higher resolution microscopy data in the Quinlan lab suggest that Spir also localizes to vesicles in the fly.

Three primary experimental approaches were conceived to dissect the mechanism of Spir—Capu synergy and test the bridging hypothesis:

1. Bead-based total internal reflection fluorescence microscopy (TIRF-M)
    - As described in the **Chapter 2** manuscript, Spir was anchored to vesicle mimics with Capu, profilin, and/or capping protein added in solution. The polymerization of fluorescently labeled actin was visualized in various conditions
2. Mutagenesis of Spir WH2 domains
    - As described in **Chapter 3** (and **Chapter 2**, in the case of the WH2-A domain), several existing mutants developed in the Quinlan lab were attractive tools for testing the contributions of Capu/Spir nucleation and/or capping/elongation to synergy in actin assembly
3. Forster resonance energy transfer (FRET) measurements via fluorescence lifetime imaging microscopy (FLIM)
    - As described in **Chapter 4**, fluorescent Spir and Capu fusions were generated to detect their interaction with high spatiotemporal precision in live cells

References

Azoury, Jessica, Karen W. Lee, Virginie Georget, Pascale Rassinier, Benjamin Leader, and Marie-Hélène Verlhac. 2008. *Spindle Positioning in Mouse Oocytes Relies on a Dynamic Meshwork of Actin Filaments*. Vol. 18.

Blatner, Nichole R., Robert V Stahelin, Karthikeyan Diraviyam, Phillip T. Hawkins, Wanjin Hong, Diana Murray, and Wonhwa Cho. 2004. "The Molecular Basis of the Differential Subcellular Localization of FYVE Domains." *The Journal of Biological Chemistry* 279(51):53818–27.

Bor, Batbileg, Justin S. Bois, and Margot E. Quinlan. 2015. "Regulation of the Formin Cappuccino Is Critical for Polarity of Drosophila Oocytes." *Cytoskeleton (Hoboken, N.J.)* 72(1):1–15.

Bor, Batbileg, Christina L. Vizcarra, Martin L. Phillips, and Margot E. Quinlan. 2012. "Autoinhibition of the Formin Cappuccino in the Absence of Canonical Autoinhibitory Domains." 23.

Bosch, Montserrat, Kim Ho Diep Le, Beata Bugyi, John J. Correia, Louis Renault, and Marie-France Carlier. 2007. "Analysis of the Function of Spire in Actin Assembly and Its Synergy with Formin and Profilin." *Molecular Cell* 28(4):555–68.

Bun, Philippe, Serge Dmitrieff, Julio M. Belmonte, François J. Nédélec, and Péter Lénárt. 2018. "A Disassembly-Driven Mechanism Explains F-Actin-Mediated Chromosome Transport in Starfish Oocytes." *ELife* 7.

Courtemanche, Naomi and Thomas D. Pollard. 2012. "Determinants of Formin Homology 1 (FH1) Domain Function in Actin Filament Elongation by Formins." *The Journal of Biological Chemistry* 287(10):7812–20.

Dahlgaard, Katja, Alexandre A. S. F. Raposo, Teresa Niccoli, and Daniel St Johnston. 2007. "Capu and Spire Assemble a Cytoplasmic Actin Mesh That Maintains Microtubule Organization in the Drosophila Oocyte." *Developmental Cell* 13(4):539–53.

Dominguez, Roberto. 2016. "The WH2 Domain and Actin Nucleation: Necessary but Insufficient." *Trends in Biochemical Sciences*.

Edwards, Marc, Adam Zwolak, Dorothy A. Schafer, David Sept, Roberto Dominguez, and John A. Cooper. 2014. "Capping Protein Regulators Fine-Tune Actin Assembly Dynamics." *Nature Reviews Molecular Cell Biology* 15(10):677–90.

Field, Christine M. and Péter Lénárt. 2011. "Bulk Cytoplasmic Actin and Its Functions in Meiosis and Mitosis." *Current Biology : CB* 21(19):R825-30.

Goode, Bruce L. and Michael J. Eck. 2007. "Mechanism and Function of Formins in the Control of Actin Assembly." *Annual Review of Biochemistry* 76(1):593–627.

Huff, Thomas, Christian S. .. Müller, Angela M. Otto, Roland Netzker, and Ewald Hannappel. 2001. "β-Thymosins, Small Acidic Peptides with Multiple Functions." *The International Journal of Biochemistry & Cell Biology* 33(3):205–20.

Ito, Takuto, Akihiro Narita, Tasuku Hirayama, Masayasu Taki, Shohei Iyoshi, Yukio Yamamoto, Yuichiro Maéda, and Toshiro Oda. 2011. “Human Spire Interacts with the Barbed End of the Actin Filament.” *Journal of Molecular Biology* 408:18–25.

Johnstone, O. and P. Lasko. 2001. “Translational Regulation and RNA Localization in Drosophila Oocytes and Embryos.” *Annual Review of Genetics* 35:365–406.

Leader, Benjamin, Hyunjung Lim, Mary Jo Carabatsos, Anne Harrington, Jeffrey Ecsedy, David Pellman, Richard Maas, and Philip Leder. 2002. “Formin-2, Polyploidy, Hypofertility and Positioning of the Meiotic Spindle in Mouse Oocytes.” *Nature Cell Biology* 4(12):921–28.

Maciver, Sutherland K. and Patrick J. Hussey. 2002. “The ADF/Cofilin Family: Actin-Remodeling Proteins.” *Genome Biology* 3(5):reviews3007.

Manseau, L., J. Calley, and H. Phan. 1996. “Profilin Is Required for Posterior Patterning of the Drosophila Oocyte.” *Development (Cambridge, England)* 122(7):2109–16.

Manseau, L. J. and T. Schupbach. 1989. “Cappuccino and Spire: Two Unique Maternal-Effect Loci Required for Both the Anteroposterior and Dorsoventral Patterns of the Drosophila Embryo.” *Genes & Development* 3(9):1437–52.

Misra, Saurav and James H. Hurley. 1999. “Crystal Structure of a Phosphatidylinositol 3-Phosphate-Specific Membrane-Targeting Motif, the FYVE Domain of Vps27p.” *Cell* 97(5):657–66.

Montaville, Pierre, Antoine Jégou, Julien Pernier, Christel Compper, Bérengère Guichard, Binyam Mogessie, Melina Schuh, Guillaume Romet-Lemonne, and Marie-France Carlier. 2014. “Spire and Formin 2 Synergize and Antagonize in Regulating Actin Assembly in Meiosis by a Ping-Pong Mechanism.” *PLoS Biology* 12(2):e1001795.

Montaville, Pierre, Sonja Kühn, Christel Compper, and Marie-France Carlier. 2015. “Role of the C-Terminal Extension of Formin 2 in Its Activation by Spire and Processive Assembly of Actin Filaments.” *The Journal of Biological Chemistry* M115.681379-.

Namgoong, Suk, Malgorzata Boczkowska, Michael J. Glista, Jonathan D. Winkelman, Grzegorz Rebowski, David R. Kovar, and Roberto Dominguez. 2011. “Mechanism of Actin Filament Nucleation by Vibrio VopL and Implications for Tandem W Domain Nucleation.” *Nature Structural & Molecular Biology* 18(9):1060–67.

Paul, Aditya S. and Thomas D. Pollard. 2009. “Review of the Mechanism of Processive Actin Filament Elongation by Formins.” *Cell Motility and the Cytoskeleton* 66(8):606–17.

Pechlivanis, Markos, Annette Samol, and Eugen Kerkhoff. 2009. “Identification of a Short Spir Interaction Sequence at the C-Terminal End of Formin Subgroup Proteins.” *The Journal of Biological Chemistry* 284(37):25324–33.

Perrin, Benjamin J. and James M. Ervasti. 2010. “The Actin Gene Family: Function Follows Isoform.” *Cytoskeleton* 67(10):630–34.

Pfender, Sybille, Vitaliy Kuznetsov, Sandra Pleiser, Eugen Kerkhoff, and Melina Schuh. 2011. “Spire-Type Actin Nucleators Cooperate with Formin-2 to Drive Asymmetric Oocyte

Division.” *Current Biology : CB* 21(11):955–60.

Pollard, T. D. 1986. “Rate Constants for the Reactions of ATP- and ADP-Actin with the Ends of Actin Filaments.” *The Journal of Cell Biology* 103(6 Pt 2):2747–54.

Pollard, T. D. and J. A. Cooper. 1986. “Actin and Actin-Binding Proteins. A Critical Evaluation of Mechanisms and Functions.” *Annual Review of Biochemistry* 55(1):987–1035.

Pylypenko, Olena, et al. Rock. 2016. “Coordinated Recruitment of Spir Actin Nucleators and Myosin V Motors to Rab11 Vesicle Membranes.” *ELife* 5:213–21.

Quinlan, Margot E. 2013. “Direct Interaction between Two Actin Nucleators Is Required in Drosophila Oogenesis.” *Development (Cambridge, England)* 140(21):4417–25.

Quinlan, Margot E., John E. Heuser, Eugen Kerkhoff, and R. Dyche Mullins. 2005. “Drosophila Spire Is an Actin Nucleation Factor.”

Quinlan, Margot E., Susanne Hilgert, Anaid Bedrossian, R. Dyche Mullins, and Eugen Kerkhoff. 2007. “Regulatory Interactions between Two Actin Nucleators, Spire and Cappuccino.” *The Journal of Cell Biology* 179(1):117–28.

Theriot, J. A. and T. J. Mitchison. 1993. “The Three Faces of Profilin.” *Cell* 75(5):835–38.

Theurkauf, W. 1994. “Premature Microtubule-Dependent Cytoplasmic Streaming in Cappuccino and Spire Mutant Oocytes.” *Science* 265(5181):2093–96.

Theurkauf, W. E., S. Smiley, M. L. Wong, B. M. Alberts, Z. Bryant, H. Ruohola-Baker, and L. Manseau. 1992. “Reorganization of the Cytoskeleton during Drosophila Oogenesis: Implications for Axis Specification and Intercellular Transport.” *Development (Cambridge, England)* 115(4):923–36.

Tittel, Janine, Tobias Welz, Aleksander Czogalla, Susanne Dietrich, Annette Samol-Wolf, Markos Schulte, Petra Schwille, Thomas Weidemann, and Eugen Kerkhoff. 2015. “Membrane Targeting of the Spir·formin Actin Nucleator Complex Requires a Sequential Handshake of Polar Interactions.” *The Journal of Biological Chemistry* 290(10):6428–44.

Vizcarra, Christina L., Batbileg Bor, and Margot E. Quinlan. 2014. “The Role of Formin Tails in Actin Nucleation, Processive Elongation, and Filament Bundling * □ S.” *Published JBC Papers in Press*.

Vizcarra, Christina L., Barry Kreutz, Avital A. Rodal, Angela V Toms, Jun Lu, Wei Zheng, Margot E. Quinlan, and Michael J. Eck. 2011. “Structure and Function of the Interacting Domains of Spire and Fmn-Family Formins.”

Vizcarra, Christina L. and Margot E. Quinlan. 2017. “Actin Filament Assembly by Bacterial Factors VopL/F: Which End Is Up?” *The Journal of Cell Biology* 216(5):1211–13.

Xu, Yingwu, James B. Moseley, Isabelle Sagot, Florence Poy, David Pellman, Bruce L. Goode, and Michael J. Eck. 2004. “Crystal Structures of a Formin Homology-2 Domain Reveal a Tethered Dimer Architecture.” *Cell* 116(5):711–23.

Zeth, Kornelius, Markos Pechlivanis, Annette Samol, Sandra Pleiser, Clemens Vonrhein, and Eugen Kerkhoff. 2011. “Molecular Basis of Actin Nucleation Factor Cooperativity: Crystal Structure of the Spir-1 Kinase Non-Catalytic C-Lobe Domain (KIND)•formin-2 Formin SPIR Interaction Motif (FSI) Complex.” *The Journal of Biological Chemistry* 286(35):30732–39.

Chapter 2: Spire stimulates nucleation by Cappuccino and binds both ends of actin filaments

Spire stimulates nucleation by Cappuccino and binds both ends of actin filaments

Alexander O. Bradley[1], Christina L. Vizcarra[1,*], Hannah M. Bailey[1], Margot E. Quinlan[1,2,#]

[1]Department of Chemistry and Biochemistry and [2]Molecular Biology Institute, University of California Los Angeles, 607 Charles E. Young Drive, Los Angeles, CA 90095, USA.

*current address: Department of Chemistry, Barnard College, New York, USA.

[#]corresponding author: margot@chem.ucla.edu

Abstract

An actin mesh fills both mouse and fly oocytes. The meshes are built by a conserved mechanism and used to establish polarity. Two actin nucleators, Spire and Cappuccino, collaborate to build actin filaments that connect vesicles and the cortex. Direct interaction between Spire and Cappuccino is required for in vitro synergistic actin assembly; however, we understand little about why the interaction is necessary. To mimic the geometry of Spire and Cappuccino in vivo, we immobilized Spire on beads. We found that increased nucleation is a major part of synergy and that Spire alone binds both barbed- and pointed-ends of actin filaments. We identified Spire's barbed-end binding domain. Partial rescue of fertility by a loss-of-function mutant indicates that barbed-end binding is not necessary for Spire's in vivo function, but that it may play a role under normal circumstances. We propose that Spire stimulates nucleation by Cappuccino in a manner similar to the collaboration between APC and mDia1.

Keywords: Spire, Cappuccino, actin, Drosophila, cytoskeleton, nucleation, microscopy, mesh, streaming, oogenesis

Introduction

Cells contain a variety of actin-based structures that fulfill distinct functional roles. The actin cytoskeleton is malleable due to dynamic structural regulation by a range of distinct actin-binding proteins. The first step to building a structure is generally catalysis of new actin filaments, so-called nucleation. Both a kinetic barrier and certain actin binding proteins, such as profilin, prevent spontaneous nucleation in the cell. Instead, actin nucleators stimulate this process in highly regulated manners. There are three known classes of actin nucleators that function by distinct mechanisms: the Arp2/3 complex, formins, and tandem-WH2 domain nucleators. A developing trend is that none of these proteins work independently. Effector proteins can inhibit or enhance the activity of actin nucleators. Usually, the effector is not a nucleator. In some cases, two independent nucleators also work together. A poorly understood example of such interplay is the collaboration between Cappuccino (Capu, a formin) and Spire (Spir, a tandem-WH2 nucleator).

Both Spir and Capu are required for oogenesis. This discovery was first made in *Drosophila* and subsequently demonstrated in mouse (Manseau and Schupbach, 1989; Leader et al., 2002; Pfender et al., 2011). In both cases, Capu (or Fmn-2, one of two mammalian homologs) and Spir (or mSpire, referring to mammalian homologs, Spire-1 and Spire-2) build a mesh of actin that fills the oocyte (Dahlgaard et al., 2007; Schuh and Ellenberg, 2008; Azoury et al., 2008; Pfender et al., 2011). The discovery that both Spir and Capu are actin nucleators led to the question of why two nucleators would be needed to build one structure (Quinlan et al., 2005). We now know that direct interaction between Spir and Capu is required for their function (Quinlan, 2013). Detailed biochemical analyses and structural biology provide insight into the interaction: the N-terminal Spir-KIND domain binds the C-terminal Capu-tail with ~100 nM affinity (**Fig. 1**) (Quinlan et al., 2007; Vizcarra et al., 2011; Pechlivanis et al., 2009; Zeth et al., 2011). However, our understanding of the functional consequences of the interaction remain

incomplete. Capu, like all formins, is a dimer. It can bind two copies of Spir and, thereby, accelerate actin assembly by Spir (Quinlan et al., 2007; Vizcarra et al., 2011). In contrast, Spir's KIND domain inhibits nucleation by Capu and competes with barbed ends for Capu binding, effectively inhibiting Capu's ability to accelerate actin assembly (Quinlan et al., 2007; Vizcarra et al., 2011). However, when a human Spire-1 construct, containing both the KIND domain and four tandem WH2 domains, is mixed with the C-terminal half of Fmn-2, actin assembly is greatly enhanced (Montaville et al., 2014). So-called ping-ponging – Spir and Fmn-2 alternately binding to the barbed end of filaments – is observed and was proposed to account for synergistic actin assembly (Montaville et al., 2014).

Spir is enriched at the cortex of the *Drosophila* oocyte, localizes to Rab11-positive vesicles in mouse oocytes, and the C-terminal mFYVE domain of mSpire-1 binds phospholipids (Quinlan et al., 2007; Quinlan, 2013; Pfender et al., 2011; Tittel et al., 2015). While Fmn-2 is also observed on Rab11-positive vesicles in mouse ooctyes, GFP-Capu appears diffuse throughout the *Drosophila* oocyte (Schuh, 2011; Dahlgaard et al., 2007; Quinlan, 2013). In the mouse oocyte, Rab11-positive vesicles that contain mSpire, Fmn-2, and Myosin V are at nodes of the actin mesh that fills the oocyte (Schuh, 2011). Mesh dynamics contribute to nucleus positioning and long distance transport of the Rab11-positive vesicles toward the cell cortex (Holubcová et al., 2013; Almonacid et al., 2015; Ahmed et al., 2018). A model to account for the long distance transport includes mSpire/Fmn-2-nucleated actin filaments growing with their barbed ends remaining near the vesicles, creating tracks that myosin V on neighboring vesicles can walk along, pulling vesicles together (Schuh, 2011). When ping-ponging was observed, Montaville et al. (Montaville et al., 2014) expanded on this model, proposing that barbed ends of filaments and/or pre-nuclei are recruited by vesicle-bound mSpire and handed off to Fmn-2 to stimulate elongation.

In order to learn more about how Spir and Capu interact to build actin filaments and structures, we combined biochemistry and fly genetics. We developed a bead-based assay, in which we attached the N-terminal half of Spir (SpirNT) to beads and added free C-terminal half of Capu (CapuCT), based on reported localization data (see **Fig. 2-1A** for construct definitions). Through this work we found that beads decorated with SpirNT and CapuCT (CapuCT/SpirNT-beads) nucleate filaments that grow with their barbed ends away from beads, protected by CapuCT, opposite to the polarity proposed earlier. We found that SpirNT alone on beads (SpirNT-beads) nucleates filaments oriented the same way. We also found that SpirNT-beads retain the pointed ends of filaments with a dwell time of ~100 seconds while neighboring SpirNT-beads capture the barbed ends of filaments for several hundreds of seconds. These data resolve an outstanding question in the literature about Spir's association with filament ends – it binds both ends. We also identified the domain necessary for Spir's high-affinity barbed-end binding. Surprisingly, barbed end binding is not necessary for oogenesis and loss of barbed-end binding increases Spir/Capu synergy *in vitro*. These genetic and biochemical data indicate that ping-ponging at the barbed end is neither the dominant source of synergy nor necessary *in vivo*. Instead, we propose that Spir and Capu collaborate by a mechanism in which Spir promotes Capu's nucleation activity through its independent nucleation activity, similar to APC/mDia1 synergy (Okada et al., 2010; Breitsprecher et al., 2012).

Results

WH2 domains are necessary for Drosophila oogenesis

The Spir-KIND domain inhibits CapuCT in pyrene-actin assays (Quinlan et al., 2007; Vizcarra et al., 2011). However, genetics indicate that Spir and Capu both play positive roles in oocyte mesh formation (Manseau and Schupbach, 1989; Dahlgaard et al., 2007; Quinlan, 2013). Combined, these data suggest that Spir's WH2 domains contribute to function in vivo. To formally test whether actin binding is required, we used full-length Spir (CG10076, splice variant

PB) with a C-terminal mEGFP tag in a genetic rescue assay. In each of Spir's four WH2 domains, we mutated three conserved, hydrophobic residues which contact actin (**Fig. 2-1A**) (Kelly et al., 2006; Chereau et al., 2005). These mutations were previously shown to dramatically decrease, if not abolish, actin monomer binding (Quinlan et al., 2005). In vitro, SpirNT with all of these mutations (SpirNT(A*B*C*D*)) does not accelerate actin assembly (**Fig. 2-8A**) (Quinlan et al., 2005). We previously demonstrated that expression of wild-type Spir-GFP, driven by germline specific nanos-Gal4-vp16, is sufficient to rescue fertility in flies that lack endogenous Spir (**Table 2-1**) (Quinlan, 2013). In contrast, expression of Spir(A*B*C*D*)-GFP failed to rescue fertility (hatch rate < 2%, **Table 2-1**). In oocytes expressing only Spir(A*B*C*D*)-GFP, the actin mesh is absent and streaming is premature, consistent with loss of actin assembly activity and loss of fertility (**Fig. 2-1C-E**). Thus, we conclude that actin binding by at least one of Spir's WH2 domains is necessary for actin assembly and oogenesis.

Barbed ends project away from CapuCT/SpirNT-beads

In order to learn more about how Spir and Capu interact to build actin filaments and structures, we developed a bead-based assay. Spir is enriched at the cortex of the *Drosophila* oocyte, localizes to Rab11-positive vesicles in mouse oocytes, and the C-terminal mSpire-mFYVE domain binds phospholipids (Quinlan et al., 2007; Quinlan, 2013; Pfender et al., 2011; Tittel et al., 2015). While Fmn2 is also observed on vesicles in the mouse oocyte, GFP-Capu appears diffuse throughout the *Drosophila* oocyte (Schuh, 2011; Quinlan, 2013). Based on these data, we immobilized SpirNT on beads and added CapuCT in solution. To do so, we biotinylated a C-terminal Avitag on SpirNT and mixed it with CapuCT and streptavidin-coated beads (**Fig. 2-1B**). We introduced the decorated beads to a sparsely biotinylated flow chamber and imaged them by total internal reflection fluorescence (TIRF) microscopy. When we added actin (20% OG-actin) and profilin to the flow chamber, extensive and rapid polymerization followed (**Fig. 2-2A, Video 1**).

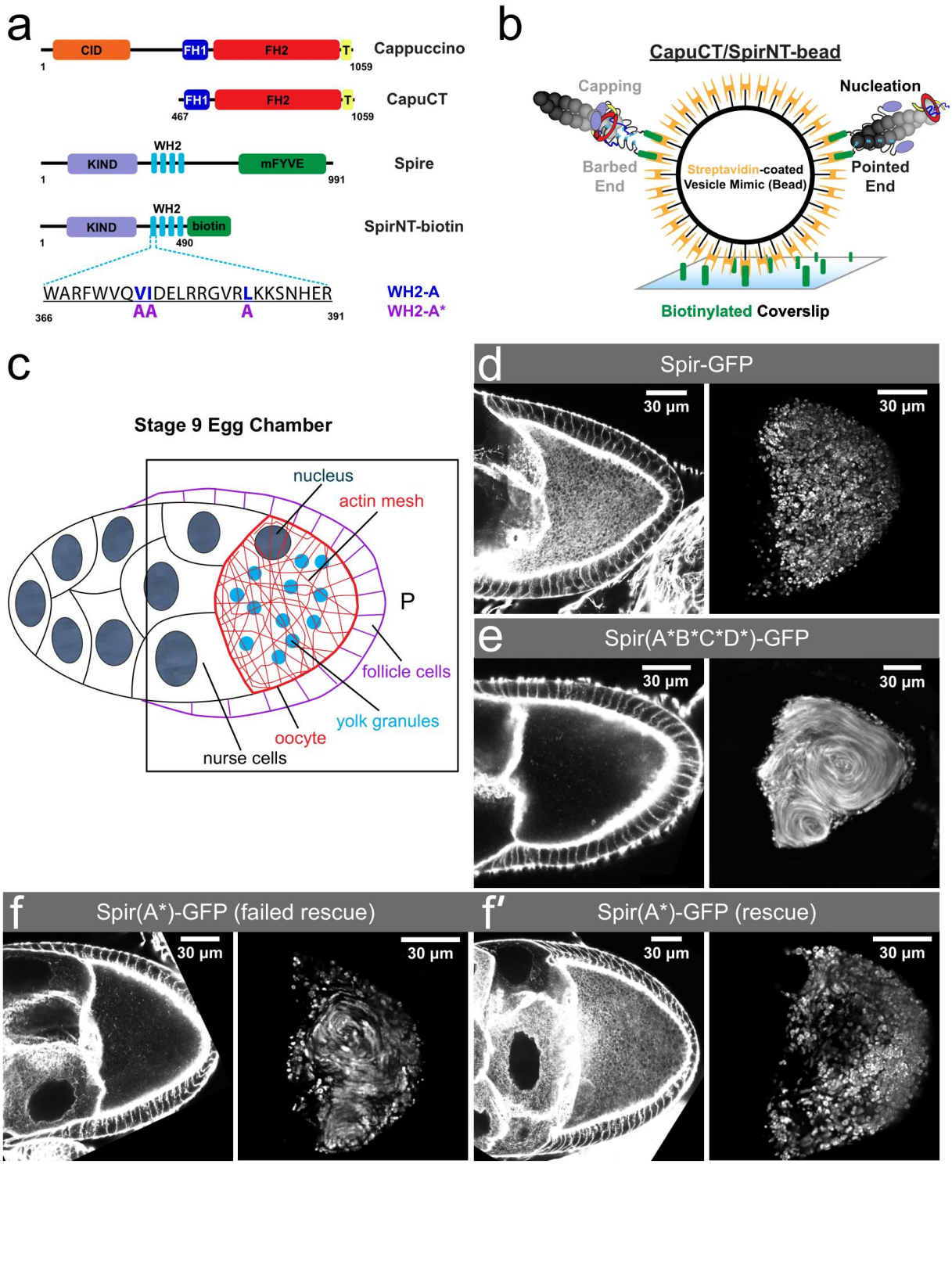
a
CID
FH1
FH2
Cappuccino
1
1059
CapuCT
467
KIND
WH2
mFYVE
Spire
991
biotin
SpirNT-biotin
490
WARFWVQVIDELRRGVRLKKSNHER
AA
A
366
391
WH2-A
WH2-A*
b
CapuCT/SpirNT-bead
Capping
Nucleation
Barbed End
Streptavidin-coated Vesicle Mimic (Bead)
Pointed End
Biotinylated Coverslip
c
Stage 9 Egg Chamber
nucleus
actin mesh
P
follicle cells
yolk granules
oocyte
nurse cells
d
Spir-GFP
30 µm
e
Spir(A*B*C*D*)-GFP
f
Spir(A*)-GFP (failed rescue)
f′
Spir(A*)-GFP (rescue)

Figure 2-1 – *WH2 domains are necessary for oogenesis*

(A) Domain architecture of Drosophila melanogaster Cappuccino (Capu), Spire (Spir), and truncations used. CID, Capu Inhibitory Domain (orange); FH1/FH2, Formin Homology domains (1, dark blue; 2, red); T, Tail (yellow); KIND, Kinase Noncatalytic C-lobe Domain (purple); WH2, Wiskott-Aldrich syndrome Homology domains (light blue); mFYVE, Modified FYVE (zinc finger) domain (green). Spir has four WH2 domains, named WH2-A through -D. The sequence of WH2-A and mutations that disrupt its actin binding are shown. (B) Bead experiment methodology. To decorate streptavidin-coated microspheres (gold) with SpirNT, and to bind the microspheres to the coverslip, biotin (green) is conjugated both to coverslips and to SpirNT. Two potential orientations of the actin filament distinguish Spir's primary activities at each end: capping filaments at their barbed ends (left) and nucleating filaments from their pointed ends (right). (C) Cartoon of a stage 9 egg chamber. P, Posterior. (D – F) Stage 9 egg chambers dissected from flies with a spir null background, expressing Spir-GFP (D), Spir(A*B*C*D*)-GFP (E), or Spir(A*)-GFP (F, F'). Egg chambers were stained with fluorescently-labeled phalloidin to detect the presence or absence of mesh (left images) and standard deviation projections of autofluorescent yolk granule positions over 2 minutes (right images) show the extent of ooplasmic streaming. Expression of Spir(A*)-GFP results in a mixture of failed (F) and successful rescues (F').

Two groups proposed that Spir/Capu-coated vesicles have filaments with barbed ends apposed to the vesicle and pointed ends growing away (**Fig. 2-1B**) (Montaville et al., 2014; Schuh, 2011). We tested this model by examining the orientation of filaments growing off of CapuCT/SpirNT-beads. By lowering the concentration of actin (600 nM), we decreased nucleation such that we could track individual filaments. Under these conditions, we observed filaments growing from but "retained" at the beads (**Videos 2 and 3**). We carefully analyzed 9 of 32 individual filaments observed. In every case, fiducial marks which do not move with respect to the bead, and increased fluorescence intensity at filament ends (i.e. ends brighter due to addition of unbleached monomers (Kovar and Pollard, 2004)), away from the bead, indicate that barbed ends grow away from the bead surface (**Fig. 2-2B, Video 3**). We expected to see the opposite case with Capu directly conjugated to the beads. For unknown reasons, Capu was not functional when attached to beads through a number of different linkers. Instead, we conjugated the formin mDia1 to beads. In this case, fiducial marks were displaced at the rate of filament elongation and the addition of unbleached monomers was no longer observed at the filament end away from the bead (**Fig. 2-2C, Video 4**), consistent with barbed-end growth at the bead surface. Together these data demonstrate that CapuCT/SpirNT-beads nucleate filaments with barbed ends growing away from the bead and suggest that CapuCT separates from SpirNT to elongate the filament.

Spir beads retain the pointed ends of nucleated actin filaments

A dense collection of filaments emanated radially from CapuCT/SpirNT-beads. Because we concluded that CapuCT-mediated elongation proceeded away from the beads, the density of actin near the bead surface suggested that the pointed ends of filaments could be retained by Spir. We repeated the experiments with SpirNT-beads, without added CapuCT or profilin, and observed similar patterns (**Fig. 2-3A, Video 5**). We found that nucleation by SpirNT-beads was

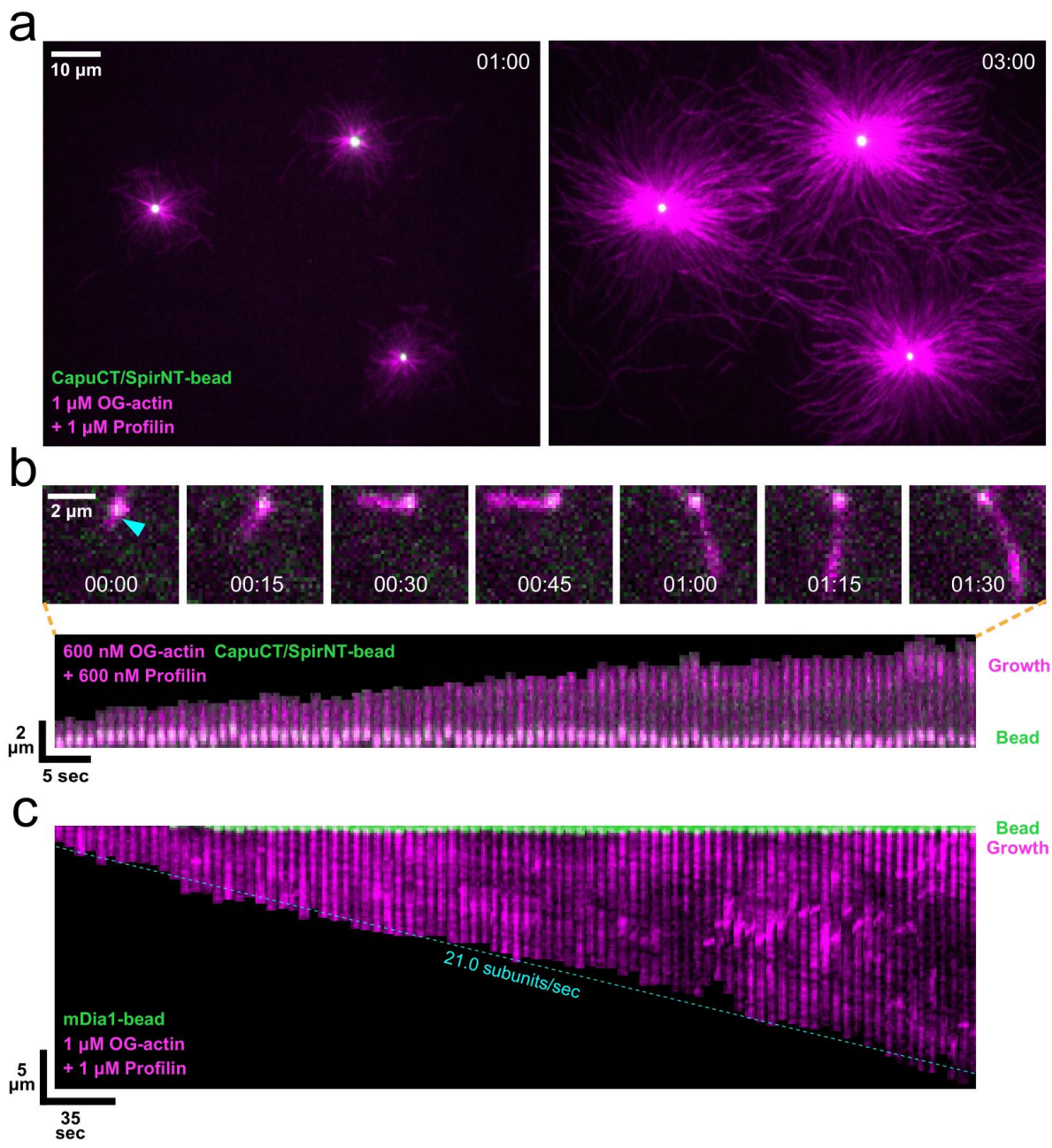

Figure 2-2 – *Barbed ends project away from CapuCT/SpirNT-beads*

(A) Actin assembles off of CapuCT/SpirNT-beads. See also, Video 1. (B) A single filament is nucleated and retained by a bead. Kymograph (bottom) shows bleaching of filament regions closest to the bead and new, labeled actin added away from the bead, indicating growth away from the bead. See also, Video 3. (C) A single filament is nucleated and elongated by a bead coated with mDia1. Filament growth is accelerated by the processive formin and profilin. Fiducial marks (e.g. dark, diagonal lines) in the kymograph are displaced from the bead at the rate of elongation, indicating growth at the bead. See also, Video 4.

suppressed enough to observe individual filaments when profilin was added back (**Fig. 2-3B**).

We again observed filaments growing from and retained at the bead surface (**Fig. 2-3C and Video 6**). The distribution of filament dwell times was well fit by a single exponential with an off rate of 0.007 ± 0.003 s^{-1} (**Fig. 2-3D**). We note that retention of filaments by SpirNT-beads occurred independent of profilin (**Fig. 2-8G and Video 7**). Furthermore, neither filament end was observed to interact with beads coated with Spir-KIND and CapuCT (**Fig. 2-8F**), indicating that retention is specifically mediated by Spir-WH2 domains.

We did not assume that filaments were oriented with their barbed ends out when nucleated by SpirNT-beads because Spir has been reported to bind both the barbed and pointed ends of filaments (Quinlan et al., 2005; Bosch et al., 2007; Ito et al., 2011). mSpire1 caps barbed ends with high affinity and SpirNT binds pointed ends weakly (nM vs μM K_ds) (Bosch et al., 2007; Montaville et al., 2014; Quinlan et al., 2005). We closely analyzed 10 of the 70 filaments included in the retention data set. All ten filaments, growing from SpirNT-beads, displayed fiducial marks which did not move with respect to the bead and typically had brighter filament ends away from the beads consistent with barbed ends being oriented away from the beads (**Fig. 2-3C**). Thus, we conclude that barbed ends grow away from SpirNT-beads and that SpirNT is sufficient to retain the pointed ends of actin filaments for >100 seconds.

SpirNT-beads capture and cap the barbed ends of actin filaments

When we examined the dense actin networks emanating from beads, we also observed apparent connections between neighboring beads (**Fig. 2-3A**). This pattern suggested to us that the barbed ends of actin filaments could also be associated with the beads. Under conditions where individual filaments could be tracked, we observed the “capture” of filaments (**Fig. 2-4**).

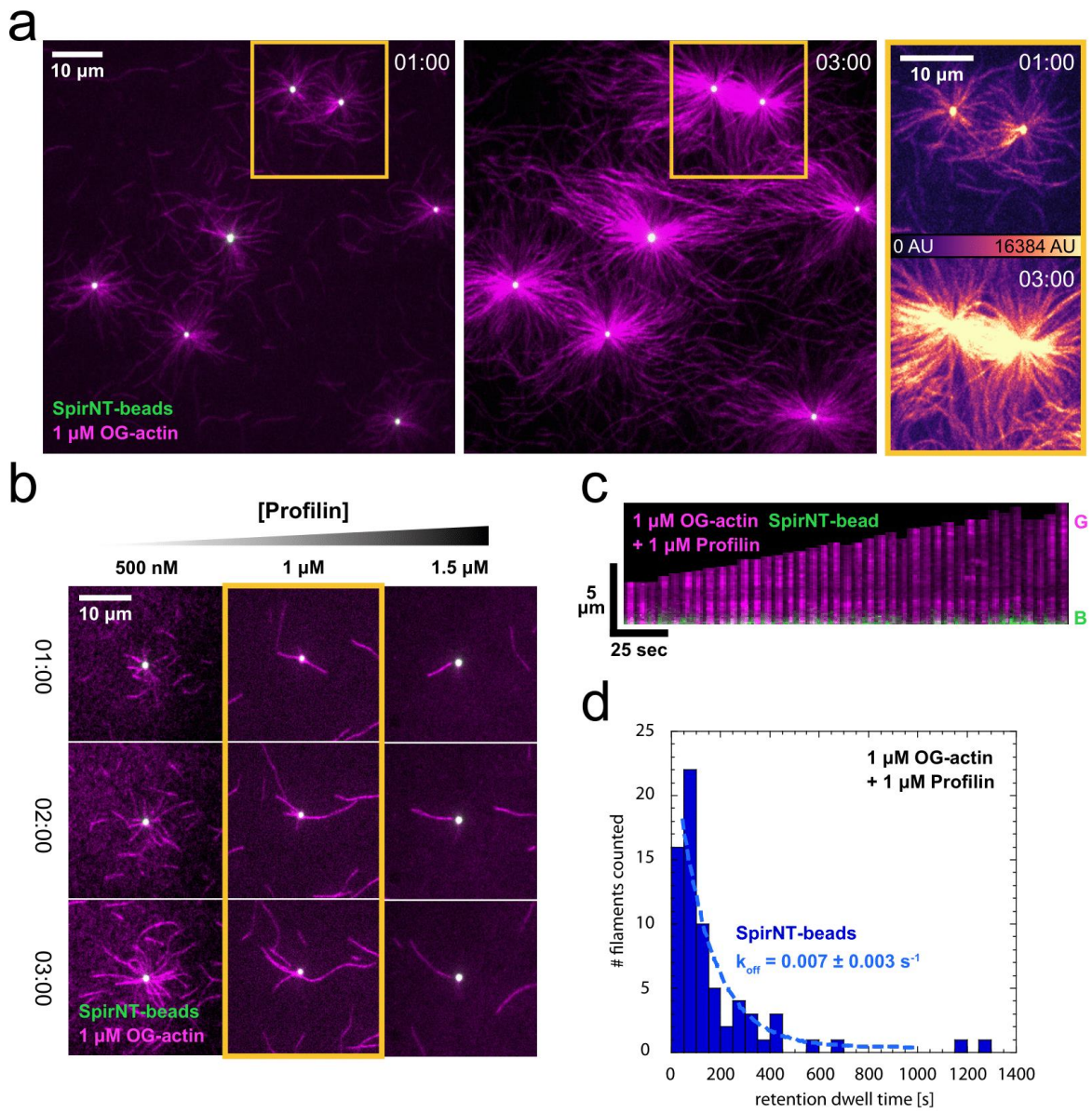

Figure 2-3 – *SpirNT-beads retain the pointed ends of nucleated actin filaments*

(A) SpirNT-beads, in the absence of Capu and profilin, also potently polymerize actin. The highlighted region (gold) is magnified and pseudocolored (right) to emphasize the enrichment of actin filaments between beads. See also, *Video 5. (B)* Nucleation by SpirNT-beads is suppressed by profilin. When added at 1 µM (gold box), profilin permits the observation of several, single filaments per bead. *(C)* SpirNT-beads also retain nucleated filaments. G, Growth; B, Bead. Fiducial marks (dark, horizontal lines) in the kymograph are not displaced as the filament elongates, indicating growth away from the bead. See also, *Video 6. (D)* Dwell times of filament pointed ends on beads. Nucleated and retained filaments were tracked from SpirNT-beads in the presence of 1 µM actin and 1 µM profilin. All bead-associated filaments were counted unless obviously captured from solution or > 1 µm in length when first visible. The data are well fit by a single exponential (k_{off} = 0.007 ± 0.003 s^{-1}, n = 70 filaments; 4 independent experiments).

The association of captured filaments with Spir beads often outlasted the single-filament imaging window (10+ minutes), precluding measurement of an off rate and suggesting that the interaction was distinct from retention.

In addition to seeing filaments between beads, we often observed capture of free filaments. We probed the orientation of captured filaments using two colors of actin. We initiated elongation in the presence of Cy3B-actin and stabilized these filaments with phalloidin after several minutes. Adding a limiting pool of OG-actin (600 nM) plus profilin to favor barbed end growth, we observed that – whether the filament had both ends free (as shown) or one end retained by a bead – only the barbed ends of filaments were captured by beads (**Fig. 2-4A, Video 8**). Filaments captured by beads did not grow measurably (**Fig. 2-4A**). Occasionally, we observed the release of a barbed end, following capture. In these cases, the filament resumed elongation at the same rate as before capture (**Fig. 2-4A**). As noted above, barbed ends do not interact with CapuCT/Spir-KIND-beads (**Fig. 2-8F**). These data indicate that the barbed ends are capped by Spir-WH2 domains, as opposed to being non-specifically stuck to the beads or KIND domain.

To further test the phenomenon of filament capture, we added capping protein and CapuCT to the experiment. Under these conditions, the sustained and accelerated growth of retained filaments confirmed that CapuCT separates from SpirNT to elongate filament barbed ends (**Fig. 2-4B**). These filaments were still captured by beads, suggesting that SpirNT displaces CapuCT from the barbed end (**Fig. 2-4B, Video 9**). Together these data demonstrate that – with or without CapuCT present – Spir-beads can nucleate and retain the pointed ends of actin filaments, while neighboring beads can capture and cap their barbed ends.

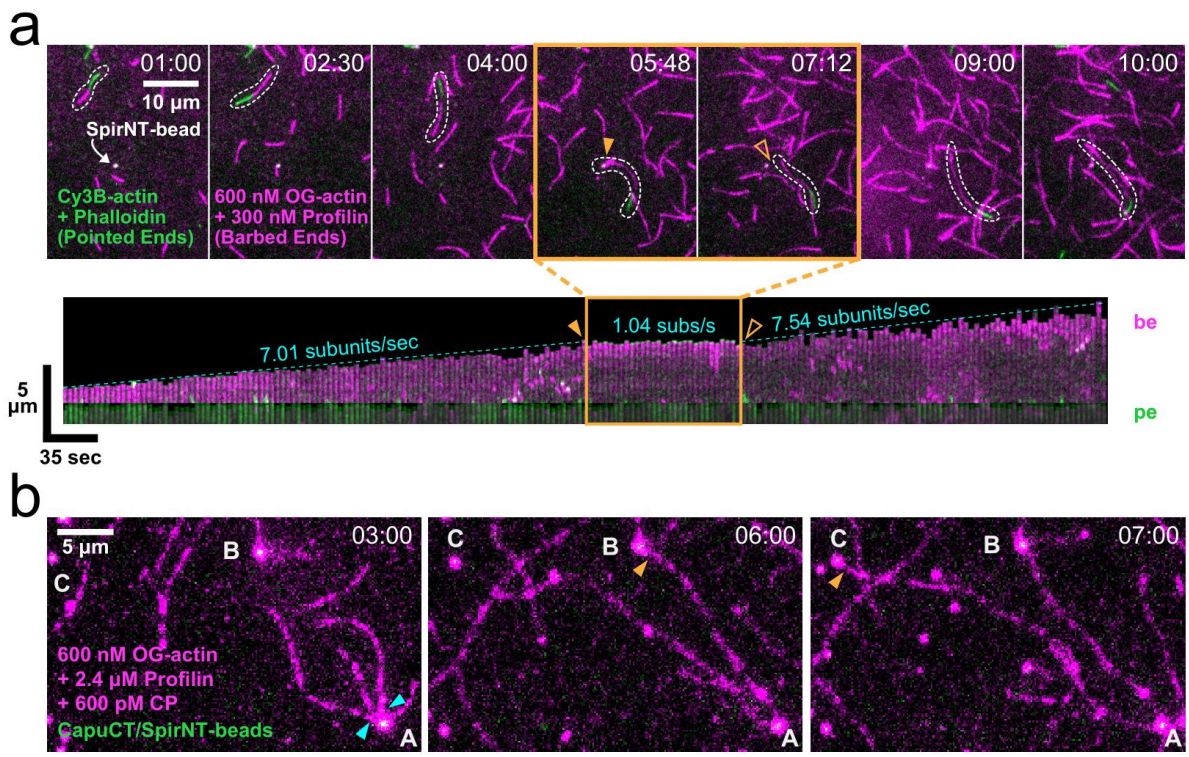

Figure 2-4 – *SpirNT-beads capture and cap the barbed ends of actin filaments*

(A) Nucleated filaments (green) grow only at their barbed ends (magenta). A free filament (dashed outline) diffuses and grows until it is captured by a SpirNT-bead (solid triangle). The filament resumes growth once released by the bead (open triangle). The kymograph shows that the growing, barbed end (magenta) is captured/capped by Spir and resumes growth after release. See also, *Video 8. (B)* Two filaments (cyan triangles) nucleated by a SpirNT/CapuCT-bead ("A") are retained for over 5 minutes. Their barbed ends are captured (gold triangles) by other CapuCT/SpirNT-beads ("B" and "C"). Accelerated growth of these filaments (~20 subunits/sec) in the presence of profilin and capping protein indicates that CapuCT is elongating and protecting their barbed ends. Filaments did not measurably grow, following capture, suggesting that CapuCT is displaced and that the barbed end is bound by SpirNT upon capture. See also, *Video 9.*

Spir's WH2-A binds filament barbed ends and reduces actin nucleation

Each of Spir's four WH2 domains contributes differently to nucleation and they bind actin monomers with a range of affinities (from ~100 nM – 1.1 μM) (Quinlan et al., 2005; Rasson et al., 2015). We reasoned that the most N-terminal WH2 domain, WH2-A, binds barbed ends of filaments, based on our earlier observation that isolated WH2-A is the only Spir-WH2 domain that slows filament growth (Rasson et al., 2015). To test the contribution of WH2-A to barbed end binding, we first established that wild-type SpirNT caps barbed ends in a seeded elongation assay, as has been shown for mSpire-1 (Bosch et al., 2007). In the presence of actin seeds, monomers, and profilin, SpirNT potently inhibits elongation (**Fig. 2-5A**). The dose dependence of inhibition indicates an apparent affinity of SpirNT for barbed ends of 20 ± 3 nM, similar to that reported for mSpire-1 (**Fig. 2-5B**). We then mutated three conserved hydrophobic residues in WH2A of SpirNT (SpirNT(A*); **Fig. 2-1A**) to remove actin monomer binding by this domain alone. When added to the seeded elongation assay, SpirNT(A*) was essentially unable to inhibit elongation (**Fig. 2-5A,B**). Thus, a functional WH2-A domain is necessary for high affinity, barbed-end capping.

In standard pyrene-actin assays, we found that SpirNT(A*) assembles actin more potently than wild type SpirNT (**Fig. 2-5C and 2-8C**). Of note, the plateau of pyrene traces does not decrease at high concentrations as is seen for wild type SpirNT, suggesting that this mutant is not a potent monomer sequesterer (**Fig. 2-5C**) (Quinlan et al., 2005). We next attached biotinylated SpirNT(A*) to beads and added actin and profilin. Consistent with increased activity in pyrene assays, we observed faster accumulation of filaments from SpirNT(A*)-beads compared to wild type SpirNT-beads (**Fig. 2-5D, Video 10**). To compare nucleation rates on beads, we measured the integrated intensity of actin within a band 1.6 μm away from the beads. At this proximity, we are minimally sensitive to filament elongation and interpret the intensity as proportional to the

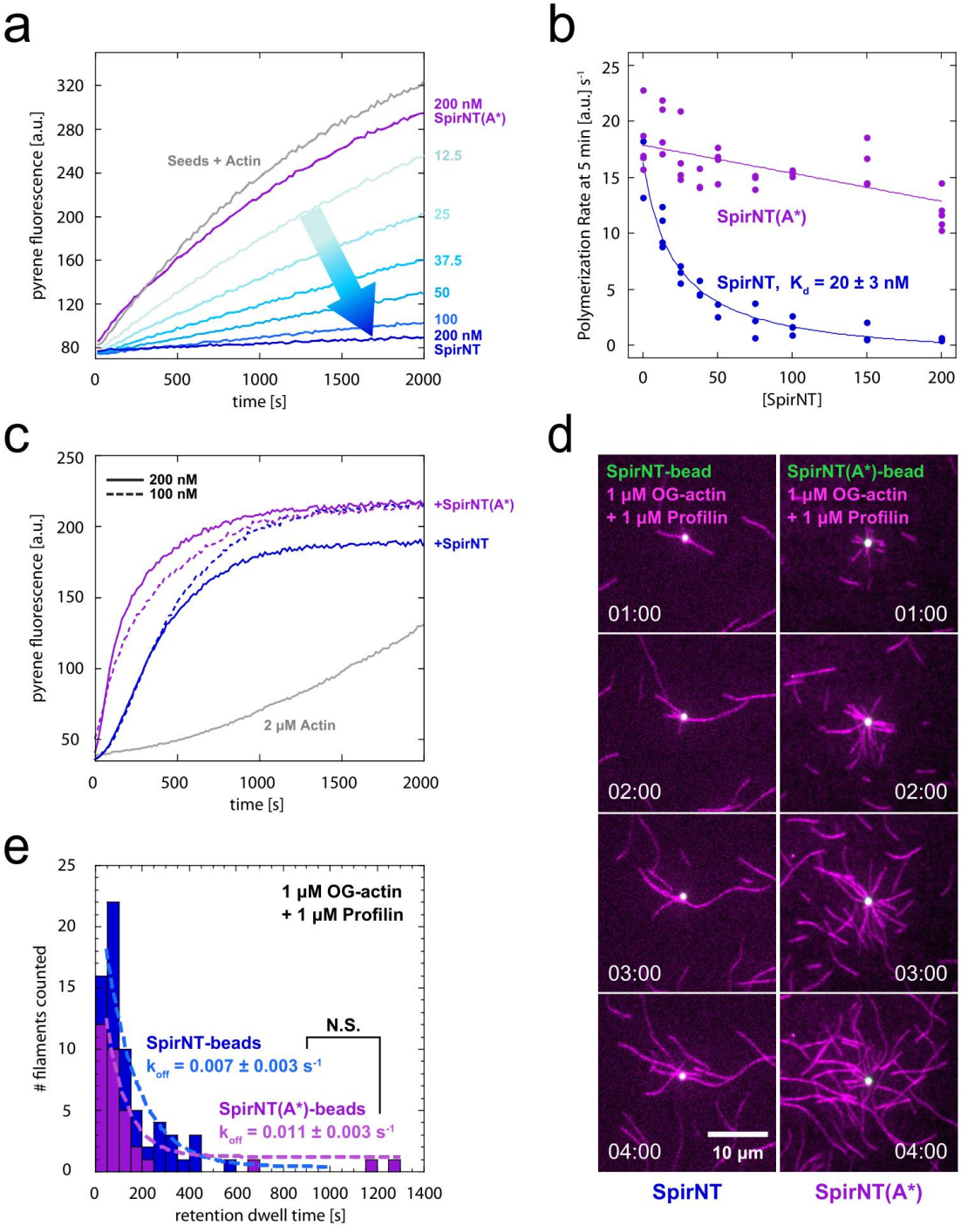
a
pyrene fluorescence [a.u.]
time [s]
Seeds + Actin
200 nM SpirNT(A*)
12.5
25
37.5
50
100
200 nM SpirNT
b
Polymerization Rate at 5 min [a.u.] s-1
[SpirNT]
SpirNT(A*)
SpirNT, Kd = 20 ± 3 nM
c
pyrene fluorescence [a.u.]
time [s]
200 nM
100 nM
+SpirNT(A*)
+SpirNT
2 µM Actin
d
SpirNT-bead
1 µM OG-actin
+ 1 µM Profilin
SpirNT(A*)-bead
1 µM OG-actin
+ 1 µM Profilin
01:00
02:00
03:00
04:00
10 µm
SpirNT
SpirNT(A*)
e
filaments counted
retention dwell time [s]
1 µM OG-actin
+ 1 µM Profilin
N.S.
SpirNT-beads
koff = 0.007 ± 0.003 s-1
SpirNT(A*)-beads
koff = 0.011 ± 0.003 s-1

Figure 2-5 – *Spir's WH2-A binds filament barbed ends and reduces actin nucleation*

(A) Seeded elongation is inhibited by the addition of 12.5 – 200 nM SpirNT (shades of blue). The addition of 200 nM SpirNT(A*) has no effect (purple). *(B)* Dose dependent elongation rates are plotted for three experiments. The data are fit by a quadratic equation, indicating that SpirNT binds the barbed end with a K_d of 20 ± 3 nM. The line is a fit to all data points and the K_d is the average of three independent experiments. Inhibition by SpirNT(A*) is negligible. *(C)* SpirNT(A*) assembles actin more potently than wild type SpirNT in a pyrene-actin assembly assay. Plateaus that are independent of Spire concentration suggest that SpirNT(A*) does not sequester actin like SpirNT (compare solid lines). *(D)* SpirNT(A*)-beads nucleate more potently than wild type. See also, *Video 10. (E)* Quantification of filament pointed end dwell times on beads (k_{off} = 0.011 ± 0.003 s^{-1},n = 33 filaments; 3 independent experiments). The off rate is not statistically different from wild type (data from Fig. 3D).

number of filaments; that is, nucleation. We measured time courses and calculated the rates of increase in OG-actin signal. The difference in rates indicates that nucleation by SpirNT(A*) is ~3x stronger than wild type SpirNT in the presence of profilin (**Fig. 2-6D,E**). We also measured the dwell times of filaments retained by SpirNT(A*)-beads. The off rate is not significantly different than that of wild type ($k_{off(\mathbf{WT})}$ = 0.007 ± 0.003 s^{-1}, $k_{off(\mathbf{A*})}$ = 0.011 ± 0.003 s^{-1}, Student's t-test, p = 0.98, **Fig. 2-5E**), indicating that WH2-A does not play an important role in filament retention. Notably, we rarely observed apparent capture events by SpirNT(A*)-beads. In several cases, filaments appeared to be close enough to a neighboring bead for capture for tens of seconds, but sustained association of the barbed end with beads was rare. Taken together, these data are consistent with the requirement of functional WH2-A for high affinity barbed end binding and demonstrate that this domain is not critical for pointed end binding.

Synergy between Spir and Capu does not require barbed end binding

Previously, synergistic actin assembly by mSpire-1 and Fmn-2 was described: the rate of actin assembly by mSpire-1+Fmn-2 is greater than the sum of assembly rates of the individual nucleators (Montaville et al., 2014). We confirmed that SpirNT and CapuCT exhibit a similar synergistic effect in pyrene-actin assembly assays (**Fig. 2-6A and 2-8D**). In the presence of profilin, the assembly rate of SpirNT+CapuCT (based on the $t_{1/2}$ at ≥ 40 nM SpirNT) was 6x and15x faster than CapuCT or SpirNT, respectively (**Fig. 2-6B**). As seen for the mammalian paralogs, direct interaction is required for synergy: SpirNT(Y232K), a mutant that does not bind Capu, does not synergize with CapuCT (Vizcarra et al., 2011; Montaville et al., 2014) (**Fig. 2-8E**). Likewise, Spir's actin binding activity is required, as demonstrated by the absence of synergy when SpirNT(A*B*C*D*) is added to CapuCT (**Fig. 2-6B and 2-8B**).

Montaville et al. (Montaville et al., 2014) concluded that actin assembly was enhanced by mSpire1 and Fmn-2 alternately binding the barbed end, which they dubbed the "ping-pong"

mechanism. Given that SpirNT(A*) does not bind to or capture barbed ends, we assume that ping-ponging is not possible with this mutant. However, when we tested SpirNT(A*) in the pyrene synergy assay, we found ~3x enhanced synergy (based on the $t_{1/2}$ at ≥ 40 nM SpirNT), as opposed to loss of activity (**Fig. 2-6A,B and S1D**). The dose dependence of synergy is indistinguishable for SpirNT and SpirNT(A*) (**Fig. 2-6B)**. We speculate that dose dependence is a function of Spir-KIND/Capu-tail binding, which should not be affected in SpirNT(A*). These data lead us to propose that nucleation – not just elongation – is enhanced when SpirNT and CapuCT interact.

To test more directly whether nucleation is increased by SpirNT and CapuCT collaborating, we returned to the bead assay. When CapuCT/SpirNT-beads are mixed with actin and profilin, we observe potent nucleation (**Fig. 2-6C**). Consistent with nucleation being a significant element of Spir/Capu synergy, the rate of filament formation is more than 6x greater than nucleation in the absence of Capu (**Figs. 2-6C,D,E**). Nucleation of profilin-actin by CapuCT/SpirNT(A*)-beads was even stronger than wild type (4x) and the synergy more pronounced (9.5x vs SpirNT(A*)-beads in the absence of Capu) with the actin signal saturating at the measured 1.6 μm radius within ~2 minutes (**Fig. 2-6C,D**). Thus, nucleation is potently enhanced when SpirNT and CapuCT are combined and loss of barbed end binding by SpirNT leads to even stronger nucleation in the presence and absence of CapuCT. These data support our conclusion that enhanced nucleation is a major source of synergy.

Barbed end binding is not necessary for oogenesis

Finally, we asked whether barbed-end binding is necessary for *Drosophila* oogenesis. To do so, we tested Spir(A*)-GFP, using the rescue strategy described above. We found that, when driven by nanos-Gal4-vp16, fertility was partially rescued (40%, **Table 2-1**). The fertility rescue is about two thirds as effective for Spir(A*)-GFP when compared to the wild type transgene.

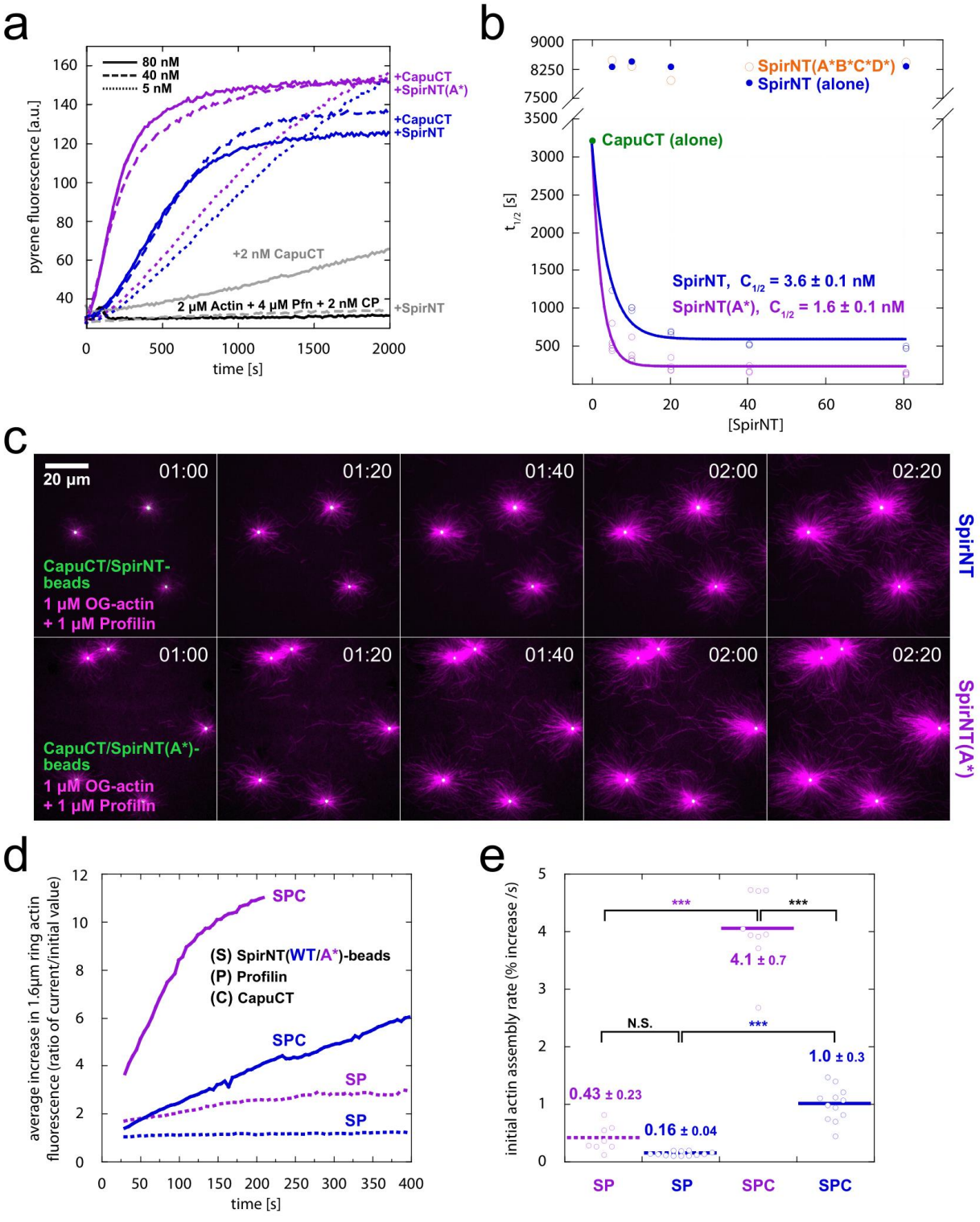
a
80 nM
40 nM
5 nM
+CapuCT
+SpirNT(A*)
+CapuCT
+SpirNT
+2 nM CapuCT
2 µM Actin + 4 µM Pfn + 2 nM CP
+SpirNT
pyrene fluorescence [a.u.]
time [s]
b
SpirNT(A*B*C*D*)
SpirNT (alone)
CapuCT (alone)
SpirNT, C1/2 = 3.6 ± 0.1 nM
SpirNT(A*), C1/2 = 1.6 ± 0.1 nM
t1/2 [s]
[SpirNT]
c
20 µm
01:00
01:20
01:40
02:00
02:20
CapuCT/SpirNT-beads
1 µM OG-actin
+ 1 µM Profilin
SpirNT
CapuCT/SpirNT(A*)-beads
SpirNT(A*)
d
SPC
(S) SpirNT(WT/A*)-beads
(P) Profilin
(C) CapuCT
SPC
SP
SP
average increase in 1.6µm ring actin fluorescence (ratio of current/initial value)
time [s]
e
***
***
4.1 ± 0.7
N.S.
***
1.0 ± 0.3
0.43 ± 0.23
0.16 ± 0.04
initial actin assembly rate (% increase /s)
SP
SP
SPC
SPC

Figure 2-6 – *Synergy between Spir and Capu does not require barbed end binding*

(A) Actin assembly assays in the presence of profilin and capping protein. CapuCT alone and SpirNT alone (solid and dashed gray lines) are weak under these conditions, but synergize in assembly when combined (blue). SpirNT(A*) synergizes more potently with CapuCT (magenta). *(B)* Dose dependence of $t_{1/2}$. Solid circles are SpirNT or CapuCT alone (blue and green, respectively; one representative experiment shown for each). Open circles indicate the addition of both proteins. SpirNT, blue; SpirNT(A*), magenta (n = 3 independent experiments, each); SpirNT(A*B*C*D*), orange (one representative experiment shown at each concentration). Raw data are shown in *Fig. S1B,D*. *(C)* Nucleation is stronger on CapuCT/SpirNT(A*)-beads than CapuCT/SpirNT-beads. *(D)* Quantification of experiments like those shown in *(C)* and Fig. 5D. Fluorescence around beads is expressed as an average percentage of initial values over time (n ≥ 4 beads, n ≥ 2 independent experiments per condition). See methods for description of data transformation. Data plotted were obtained using 1 µm diameter beads, 1 µM actin, and 1 µM profilin, with or without CapuCT (solid or dashed lines, respectively). S, SpirNT-beads; P, profilin; C, CapuCT. SpirNT-bead data are plotted in blue and SpirNT(A*)-bead data, in magenta. (*E*) Rates of fluorescence increase, from (*D*). Mean ± SEM are indicated for each condition. The initial 50 s of images (t = ~30–80 s) were used to determine rates. A Student's t-test was performed on each pair of conditions indicated (black brackets). ***, $p < 0.0001$. The difference in activity by SpirNT(A*/WT)-beads (without Capu) was not statistically significant (unequal variance; $p = 0.13$).

Consistently, the mesh is present and streaming is properly regulated in about half of the oocytes (**Fig. 2-1F,F'**) Thus, barbed-end binding is not necessary for mesh formation or oogenesis, though the fertility decrease suggests that it may contribute under normal conditions.

Table 2-1 – *Fertility experiments*

Transgene ($spir^1/Df(2L)Exel^{6046}$)[a]	% Hatched[b]	Number counted[b]
Spir-GFP[c]	59	606
Spir(A*B*C*D*)-GFP	<2	431
Spir(A*)-GFP	40	619

[a] Genetic background is in parentheses.
[b] % hatched is reported as the average of at least three independent trials. Number counted is the sum of eggs counted from all trials.
[c] (Quinlan 2013)

% hatched is measured 24 hours after egg lay. ~95% w^{1118} hatch; 0% $spir^1/Df(2L)Exel^{6046}$ hatch.

Discussion

Spir binds both ends of actin filaments

The bead assay facilitated observation of several steps in actin assembly by Spir and Capu. We found that filaments nucleated on CapuCT/SpirNT-beads grow with their barbed ends away from the bead with enhanced rates, accelerated by CapuCT. Thus, SpirNT and CapuCT separate after nucleation, consistent with genetics results (Quinlan, 2013). We also found that CapuCT-bound barbed ends would subsequently stop growing if they encountered CapuCT/SpirNT-beads, suggesting that the barbed-end was passed from CapuCT to SpirNT. To our surprise, we found that SpirNT-beads were sufficient to bind both ends of actin filaments. There are conflicting reports regarding filament-end binding for two classes of tandem-WH2 nucleators: Spir and VopF/L (Liverman et al., 2007; Yu et al., 2011; Pernier et al., 2013, 2016; Burke et al., 2017). The N-termini of WH2 domains bind actin monomers between subdomains 1 and 3 of actin – the surface exposed at the barbed ends of filaments (Chereau et al., 2005; Hertzog et al., 2004). It was, therefore, reasonable to expect tandem-WH2 nucleators to associate with filament barbed ends and surprising when both VopL and Spir were reported to bind filament pointed ends (Quinlan et al., 2005; Namgoong et al., 2011; Yu et al., 2011). Spir nucleates filaments with free barbed ends and inhibits depolymerization of gelsolin-capped filaments, albeit weakly (Quinlan et al., 2005). Spir also caps barbed ends of growing filaments but with nanomolar affinity (Bosch et al., 2007; Montaville et al., 2014). Here we present evidence that these apparently conflicting data are both correct. This is not unprecedented. Namgoong et al. (Namgoong et al., 2011) and Burke et al. (Burke et al., 2017) reported that VopL/F can interact with both ends of actin filaments, depending on the conditions.

Earlier, we did not observe barbed-end binding by Spir when assayed by inhibition of depolymerization (Quinlan et al., 2005). We now report high affinity barbed-end binding in inhibition of elongation assays. Possibly, Spir only binds barbed ends in the presence of actin

monomers as was described for N-Wasp (Co et al., 2007). This contrasts with VopL/F that primarily bind barbed ends of preformed filaments in the absence of free monomer (Burke et al., 2017). The first of Spir's tandem WH2 domains, WH2-A, is necessary to cap barbed ends. It is curious that removing function of this WH2 domain increases the activity of SpirNT. In earlier work, we did not observe a significant difference in actin assembly, with or without WH2-A (Quinlan et al., 2005). The original data were acquired with higher concentrations of both SpirNT and actin, which may have masked the difference. In addition, the data were acquired with a slightly longer construct: 1-520 vs 1-490. One possible explanation for enhanced actin nucleation by SpirNT(A*) is that loss of capping leads to fewer so-called SA_4 complexes (Spir bound to four actin monomers). We and others observed SA_4 complexes when Spir is mixed with actin under polymerizing conditions (Quinlan et al., 2005; Bosch et al., 2007). We originally interpreted these structures as pre-nuclei. In contrast, Bosch (Bosch et al., 2007) proposed that they are stable structures that sequester actin monomers. Whether there are two paths (i.e. nucleation vs. SA_4 complex), or one (nucleation, with formation of the nucleus from the SA_4 complex being a rate limiting step), removing capping would likely destabilize the SA_4 structure and could favor nucleation.

How do tandem-WH2-domain nucleators bind filament pointed ends? Single molecule observations showed that VopL/F remains associated with the pointed ends of filaments it nucleates for ~100 s (Burke et al., 2017). In the absence of actin monomers, VopL/F binds pointed ends for shorter times (~25 s). Higher affinity binding is likely due to the contribution of the VopL/F C-terminal domain, that dimerizes and binds the pointed end. In the case of Spir, weak inhibition of depolymerization may be mediated by a linker or a domain straddling the WH2 domains. Side binding by the C-terminal portion of tandem WH2 domains may enhance relatively weak pointed end binding of both Spir and VopL/F. Side binding by Spir is consistent with the fact that it can sever filaments (Bosch et al., 2007; Chen et al., 2012). We speculate

that the ability to retain the pointed ends of filaments nucleated by Spir on beads reflects enhanced binding due to clustering on beads (**Fig. 2-7A**). Multiple cases of emergent behavior of clustered WH2 domains have been reported. Spir nucleates more potently when clustered on gold particles (Ito et al., 2011). VopL retains the pointed end of ~10% of nucleated filaments for several minutes (compared to seconds for ~80% of filaments) and accelerates barbed end elongation of ~8% of filaments when clustered on Qdots (Namgoong et al., 2011); and Ena/VASP are potent elongation factors when clustered on beads (Breitsprecher et al., 2008; Winkelman et al., 2014). In sum, WH2 domains can bind both ends of actin filaments but they are likely to be part of a larger context which dictates their activity (Dominguez, 2016).

How do Spir and Capu synergize?

Synergy of actin assembly can be explained by enhanced nucleation and/or elongation. In the cases of Bud6/Bni1 and APC/mDia1, nucleation is enhanced (Graziano et al., 2011; Breitsprecher et al., 2012). We propose that increased nucleation is also the dominant source of synergy for Spir/Capu. The ping-pong model, initially proposed, suggests that Spir and Capu (Fmn2) enhance elongation by dynamic exchange at the barbed ends of filaments. A key element of the ping-pong model is that Fmn2 binds barbed ends with a slow on-rate. Thus, by recruiting Fmn2 to barbed ends, Spir increases the fraction of time that elongation is enhanced by the formin. We found that synergistic assembly of profilin-actin is actually improved in the absence of Spir binding to barbed ends (CapuCT+SpirNT(A*)). We also directly observed increased nucleation in bead assays: CapuCT/SpirNT-beads nucleate 6x and 10x more potently than SpirNT-beads, with or without a functional WH2-A, respectively (**Figs. 2-5D, 2-6C-E**). A full comparison (i.e. nucleation by SpirNT-beads and CapuCT-beads, versus CapuCT/SpirNT-beads) was precluded by the inactivity of CapuCT-beads, regardless of the coupling method. Finally, we see a 4–fold increase in nucleation by CapuCT/SpirNT(A*)-beads compared to wild type CapuCT/SpirNT-beads, similar to the ~3x decrease in $t_{1/2}$ in bulk assays

(**Fig. 2-6B**). Thus, we conclude that nucleation is the major source of enhanced actin assembly mediated by Spir/Capu synergy.

Ping-ponging may still take place and contribute to mesh assembly. We observe transfer of Capu-bound barbed ends to Spir (**Fig. 2-4B**, **Video 9**), consistent with one half of ping-pong. We do not see transfer in the other direction but our bead-based assay is not well suited to studying this process, as we do not have excess Spir or Capu in solution (The original observation of ping-pong was made with all proteins in solution (Montaville et al., 2014)). Importantly, the intermediate phenotype we observe in flies expressing Spir(A*)-GFP (**Fig. 2-1F and Table 2-1**) could indicate that, while not necessary, ping-ponging may enhance mesh assembly in the oocyte. Perhaps Spir helps Capu fall off of filaments when they reach their target. Additionally, Spir could pass the filament to another protein that anchors it at the vesicle even more stably, influencing the dynamics of the mesh. It is also possible that capping serves an important role in vivo, independent of the processes we are studying here.

The classical nucleation promoting factors (NPFs), N-Wasp and Scar, bind actin monomers and the Arp2/3 complex to stimulate nucleation by the Arp2/3 complex (Machesky et al., 1999; Welch and Mullins, 2002). Similarly, the yeast NPF, Bud6, binds an actin monomer and the formin Bni1 to stimulate nucleation by Bni1 (Park et al., 2015; Graziano et al., 2011; Tu et al., 2012). In each of these cases, the NPF has negligible independent activity. In contrast, APC and Spir can nucleate alone, as well as synergize with a formin (Moseley et al., 2007; Okada et al., 2010; Quinlan et al., 2005; Montaville et al., 2014). We note that Spir's nucleation activity, in the presence of profilin, correlates with synergy: in the absence of nucleation by SpirNT(A*B*C*D*), no synergy is observed; when nucleation is augmented, (SpirNT(A*) nucleation is ~3x stronger than SpirNT), synergy with Capu is also enhanced over wild type (~4x). These are only two data points, but they suggest that Spir's nucleation contributes to

synergy, as opposed to Spir acting as a passive actin binding protein, or NPF. In fact, if monomer delivery were Spir's role, one might expect SpirNT(A*) to be a weaker Capu activator because it has fewer functional WH2 domains. Thus, we conclude that Spir and Capu collaborate by a mechanism similar to that proposed for APC/mDia1 – Spir nucleates seeds that are elongated by Capu (**Fig. 2-7B**).

In vivo implications

The filament orientation we observe, barbed-ends away from the bead, reflects the fact that Spir is attached to the beads and Capu is bound to Spir in our assays. As we and others have shown, when a formin is bound to a bead, filaments grow with their barbed ends at the bead surface. Both mSpire and Fmn-2 are enriched on Rab-11 vesicles. We speculate that Fmn2 is affiliated by binding mSpire as opposed to an independent association with the vesicle. We base this on the finding that mSpire binds directly to membranes and the fact that, in flies, GFP-Capu is diffuse throughout the oocyte (Tittel et al., 2015; Quinlan, 2013). If we are correct, then the geometry in our assays mimics the situation *in vivo* and indicates that the actin filaments are oriented opposite to what was originally proposed by others (Schuh, 2011; Montaville et al., 2014). Long distance transport is still possible with this orientation of filaments (**Fig. 2-7C**). Instead of myosin V capturing filaments from a neighboring vesicle, Spir or another protein could capture a growing filament and myosin V on the vesicle from which the filament originated could walk along the filament pulling the vesicle towards its neighbor (**Fig. 2-7C'**). In this case, pointed end attachment would not have to be as long lasting as barbed end retention. These conditions are surprisingly well satisfied in our simplified system.

Increased Capu expression is sufficient to build a mesh in the absence of Spir or in the absence of direct interaction with Spir (Dahlgaard et al., 2007; Quinlan, 2013). In these cases, the mesh is not as dense or as long lived. No mesh is built when exogenous Spir expression is driven in

the absence of Capu (Dahlgaard et al., 2007). Thus we propose that Spir's primary role is to enhance Capu's actin assembly activity in vivo. The fact that Spir(A*)-GFP expression partially rescues loss of Spir indicates that barbed-end binding by Spir is not necessary. We note, however, that actin nucleation is enhanced, which could compensate for loss of ping-ponging or other barbed end binding roles of Spir. Why do formins need NPFs? In addition to adding another level of control in the cell, nucleation by many formins is dampened by profilin. In the case of the fly oocyte, we also note that the cytoplasm is enriched with microtubules which potently inhibit Capu by binding to its tail, where the Spir-KIND domain also binds (Roth-Johnson et al., 2014). Thus Spir is well suited to simultaneously protect Capu from inhibitory factors and amplify its activity.

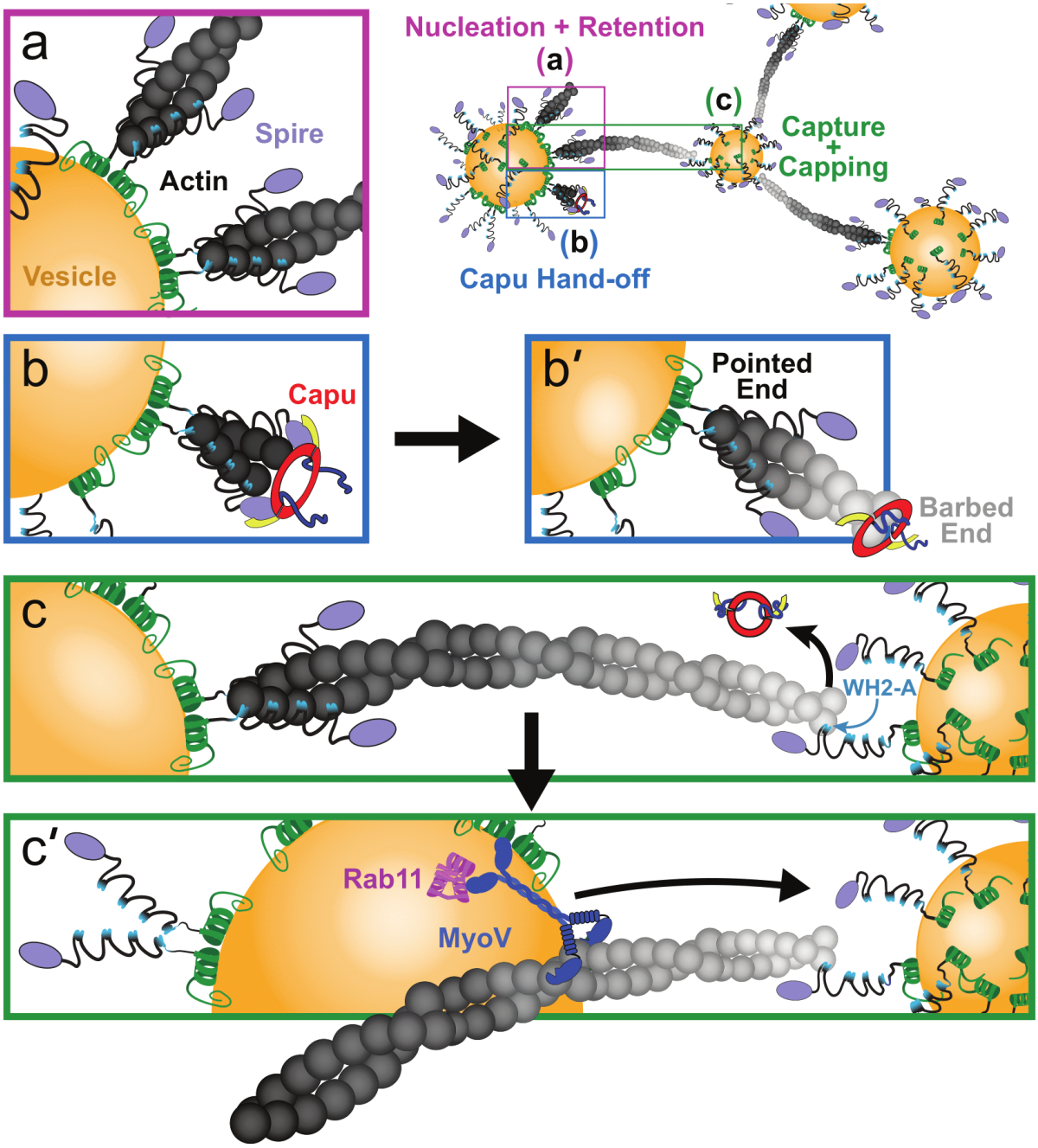

Figure 2-7 – *Model of Spir—Capu synergy*

(A) Spir is directed to vesicles through its phospholipid-binding mFYVE domain (green helix). The clustering of Spir on vesicles may enhance its affinity for filament pointed-ends. Each of Spir's tandem, WH2 domains (light blue) can bind to an actin subunit (dark gray spheres). *(B)* Spir and Capu interact through their respective KIND (purple) and tail (yellow) domains. *(B')* Spir retains a filament's pointed end (dark gray), while Capu separates from Spir to elongate its barbed end (light gray). *(C)* A filament's barbed end is captured and capped by Spir's WH2-A domain (light blue), displacing Capu. Spir's bipolar filament binding may tether vesicles, as shown. *(C')* Associated with Rab11 (pink) and Spir on vesicles, MyoV (dark blue) may tow a nucleating vesicle (left) toward another, receiving (filament capturing) vesicle (right).

Materials and Methods

DNA constructs

CapuCT (aa 467-1059) constructs were expressed from a modified pET15b vector with an N-terminal hexahistidine tag (Vizcarra et al., 2011). All other proteins were expressed from a modified pET20b(+) vector with no affinity tag. A native poly-histidine region within the Spir-KIND domain is sufficient for binding of these constructs to TALON® resin (Clontech). Gibson cloning was employed for the scar-free introduction of Avidity's 45 bp Avitag™ (translated sequence: GLNDIFEAQKIEWHE) to all proteins requiring biotinylation for bead-conjugation. This tag was introduced to the C-terminus of all constructs.

Expression, purification, and biotinylation of proteins

Actin was purified from *Acanthamoeba castellani* as described (Zuchero, 2007) and stored in G-buffer (2 mM Tris-Cl, pH 8.0, 0.1 mM $CaCl_2$, 0.2 mM ATP, 0.5 mM TCEP, 0.04% sodium azide). Expression was induced in Rosetta™(DE3) cells (EMD Biosciences). Bacteria were grown in Terrific Broth medium supplemented with 100 mg⁄L ampicillin and 32 mg⁄L chloramphenicol. Cells were grown to an OD of 0.6 at 37°C, cooled to 18°C for 1 hour, induced with 250 µM IPTG, and shaken for 18 hours at 18°C. Bacteria were harvested by centrifugation. Pellets were washed once with ice-cold PBS, flash-frozen in liquid nitrogen, and stored at −80°C.

All purification steps were carried out at 4°C or on ice. Thawed cells were diluted at least two-fold with lysis buffer (50 mM sodium phosphate pH 8.0, 1 mM β-ME, 300 mM NaCl) supplemented with 1 mM phenylmethylsulfonyl fluoride (PMSF) and 2 µg⁄mL DNaseI and then lysed by microfluidizing, 2-3x. Cell debris was removed by centrifugation at 20,000×g for 20min at 4°C. Clarified lysates were then rocked with TALON® resin for 1 hour at 4°C (4 mL slurry for every 1 L culture pellet). The TALON® resin was washed with 20 column volumes of lysis buffer, followed by washing with 20 column volumes of wash buffer (lysis buffer, at pH 7.0).

Proteins were eluted with elution buffer (wash buffer, plus 200 mM imidazole), until little or no protein remained on the column, as determined by a Coomassie-stained dot-blot of the eluates.

TALON® eluates were pooled and dialyzed 2 x 2 hours and once overnight against 1 L volumes of 10 mM Tris, 1 mM DTT, pH 8.0; or, 5 mL of the most concentrated eluates were buffer exchanged into the same, using a PD-10 desalting column (GE Life Sciences). Protein was loaded onto a MonoQ anion exchange column (GE Life Sciences) and eluted using a gradient of 50–500 mM KCl over 60 column volumes for Spir-KIND, 50–250 mM KCl over 100 column volumes for CapuCT, or 0–500 mM KCl over 60 column volumes for SpirNT. Pooled fractions from the MonoQ column were again dialyzed or buffer exchanged as described above. Unless tagged with an Avitag™, 50% glycerol was added to the overnight dialysis step (1:1 glycerol:buffer). The protein was flash-frozen in liquid nitrogen in 10-50 µL aliquots and stored at -80°C.

If tagged with an Avitag™, 2 mL of the protein was added to 223 µL Biomix B and 5 µL (5 µg) BirA (both from Avidity) and rocked overnight at 4°C. The reaction was again loaded onto a MonoQ anion exchange column and eluted as described above. Pooled fractions from the MonoQ column were dialyzed or buffer exchanged as described above, with 50% glycerol added to the overnight dialysis step and flash-frozen in liquid nitrogen.

Spir-KIND, SpirNT, and CapuCT concentrations were calculated based on their absorbances at 280nm (ε_{280} = 17,452 $cm^{-1}M^{-1}$ for KIND, 25,575 $cm^{-1}M^{-1}$ for Spir-NT, and 75,200 $cm^{-1}M^{-1}$ for Capu-CT) (Quinlan et al., 2007).

Purified VopL and mDia1-CT proteins were generously provided by the Kovar lab (U Chicago).

Pyrene actin assembly assays

Bulk actin assembly assays were carried out essentially as described (Zuchero, 2007). Briefly, actin (5% pyrene labeled) was incubated for 2 min at 25°C with 200 µM EGTA and 50 µM $MgCl_2$ to convert Ca-actin to Mg-actin. When included in the experiment, *Schizosaccharomyces pombe* profilin (typically 2:1 profilin:actin) was incubated with actin for 2 min at 25°C before conversion to Mg-actin. Polymerization was initiated by adding polymerization buffer (KMEH, final concentration: 10 mM HEPES, pH 7.0, 1 mM EGTA, 50 mM KCl, 1 mM $MgCl_2$) to the Mg-actin. Additional components, such as CapuCT, SpirNT, and capping protein were combined in the polymerization buffer before addition to Mg-actin. Fluorescence was monitored in a TECAN F200 with λ_{ex} = 360 ± 17 nm and λ_{em} = 400 ± 10 nm.

Actin seeds were prepared by polymerizing 5 µM actin at 25°C for 1 hour in KMEH. The filaments were dispensed in 5 µL aliquots and allowed to re-equilibrate for 2–3 hours at 25°C. SpirNT was incubated with filaments for 3 min at 25°C. During this incubation time, monomeric actin was converted to Mg-actin. Using a cut pipette tip to prevent shearing, polymerization buffer was added to Mg-actin and then mixed with seeds plus SpirNT. The slope of the pyrene fluorescence trace between 200 and 500 s was considered the elongation rate.

TIRF microscopy assays

Coverslips were prepared and functionalized with polyethylene glycol (final surface composition, 97% methoxy-PEG and 3% biotin-PEG; JenKem Technology, Allen, TX) as previously described (Bor et al., 2012). Biotinylated coverslips were stored in a sealed container at 4°C for up to 2 months before use. Flow cells with volumes of ~10–15 µl were assembled using thin strips of double-stick tape. Streptavidin-coated microspheres were either colorless or Flash Red fluorescent, with mean diameters of ~100 nm or ~1 µm (Bangs Laboratories), respectively. Spheres were washed 2x with ~20 volumes of KMEH, resuspended in 1 volume of KMEH + 1

mg/mL BSA, and added in 10 µL aliquots to 40 µL pre-mixed protein mixtures in KMEH. After a 10 min incubation on ice, spheres were spun for 10 min at 10,000x RPM and 4°C. Pellets were gently resuspended in 30 µL KMEH. Pellets were briefly sonicated (~5 s) if clumped and not well dispersed when visualized by TIRF microscopy.

All buffers were flowed into cells in 25 µL volumes in the following order: 1) blocking buffer (1x PBS, pH 8.0, 1% pluronic, 0.1 mg/mL casein) with 2 min incubation; 2) TIRF buffer (50 mM KCl, 1 mM $MgCl_2$, 1 mM EGTA, 10 mM HEPES, pH 7.0, 0.2 mM ATP, 50 mM DTT, 0.2% methylcellulose, 20 mM glucose); 3) beads (5 µL resuspended beads, 25 µL TIRF buffer) with 2 min incubation; 4) TIRF buffer; 5) TIRF buffer, supplemented with GCC mix (0.25 mg/mL glucose oxidase, 0.05 mg/mL catalase, 0.8 mg/mL casein), actin (typically 1 µM, 20% Oregon Green labeled), and profilin and/or capping protein, when appropriate. In this final step, actin and profilin (when present) were mixed and incubated for 1 min, then added to the other buffer components immediately before being flowed into the cell.

Time zero was defined as the moment the final 25 uL mix, including actin, was entirely added. Polymerization was visualized immediately (typically, t = ~30 s) on a DMI6000B TIRF microscope (Leica, Wetzlar, Germany), controlled by LAS X (Leica software). Images were acquired with a DU897 EMCCD camera (Andor) and 100x/1.47 HCX PL APO objective (Leica) at ~25°C. All analyses were performed on raw data in FIJI. The brightness and contrast of figure images were minimally adjusted for clarity of image features. Filament lengths, elongation rates, and kymographs were analyzed/prepared with JFilament incorporated in FIJI (Smith et al., 2010). Plots were made and statistical analyses conducted in Kaleidagraph. Filament dwell times were obtained by manually tracking individual, retained filaments until clearly released from a bead. Some filaments did not become clearly visible in the TIRF plane until some growth had already occurred. In these cases, time was added to the measured retention period,

proportional to the initial length of the filament and the average filament elongation rate observed in the experiment.

For 2-color experiments, 1 μM Cy3B-labeled actin was introduced to the functionalized, bead-bound flow cell. Following this (step 5 of the aforementioned protocol), and after allowing beads to briefly (1–2 mins) polymerize the Cy3B-actin, the following components were flowed in: 6) TIRF buffer supplemented with 1 μM phalloidin, with 2 min incubation; 7) TIRF buffer supplemented with GCC mix, 600 nM 20% labeled OG-actin, and 300 nM profilin. Polymerization was visualized as described above.

For the plots generated in Fig. 6D/E, circles of 10 and 11 px radii (1.6 and 1.76 μm, respectively) were drawn around the centroids of each bead. Actin fluorescence was measured within these circles over time. The integrated density measurements of the 10 px circles were subtracted from those of their concentric, 11 px circles, to measure 1 px-wide (160 nm) bands of actin fluorescence, 1.6 μm away from beads. A script that performs these operations in FIJI is available upon request.

Fluorescence measurements in Fig. 6D/E are expressed as a fraction of their initial values (i.e. a 10% increase = 1.1). Discrepancies in initial fluorescence values for different bead types were observed, in part, due to real differences in assembly rates, because actin polymerization could not be observed instantly. To scale these differences in assembly prior to image collection, the average starting values of each bead type were compared. The larger ratio of these two values was used as a multiplier for the more active bead type. For example, if measurements of SpirNT(A*)- and SpirNT-beads were 110% their initial values, these quantities would each be plotted as “1.1.” However, if the average, initial values of SpirNT(A*)-beads were twice those of

SpirNT-beads, the quantities would be plotted as “2.2” and “1.1,” respectively, reflecting the 2-fold greater assembly by SpirNT(A*)-beads prior to image collection.

Drosophila stocks

The following stocks were obtained from the Bloomington Drosophila Stock Center (NIH P40OD018537): *spir*^{1} and *capu*^{1} (Manseau and Schüpbach, 1989); Df(2L)Exel^{6046} (Exelixis); and nos-GAL4-vp16 (Van Doren et al., 1998). Mutant SpirB-GFP transgenes were generated by inserting the coding region of spir (CG10076-RB) with point mutations created by QuikChange mutagenesis, between the KpnI and SpeI sites of pTIGER (Ferguson et al., 2012) with mEGFP inserted between the BamHI and XbaI sites. pTIGER plasmids were integrated at the attP2 landing site by BestGene.

Fertility assays

Approximately 100 test females were crossed to 40 wild-type males and kept on apple plates for 2 nights at 25°C. Flies were pre-cleared on a fresh plate with yeast paste for at least 1.5 hours, the plate was changed and eggs laid over the next 3 hours were collected. Typically, 100 eggs were laid in this time period. Eggs were transferred to a fresh plate and stored at 25°C. The number of eggs that hatched after 24 hours was recorded. Each trial was repeated at least three times with independent crosses.

Fly oocyte microscopy and staining

The visualization of cytoplasmic flows and the actin mesh were performed on a Leica SPE I inverted confocal microscope. Flies were kept at 25°C and fed yeast paste for ~24 hours before an experiment. Flows were visualized by imaging autofluorescent yolk granules of egg chambers teased apart in Halocarbon oil 700. The actin mesh was stained as described by Dahlgaard et al. (Dahlgaard et al., 2007) with modifications. Briefly, ovaries were dissected,

teased apart and fixed in 10% paraformaldehyde/PBS (pH 7.4) for a total of less than 20 minutes. Samples were stained with 1 µM AlexaFluor488-phalloidin diluted in 0.3% Triton X-100/PBS for 25 minutes at room temperature. Samples were then washed extensively and mounted in ProLong Gold with DAPI. Images were recorded within 24 hours of staining because phalloidin staining quality degraded over time, as has been reported (Dahlgaard et al., 2007).

References

Ahmed, W.W., É. Fodor, M. Almonacid, M. Bussonnier, M.-H. Verlhac, N. Gov, P. Visco, F. van Wijland, and T. Betz. 2018. Active Mechanics Reveal Molecular-Scale Force Kinetics in Living Oocytes. *Biophys. J.* 114:1667–1679. doi:10.1016/j.bpj.2018.02.009.

Almonacid, M., W.W. Ahmed, M. Bussonnier, P. Mailly, T. Betz, R. Voituriez, N.S. Gov, and M.H. Verlhac. 2015. Active diffusion positions the nucleus in mouse oocytes. *Nat Cell Biol*. 17:470–479. doi:10.1038/ncb3131.

Azoury, J., K.W. Lee, V. Georget, P. Rassinier, B. Leader, and M.-H. Verlhac. 2008. Spindle Positioning in Mouse Oocytes Relies on a Dynamic Meshwork of Actin Filaments. *Current Biology*. 18:1514–1519. doi:10.1016/j.cub.2008.08.044.

Bor, B., C.L. Vizcarra, M.L. Phillips, and M.E. Quinlan. 2012. Autoinhibition of the formin Cappuccino in the absence of canonical autoinhibitory domains. *Mol. Biol. Cell*. 23:3801–3813. doi:10.1091/mbc.E12-04-0288.

Bosch, M., K.H.D. Le, B. Bugyi, J.J. Correia, L. Renault, and M.-F. Carlier. 2007. Analysis of the Function of Spire in Actin Assembly and Its Synergy with Formin and Profilin. *Molecular Cell*. 28:555–568. doi:10.1016/j.molcel.2007.09.018.

Breitsprecher, D., R. Jaiswal, J.P. Bombardier, C.J. Gould, J. Gelles, and B.L. Goode. 2012. Rocket Launcher Mechanism of Collaborative Actin Assembly Defined by SingleMolecule Imaging. *Science*. 336:1164–1168. doi:10.1126/science.1218062.

Breitsprecher, D., A.K. Kiesewetter, J. Linkner, C. Urbanke, G.P. Resch, J.V. Small, and J. Faix. 2008. Clustering of VASP actively drives processive, WH2 domain-mediated actin filament elongation. *EMBO J.* 27:2943–2954. doi:10.1038/emboj.2008.211.

Burke, T.A., A.J. Harker, R. Dominguez, and D.R. Kovar. 2017. The bacterial virulence factors VopL and VopF nucleate actin from the pointed end. *J Cell Biol*. 216:1267–1276. doi:10.1083/jcb.201608104.

Chen, C.K., M.R. Sawaya, M.L. Phillips, E. Reisler, and M.E. Quinlan. 2012. Multiple forms of Spire-actin complexes and their functional consequences. *J. Biol. Chem.* 287:10684–10692. doi:10.1074/jbc.M111.317792.

Chereau, D., F. Kerff, P. Graceffa, Z. Grabarek, K. Langsetmo, and R. Dominguez. 2005. Actinbound structures of Wiskott–Aldrich syndrome protein (WASP)-homology domain 2 and the implications for filament assembly. *PNAS*. 102:16644–16649. doi:10.1073/pnas.0507021102.

Co, C., D.T. Wong, S. Gierke, V. Chang, and J. Taunton. 2007. Mechanism of Actin Network Attachment to Moving Membranes: Barbed End Capture by N-WASP WH2 Domains. *Cell*. 128:901–913. doi:10.1016/j.cell.2006.12.049.

Dahlgaard, K., A.A. Raposo, T. Niccoli, and D. St Johnston. 2007. Capu and Spire assemble a cytoplasmic actin mesh that maintains microtubule organization in the Drosophila oocyte. *Dev Cell*. 13:539–53. doi:10.1016/j.devcel.2007.09.003.

Dominguez, R. 2016. The WH2 Domain and Actin Nucleation: Necessary but Insufficient. *Trends in Biochemical Sciences*. 41:478–490. doi:10.1016/j.tibs.2016.03.004.

Graziano, B.R., A.G. DuPage, A. Michelot, D. Breitsprecher, J.B. Moseley, I. Sagot, L. Blanchoin, and B.L. Goode. 2011. Mechanism and cellular function of Bud6 as an actin nucleation–promoting factor. *MBoC*. 22:4016–4028. doi:10.1091/mbc.e11-05-0404.

Hertzog, M., C. van Heijenoort, D. Didry, M. Gaudier, J. Coutant, B. Gigant, G. Didelot, T. Préat, M. Knossow, E. Guittet, and M.-F. Carlier. 2004. The β-Thymosin/WH2 Domain: Structural Basis for the Switch from Inhibition to Promotion of Actin Assembly. *Cell*. 117:611–623. doi:10.1016/S0092-8674(04)00403-9.

Holubcová, Z., G. Howard, and M. Schuh. 2013. Vesicles modulate an actin network for asymmetric spindle positioning. *Nat Cell Biol*. 15:937–947. doi:10.1038/ncb2802.

Ito, T., A. Narita, T. Hirayama, M. Taki, S. Iyoshi, Y. Yamamoto, Y. Maéda, and T. Oda. 2011. Human Spire Interacts with the Barbed End of the Actin Filament. *Journal of Molecular Biology*. 408:18–25. doi:10.1016/j.jmb.2010.12.045.

Kelly, A.E., H. Kranitz, V. Dotsch, and R.D. Mullins. 2006. Actin binding to the central domain of WASP/Scar proteins plays a critical role in the activation of the Arp2/3 complex. *J Biol Chem*. 281:10589–97. doi:10.1074/jbc.M507470200.

Kovar, D.R., and T.D. Pollard. 2004. Insertional assembly of actin filament barbed ends in association with formins produces piconewton forces. *Proc Natl Acad Sci U S A*. 101:14725–30.

Leader, B., H. Lim, M.J. Carabatsos, A. Harrington, J. Ecsedy, D. Pellman, R. Maas, and P. Leder. 2002. Formin-2, polyploidy, hypofertility and positioning of the meiotic spindle in mouse oocytes. *Nat Cell Biol*. 4:921–8. doi:10.1038/ncb880.

Liverman, A.D., H.C. Cheng, J.E. Trosky, D.W. Leung, M.L. Yarbrough, D.L. Burdette, M.K. Rosen, and K. Orth. 2007. Arp2/3-independent assembly of actin by Vibrio type III effector VopL. *Proc Natl Acad Sci U S A*. 104:17117–22. doi:10.1073/pnas.0703196104.

Machesky, L.M., R.D. Mullins, H.N. Higgs, D.A. Kaiser, L. Blanchoin, R.C. May, M.E. Hall, and T.D. Pollard. 1999. Scar, a WASp-related protein, activates nucleation of actin filaments by the Arp2/3 complex. *Proc Natl Acad Sci U S A*. 96:3739–44.

Manseau, L.J., and T. Schupbach. 1989. cappuccino and spire: two unique maternal-effect loci required for both the anteroposterior and dorsoventral patterns of the Drosophila embryo. *Genes Dev*. 3:1437–52.

Montaville, P., A. Jégou, J. Pernier, C. Compper, B. Guichard, B. Mogessie, M. Schuh, G. Romet-Lemonne, and M.-F. Carlier. 2014. Spire and Formin 2 Synergize and Antagonize in Regulating Actin Assembly in Meiosis by a Ping-Pong Mechanism. *PLOS Biology*. 12:e1001795. doi:10.1371/journal.pbio.1001795.

Moseley, J.B., F. Bartolini, K. Okada, Y. Wen, G.G. Gundersen, and B.L. Goode. 2007. Regulated Binding of Adenomatous Polyposis Coli Protein to Actin. *J. Biol. Chem.*

282:12661–12668. doi:10.1074/jbc.M610615200.

Namgoong, S., M. Boczkowska, M.J. Glista, J.D. Winkelman, G. Rebowski, D.R. Kovar, and R. Dominguez. 2011. Mechanism of actin filament nucleation by Vibrio VopL and implications for tandem W domain nucleation. *Nat Struct Mol Biol*. 18:1060–7. doi:10.1038/nsmb.2109.

Okada, K., F. Bartolini, A.M. Deaconescu, J.B. Moseley, Z. Dogic, N. Grigorieff, G.G. Gundersen, and B.L. Goode. 2010. Adenomatous polyposis coli protein nucleates actin assembly and synergizes with the formin mDia1. *J Cell Biol*. 189:1087–96. doi:10.1083/jcb.201001016.

Park, E., B.R. Graziano, W. Zheng, M. Garabedian, B.L. Goode, and M.J. Eck. 2015. Structure of a Bud6/Actin Complex Reveals a Novel WH2-like Actin Monomer Recruitment Motif. *Structure*. 23:1492–1499. doi:10.1016/j.str.2015.05.015.

Pechlivanis, M., A. Samol, and E. Kerkhoff. 2009. Identification of a short Spir interaction sequence at the C-terminal end of formin subgroup proteins. *J Biol Chem*. 284:25324–33. doi:10.1074/jbc.M109.030320.

Pernier, J., J. Orban, B.S. Avvaru, A. Jégou, G. Romet-Lemonne, B. Guichard, and M.-F. Carlier. 2013. Dimeric WH2 domains in Vibrio VopF promote actin filament barbed-end uncapping and assisted elongation. *Nat Struct Mol Biol*. 20:1069–1076. doi:10.1038/nsmb.2639.

Pernier, J., S. Shekhar, A. Jegou, B. Guichard, and M.-F. Carlier. 2016. Profilin Interaction with Actin Filament Barbed End Controls Dynamic Instability, Capping, Branching, and Motility. *Developmental Cell*. 36:201–214. doi:10.1016/j.devcel.2015.12.024.

Pfender, S., V. Kuznetsov, S. Pleiser, E. Kerkhoff, and M. Schuh. 2011. Spire-Type Actin Nucleators Cooperate with Formin-2 to Drive Asymmetric Oocyte Division. *Current Biology*. 21:955–960. doi:10.1016/j.cub.2011.04.029.

Quinlan, M.E. 2013. Direct interaction between two actin nucleators is required in *Drosophila* oogenesis. *Development*. 140:4417–4425. doi:10.1242/dev.097337.

Quinlan, M.E., J.E. Heuser, E. Kerkhoff, and R.D. Mullins. 2005. Drosophila Spire is an actin nucleation factor. *Nature*. 433:382–8.

Quinlan, M.E., S. Hilgert, A. Bedrossian, R.D. Mullins, and E. Kerkhoff. 2007. Regulatory interactions between two actin nucleators, Spire and Cappuccino. *J Cell Biol*. 179:117–28. doi:10.1083/jcb.200706196.

Rasson, A.S., J.S. Bois, D.S.L. Pham, H. Yoo, and M.E. Quinlan. 2015. Filament assembly by Spire: key residues and concerted actin binding. *J. Mol. Biol.* 427:824–839. doi:10.1016/j.jmb.2014.09.002.

Roth-Johnson, E.A., C.L. Vizcarra, J.S. Bois, and M.E. Quinlan. 2014. Interaction between microtubules and the Drosophila formin Cappuccino and its effect on actin assembly. *J. Biol. Chem.* 289:4395–4404. doi:10.1074/jbc.M113.499921.

Schuh, M. 2011. An actin-dependent mechanism for long-range vesicle transport. *Nature Cell Biology*. 13:ncb2353. doi:10.1038/ncb2353.

Schuh, M., and J. Ellenberg. 2008. A New Model for Asymmetric Spindle Positioning in Mouse Oocytes. *Current Biology*. 18:1986–1992. doi:10.1016/j.cub.2008.11.022.

Tittel, J., T. Welz, A. Czogalla, S. Dietrich, A. Samol-Wolf, M. Schulte, P. Schwille, T. Weidemann, and E. Kerkhoff. 2015. Membrane Targeting of the Spir·Formin Actin Nucleator Complex Requires a Sequential Handshake of Polar Interactions. *J. Biol. Chem.* 290:6428–6444. doi:10.1074/jbc.M114.602672.

Tu, D., B.R. Graziano, E. Park, W. Zheng, Y. Li, B.L. Goode, and M.J. Eck. 2012. Structure of the formin-interaction domain of the actin nucleation-promoting factor Bud6. *Proc. Natl. Acad. Sci. U.S.A.* 109:E3424-3433. doi:10.1073/pnas.1203035109.

Vizcarra, C.L., B. Kreutz, A.A. Rodal, A.V. Toms, J. Lu, W. Zheng, M.E. Quinlan, and M.J. Eck. 2011. Structure and function of the interacting domains of Spire and Fmn-family formins. *PNAS*. 108:11884–11889. doi:10.1073/pnas.1105703108.

Welch, M.D., and R.D. Mullins. 2002. Cellular Control of Actin Nucleation. *Annual Review of Cell and Developmental Biology*. 18:247–288. doi:10.1146/annurev.cellbio.18.040202.112133.

Winkelman, J.D., C.G. Bilancia, M. Peifer, and D.R. Kovar. 2014. Ena/VASP Enabled is a highly processive actin polymerase tailored to self-assemble parallel-bundled F-actin networks with Fascin. *PNAS*. 111:4121–4126. doi:10.1073/pnas.1322093111.

Yu, B., H.C. Cheng, C.A. Brautigam, D.R. Tomchick, and M.K. Rosen. 2011. Mechanism of actin filament nucleation by the bacterial effector VopL. *Nat Struct Mol Biol*. 18:1068–74. doi:10.1038/nsmb.2110.

Zeth, K., M. Pechlivanis, A. Samol, S. Pleiser, C. Vonrhein, and E. Kerkhoff. 2011. Molecular basis of actin nucleation factor cooperativity: crystal structure of the Spir-1 kinase noncatalytic C-lobe domain (KIND)•formin-2 formin SPIR interaction motif (FSI) complex. *J. Biol. Chem.* 286:30732–30739. doi:10.1074/jbc.M111.257782.

Zuchero, J.B. 2007. In vitro actin assembly assays and purification from Acanthamoeba. *Methods Mol. Biol.* 370:213–226. doi:10.1007/978-1-59745-353-0_15.

Appendix

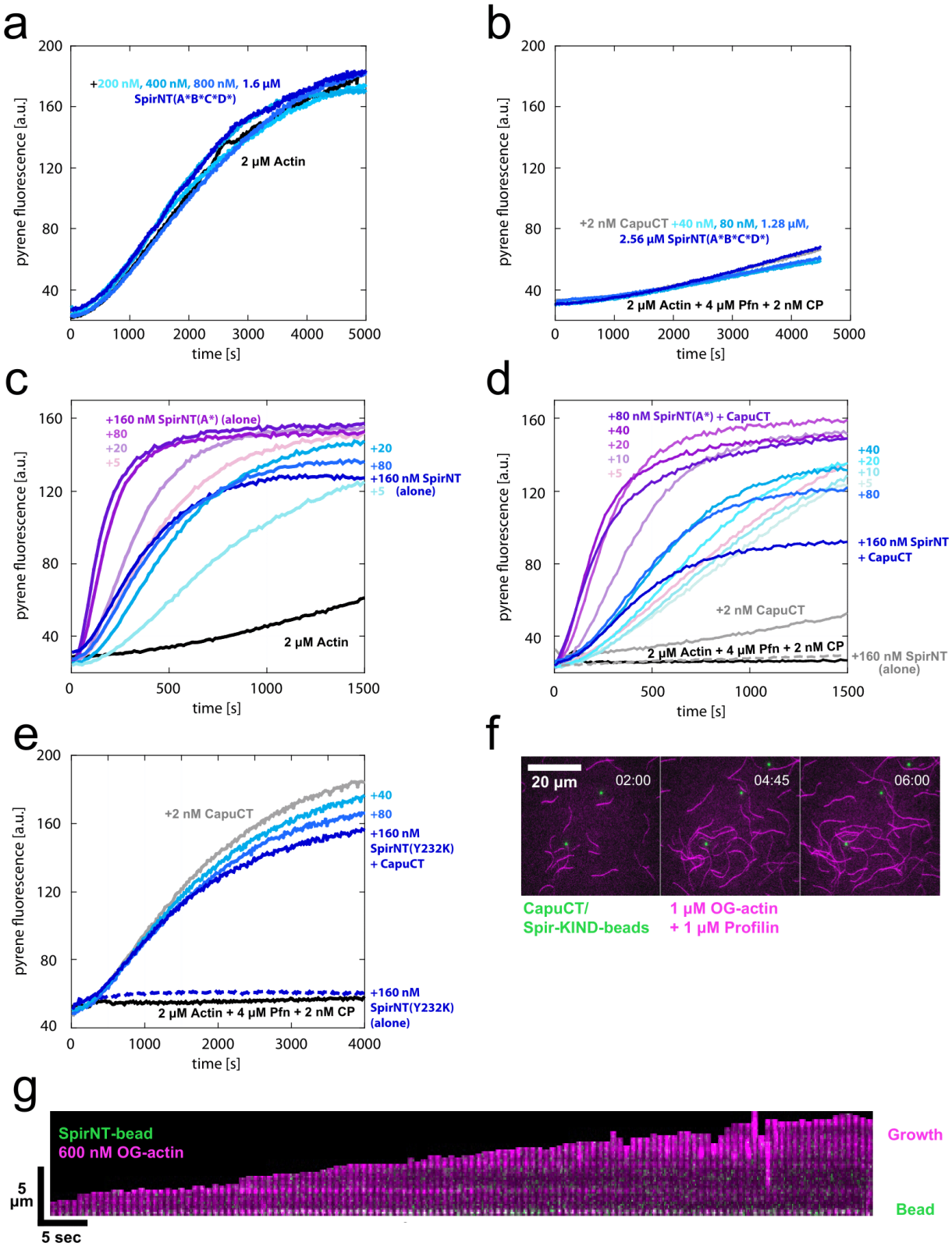
a
pyrene fluorescence [a.u.]
time [s]
+200 nM, 400 nM, 800 nM, 1.6 µM SpirNT(A*B*C*D*)
2 µM Actin
b
pyrene fluorescence [a.u.]
time [s]
+2 nM CapuCT +40 nM, 80 nM, 1.28 µM, 2.56 µM SpirNT(A*B*C*D*)
2 µM Actin + 4 µM Pfn + 2 nM CP
c
pyrene fluorescence [a.u.]
time [s]
+160 nM SpirNT(A*) (alone)
+80
+20
+5
+20
+80
+160 nM SpirNT (alone)
+5
2 µM Actin
d
pyrene fluorescence [a.u.]
time [s]
+80 nM SpirNT(A*) + CapuCT
+40
+20
+10
+5
+40
+20
+10
+5
+80
+160 nM SpirNT + CapuCT
+2 nM CapuCT
2 µM Actin + 4 µM Pfn + 2 nM CP
+160 nM SpirNT (alone)
e
pyrene fluorescence [a.u.]
time [s]
+2 nM CapuCT
+40
+80
+160 nM SpirNT(Y232K) + CapuCT
+160 nM SpirNT(Y232K) (alone)
2 µM Actin + 4 µM Pfn + 2 nM CP
f
20 µm
02:00
04:45
06:00
CapuCT/ Spir-KIND-beads
1 µM OG-actin + 1 µM Profilin
g
SpirNT-bead
600 nM OG-actin
Growth
Bead
5 µm
5 sec

Figure 2-8 – *Supplementary data*

(A) SpirNT(A*B*C*D*) does not assemble actin. *(B)* SpirNT(A*B*C*D*) does not synergize with CapuCT to assemble actin. *(C)* SpirNT(A*) is a superior actin nucleator and does not sequester actin like wild-type SpirNT. *(D)* SpirNT(A*) demonstrates enhanced synergy/actin assembly with CapuCT and does not sequester actin like wild-type SpirNT. *(E)* A Capu-binding mutant, SpirNT(Y232K), does not synergize with CapuCT to assemble actin. *(F)* Spir-KIND/CapuCT-beads do not assemble actin or bind actin filaments. *(G)* Retention of nucleated filaments by SpirNT-beads is not dependent on the presence of CapuCT or profilin. Fiducial marks (bright, horizontal lines) in the kymograph are not displaced as the filament elongates, indicating growth away from the bead. See also, *Video 7.*

Chapter 3: Unique domain functions in Spire—Cappuccino synergy

Introduction

Nucleation vs. capping: what are they good for?

As noted in Chapter 1, a long-standing point of contention in the cytoskeleton field has been the question of which end of the actin filament Spir binds. Early evidence showed a weak (μM) interaction with pointed ends (**Fig. 1-4**) (Quinlan et al. 2005), while subsequent work with mammalian Spir-1 showed a stronger (nM) interaction with barbed ends (Ito et al. 2011; Montaville et al. 2014). The distinction of which filament end Spir interacts with is crucial, as the models describing synergy with Capu conflict on this detail: Ping-pong occurs at barbed ends, while Hand-off occurs at pointed ends.

The data presented in Chapter 2 satisfyingly show that Spir can bind both ends of the filament, at least when Spir is clustered on a bead. With this geometry, a primary tenet of each model was observed – Spir handing nucleated filaments to Capu, and Spir displacing Capu from growing filaments. However, the core and more difficult-to-test discrepancy between the two models lies in the actual Spir function purportedly driving synergy: nucleation (Hand-off) or capping (Ping-pong) of filaments. Because nucleation by SpirNT-beads was greatly enhanced in the presence of Capu, the data from Chapter 2 make a strong argument for nucleation driving synergy (**Fig. 2-6C-E**).

In Chapter 2, the mutant SpirNT(A*) was also introduced, whose capping function is lost and whose nucleation function is augmented. This mutant demonstrated enhanced nucleation and synergy with Capu on beads, further supporting the role of nucleation by Spir as the driver of synergy (**Fig. 2-6C-E**). However, our understanding is incomplete. In the fly, rescue by Spir(A*)-GFP was less than 70% as efficient as its wild-type counterpart, suggesting that capping may still be important in vivo (**Table 2-1**). Furthermore, forthcoming data from Spir(D*)-GFP experiments in the Quinlan lab suggest that rescue by this mutant is significantly better than

Spir(A*)-GFP (data not shown). Because a non-functional fourth WH2 domain (D*) has been shown to dramatically decrease Spir's nucleation activity (Quinlan et al. 2005), efficient rescue by Spir(D*)-GFP introduces the possibility that Spir nucleation is not essential for synergy in vivo, either.

Discrepancies in Spir activity

At least one WH2 domain is necessary for Spir to assemble actin and synergize with Capu (**Fig. 2-8A,B)**. Although the fly data are not yet fully understood, the WH2-A and WH2-D Spir mutants have proven to be excellent tools for disentangling Spir's nucleation and capping activities. Do mutants of the remaining WH2 domains – B and C – offer further modulation of these activities? In fact, mutations which disrupt actin binding were generated and tested for each of the four WH2 domains when Dr. Quinlan first published on Spir. At this time, SpirNT(A*) demonstrated only a moderate increase in actin assembly, while assembly by SpirNT(B*) and SpirNT(C*) was moderately diminished (**Fig. 3-1**) (Quinlan et al. 2005). When we revisited the SpirNT(A*) mutant and observed a more dramatic increase in assembly (**Fig. 2-5C**), we noted that the difference might be attributed to a truncation of the protein.

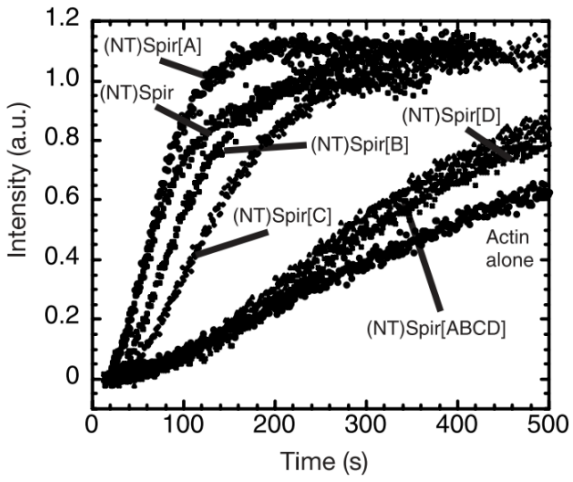

Figure 3-1 – *Nucleation by SpirNT and WH2 mutants*

From Quinlan 2005. Actin-binding mutations within each of Spir's four WH2 domains have different effects on nucleation by SpirNT *(here, (NT)Spir)*

Dr. Quinlan's experiments were performed with SpirNT(1-520), while those presented in Chapter 2 were performed with SpirNT(1-490). Thus, we hypothesized that the 30-amino acid stretch following 490aa was involved in inhibiting actin assembly by Spir and/or synergy with Capu. Notably, recent and intriguing data in the Quinlan lab have also identified these residues to be

necessary for Myosin V (MyoV) binding. If the presence of Spir residues 490-520aa does, in fact, hamper actin assembly, then this domain presents another potential avenue for Spir, Capu, and mesh regulation. Preliminary insights into the role of these amino acids in actin assembly are presented in the results that follow.

Clustering hypothesis

In addition to discrepancies in the pyrene-actin assembly assay, we noted that the surprising association of filament pointed ends with SpirNT-beads (**Chapter 2**) happened reliably and often. Because Spir's affinity for pointed ends was previously demonstrated to be very weak with Spir free in solution (Quinlan et al. 2005), we speculated that clustering on beads and/or dimerization of Spir strengthens its interaction with pointed ends. When we conjugated a dimeric, GST-tagged fusion of SpirNT to beads, no increase in nucleation or filament retention was apparent (data not shown). Because nucleation by GST-SpirNT is markedly increased in the pyrene assay and closely mimics synergistic assembly by SpirNT and CapuCT in the conditions tested (Vizcarra et al. 2011), we hypothesized that the clustering of Spir on beads (or membranes, in vivo) mimics the dimerization of Spir, making it a better nucleator and enhancing Spir's affinity for filament ends – that is, its ability to retain and capture filaments.

Although SpirNT(A*) is unable to cap barbed ends in vitro (Rasson et al. 2015), we noted that SpirNT(A*)-beads were capable of capturing – albeit very rarely – the barbed ends of filaments in TIRF-M. Furthermore, while SpirNT(D*) could not nucleate in pyrene-actin assembly assays (Quinlan et al. 2005), pilot experiments suggested that it was not entirely inactive when conjugated to beads (**Fig. 3-2**). SpirNT(D*)-beads observed were also capable of retaining the few filaments they nucleated. If clustering increases Spir's affinity for either end of the filament, we suspected that tuning the density of Spir on beads would measurably affect these

interaction(s). In this chapter, we present preliminary data testing the clustering hypothesis by examining the effect of diluting SpirNT (wild type, A*, and D*) on beads.

Capu's role in synergy

A significant increase in filament assembly by SpirNT-beads is observed when CapuCT is added (**Fig. 2-6C-E**), similar to the synergistic effect observed in pyrene assays (**Fig. 2-6A,B**). We showed in Chapter 2 that this synergy in actin assembly scales with the nucleation potency of Spir. Next, we asked how Capu might reciprocally be enhancing Spir.

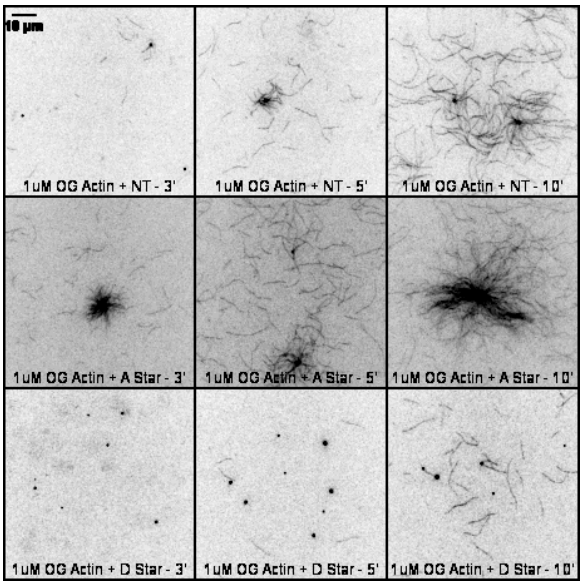

Figure 3-2 – *Nucleation by SpirNT-beads is affected by mutations to WH2 domains*

(*Top Row*) SpirNT-beads nucleate actin. (*Middle Row*) SpirNT(A*)-beads have enhanced nucleation. (*Bottom Row*) SpirNT(D*)-beads have diminished nucleation. Images for each row were acquired at 1' (*Left Column*), 5' (*Center Column*) and 10' (*Right Column*) following the introduction of G-actin. Scale bar = 10 µm

An existing asset of the Quinlan lab, the CapuCT(I706A) mutant bears a canonical, "formin-killing" FH2 domain mutation (Xu et al. 2004). This mutation was previously verified to abolish nucleation by CapuCT while still enhancing SpirNT's activity in vitro, presumably by increasing the rate of SpirNT nucleation via dimerization (Quinlan et al. 2007). However, this enhancement is not sufficient in vivo, based on the observation that Capu(I706A) fails to rescue the mesh defect in *capu* null flies (Quinlan 2013). These observations are consistent with the hypothesis that dimerization of Spir by Capu increases nucleation but is not as important an activity in vivo due to the already clustered geometry of Spir. Thus, the enhancement of actin assembly by SpirNT-beads seen in the presence of CapuCT(I706A) makes this mutant an attractive tool to further probe the role(s) of Capu in synergy – in addition to nucleation and the dimerization of Spir. We study the activities of the CapuCT(I706A) mutant in greater detail in this chapter.

Results

Residues 490-520 inhibit nucleation by SpirNT

We observed that SpirNT(A*) was much more active than initially reported and hypothesized that this was due to the use of different truncations of Spir. Before testing for similar discrepancies in the remaining WH2 domain mutants, we addressed the question of whether or not the discrepant amino acids (490-520) impact the activity of wild type Spir. Comparing the two truncations in the pyrene assay, we found the presence of this 30-amino acid stretch to be meaningful. Plotting the half time to reach maximal F-actin signal ($t_{1/2}$) at various concentrations of SpirNT, we observed that SpirNT(1-490) is a stronger nucleator than SpirNT(1-520) (**Fig. 3-3**).

Next, we asked if the presence of residues 490-520 also alters the activity of WH2 mutants. Having already observed the surprising increase in assembly by SpirNT(A*) relative to the activity reported in 2005, we interrogated the effect of mutations within the second and third WH2 domains, SpirNT(B*) and SpirNT(C*).

A non-functional WH2-B enhances nucleation by SpirNT(1-490)

We found that a non-functional WH2-B domain improves nucleation by SpirNT(1-490) in a manner similar to SpirNT(A*) (**Fig. 3-4**). At this point, it was unsurprising that the absence of 490-520aa enhanced actin assembly by SpirNT(B*). However, these data curiously contrasted with the slight inhibition of actin assembly, relative to wild type, originally reported for this mutant (**Fig. 3-1**) (Quinlan et al. 2005). We proceeded to confirm that SpirNT(B*,1-490) is not only better than SpirNT(B*,1-520), but that it is also superior to a wild type Spir of the same length in a basic pyrene-actin assay (**Fig. 3-5**).

Under conditions which tested synergy with Capu, we again found that SpirNT(B*,1-490) is superior to its wild type counterpart (**Fig. 3-6**). These results further support the conclusion of Chapter 2, that nucleation by Spir is a major driver of synergy with Capu. However, we had expected SpirNT(B*) to be impaired in nucleation, which would have offered a tool to test whether a reduction in Spir nucleation results in a commensurate decrease in synergy.

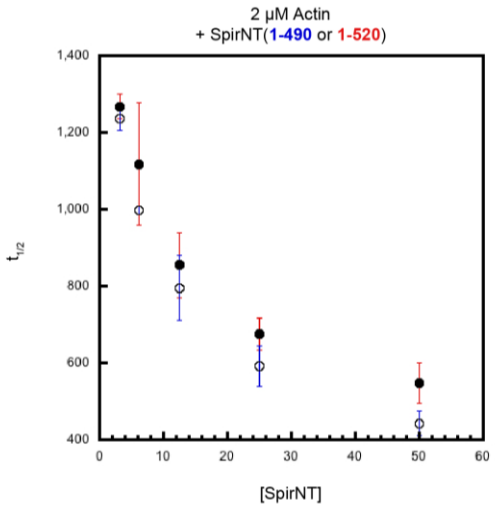

Figure 3-3 – *SpirNT(1-490) is a stronger nucleator than SpirNT(1-520)*

The time to reach the half-maximal polymerization ($t_{1/2}$) of actin by SpirNT(1-490) (*open circles; S.D. shown in blue*) is increased by the presence of 490-520aa (*closed circles; S.D. shown in red*).

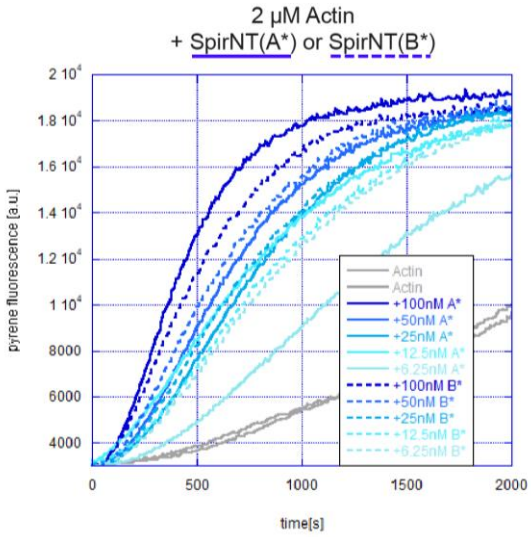

Figure 3-4 – *Nucleation by SpirNT(B*,1-490) is comparable to SpirNT(A*,1-490)*

SpirNT(B*,1-490) (*dashed lines*) assembles actin with a dose dependence (*shades of blue*) comparable to SpirNT(A*, 1-490) (*solid lines*)

A non-functional WH2-C enhances nucleation by SpirNT(1-490)

In search of an intermediate nucleator, we next tested the role of WH2-C in the pyrene assay. We found that nucleation by SpirNT(C*) was also enhanced in the absence of 490-520aa (**Fig. 3-7**). While further characterization of this mutant is needed, preliminary data suggest that SpirNT(C*,1-490) also demonstrates enhanced synergy with CapuCT (data not shown). While these results again supported the conclusion that Spir nucleation drives synergy with Capu, no

WH2 domains remained to mutate in search of an impaired nucleator. Thus, a strategic combination of WH2 mutants will be required, as noted in the discussion that later follows.

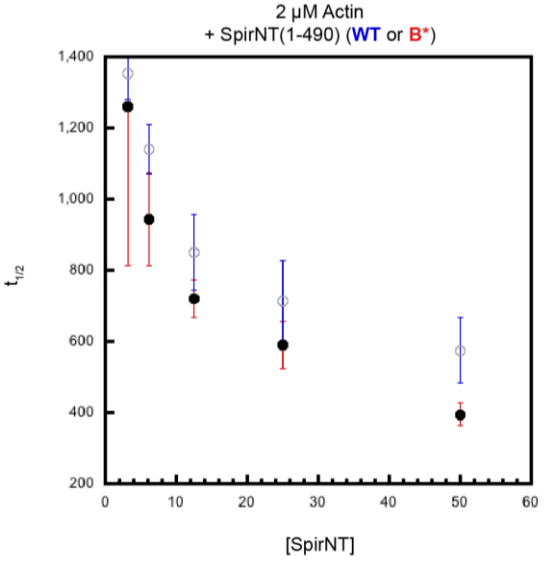

Figure 3-5 – *SpirNT(B*,1-490) is a stronger nucleator than wild type SpirNT(1-490)*

The time to reach the half-maximal polymerization ($t_{1/2}$) of actin by SpirNT(1-490) (*open circles; S.D. shown in blue*) is reduced by mutating WH2-B (*solid circles; S.D. shown in red*)

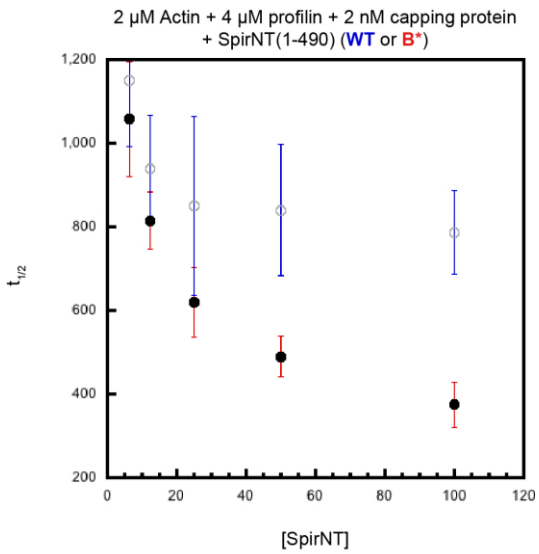

Figure 3-6 – *SpirNT(B*,1-490) has stronger synergy with CapuCT than wild type SpirNT(1-490)*

The time to reach the half-maximal polymerization ($t_{1/2}$) of actin by SpirNT(1-490) (*open circles; S.D. shown in blue*) in the presence of profilin, capping protein, and CapuCT reflects Spir—Capu synergy. The $t_{1/2}$ is reduced (synergy is enhanced) by mutating WH2-B (*solid circles; S.D. shown in red*)

Spir clustering may be important for nucleation, retention, and capture

Having determined that the mutation of WH2-A, -B, or -C consistently enhanced SpirNT(1-490) nucleation and synergy, we wanted to probe the effect of these mutations on two other activities of Spir, revealed in Chapter 2: the retention and capture of actin filaments. To test the hypothesis that clustering Spir enhances these functions, we endeavored to preserve the vesicular-like geometry of Spir on a bead while tuning its density in two different ways: 1) by modifying bead size, or 2) by adjusting Spir's concentration during the bead incubation step. In addition to observing any effect of these changes by TIRF-M, we took a bulk measurement approach and conducted pulldown experiments.

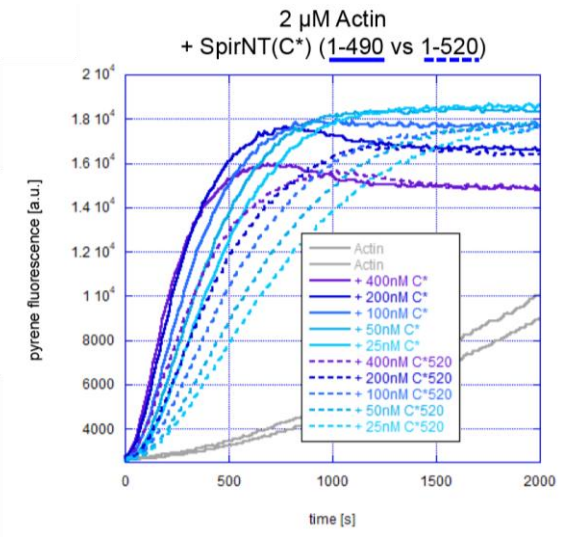

Figure 3-7 – *SpirNT(C*,1-490) is a stronger nucleator than SpirNT(C*,1-520)*

Dose-dependent actin assembly (*shades of blue/ purple*) by SpirNT(C*,1-490) (*solid lines*) is inhibited by the presence of 490-520aa (*dashed lines*). Notably, trace plateaus are affected equivalently, indicating that mutation of WH2-C and the presence/ absence of 490-520aa do not affect sequestration of actin

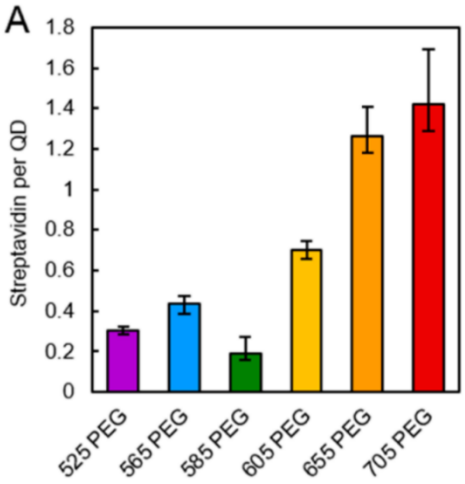

Figure 3-8 – *Qdots average only one or no streptavidins per dot*

From Lippert et al. (2016). Commercially available (Life Technologies), PEG-coated and streptavidin-conjugated Qdots fail to display even one (*525-605 nm light-emitting variants*) or more than one (*655 nm and 705 nm variants; orange and red bars*) streptavidin molecule per dot, on average

Reducing the size of the bead should result in fewer possible points of conjugation to Spir. The experiments we performed with the smallest, commercially available streptavidin-coated microspheres (100 nm average diameter) resulted in the same star-like explosions of actin polymerization we observed with the larger spheres (1 µm average diameter). We identified an even smaller, intrinsically fluorescent vessel to conjugate SpirNT to: the quantum dot (Qdot). We found precedence for such an approach with another tandem WH2 domain nucleator, VopL/F. Burke et al. attached VopL and VopF to Qdots and measured their interaction at both ends of actin filaments (Burke et al. 2017; Vizcarra and Quinlan 2017).

Unfortunately, after conjugating SpirNT to multiple Qdots of various sizes (their size scales with their emitted fluorescence wavelength), we found that effectively no Qdot was capable of polymerizing actin. In fact, too late we discovered a study that showed the reported binding

capacities of these commercial Q-dots to be woefully greater than their actual capacities (**Fig. 3-8**) (Lippert et al. 2016). Despite several adhesion points being advertised for the largest dots, we could not observe any actin assembly when SpirNT was incubated with them, suggesting unsuccessful conjugation. With no early success, we turned to the strategy of dilution.

If clustering enhances Spir nucleation, we expected to observe a non-linear relationship between Spir concentration and actin assembly. As less Spir was introduced to beads, we observed obvious differences in nucleation, with a particularly steep drop-off in activity for the first dilution (**Fig 3-9**). We did not closely quantify these data, as we were interested in interrogating the activities of retention and capture and the experiment and analysis methodology required significant optimization to monitor changes in more than bulk nucleation activity.

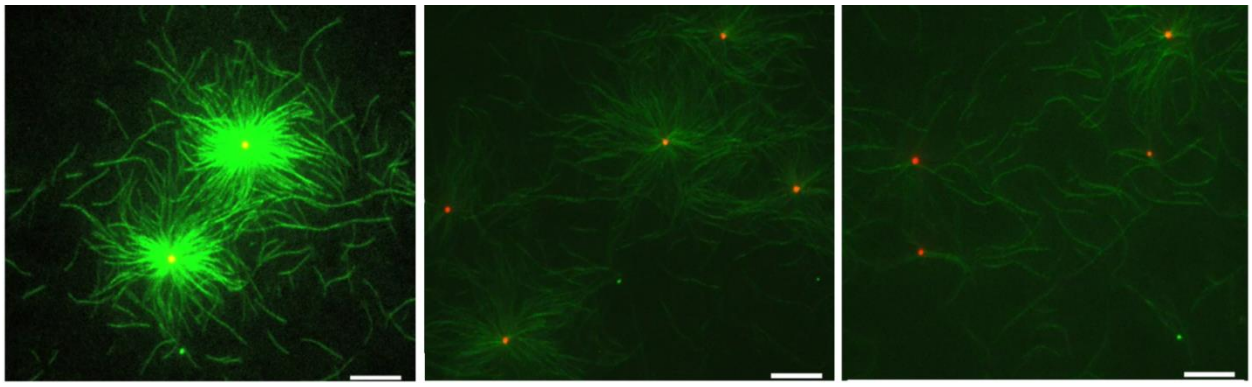

Figure 3-9 – *Dilution of SpirNT on beads significantly alters nucleation*

(*Left*) Beads incubated with 400 nM SpirNT nucleate large stars of actin. (*Middle*) Beads incubated with 200 nM SpirNT and 200 nM KIND demonstrate less nucleation. (*Right*) Beads incubated with 100 nM SpirNT and 300 nM KIND are even less active. Scale bars = 10 μm. All images taken at 3' after the introduction of G-actin.

To address the question of whether clustering also augments Spir's affinity for barbed and/or pointed ends, we supplemented our TIRF experiments with higher throughput measurements. Employing the same titration approach shown in **Fig. 3-9**, we allowed SpirNT-beads to incubate briefly with either F-actin or G-actin in the tube, rather than within a flow cell on the microscope.

We then used centrifugation to pellet and wash the beads before running them on a gel to see how much actin they pulled down.

In the context of G-actin incubation, we anticipated that any pelleted actin should be associated with SpirNT-beads via their nucleation and retention of pointed ends. In the case of F-actin incubation, we expected the enrichment of actin in the pellet to be due to the capture of barbed ends by SpirNT-beads. Unfortunately, several attempts at this experiment failed to produce consistent data. Differences in actin band intensities were subtle in the gels and often significantly different from one iteration to the next. This was likely due primarily to inconsistency in pelleting and the aspiration of supernatants (i.e. the loss of beads). Due to the limitations of this methodology, we obtained narrow dynamic ranges and large variances in the data – two undesirable traits. A more thorough discussion of the problems encountered, and their potential answers, later follows.

Despite the methodological hurdles and noisiness of the data, some interesting results were still extracted. By additionally incubating SpirNT-beads with either GFP-biotin or mCherry-biotin, I was able to account for the loss of beads during pelleting steps to some extent. Using the abundance of GFP or mCherry as a reference for the total beads left in the pellet at the end of the experiment, the data were normalized and non-linear relationships between Spir concentration and actin in the pellet were apparent (**Figs. 3-10** and **3-11**). However, the trends were opposite to our expectations. We observed non-linear increases in the presumed “capture” and “retention” activities of SpirNT as it was diluted on beads.

The transformations of these data were performed simply: the concentration of actin measured from each pellet was multiplied by the dilution factor of SpirNT incubated with the beads. Thus, the relative ratios of actin:GFP plotted in **Figs. 3-10** and **3-11** should be equal for all dilutions if

clustering has no effect on capture or retention. Instead, both the capture and retention of filaments are enhanced as lower concentrations of SpirNT are incubated with beads. It is confounding that this relationship holds true even for the WH2-A and -D mutants. SpirNT(D*)-beads appeared expectedly less potent than SpirNT(WT/A*)-beads in the retention-testing pulldown experiment (which should be dependent on the nucleation of actin) (**Fig. 3-11**). However, SpirNT(A*) beads were not impaired in capture (**Fig. 3-10**), despite the very infrequent observation of this phenomenon at SpirNT(A*)-beads in TIRF-M. Taken together, these data suggest an interesting relationship between clustering and the functions of Spir studied here – nucleation, retention, and capture. Optimization of this methodology offers a possible means of further studying these relationships in medium-throughput.

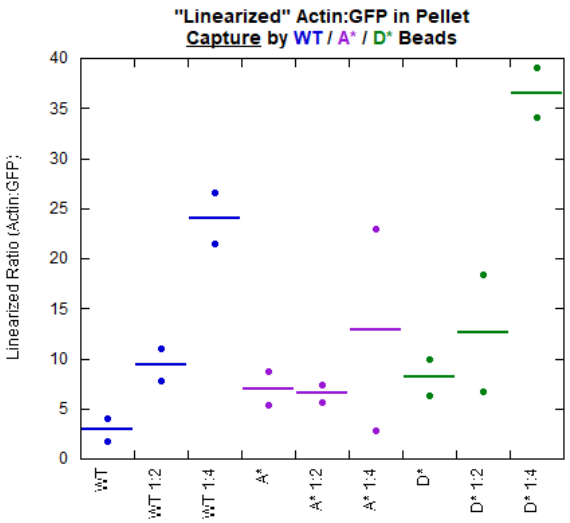

Figure 3-10 – *Spir clustering may affect the capture of actin filaments*

Pulldown of phalloidin-stabilized actin filaments via incubation with beads conjugated to SpirNT(WT) (*blue*), SpirNT(A*) (*purple*), or SpirNT(D*) (*green*). 400 nM SpirNT alone, 200 nM SpirNT and 200 nM KIND, or 100 nM SpirNT and 300 nM KIND (*Left-to-right for each variant*) were conjugated to beads. The data have been transformed so that the average number of filaments per bead (*solid lines*) is altered by dilution only if pelleted actin and SpirNT concentrations do not share a 1:1 relationship

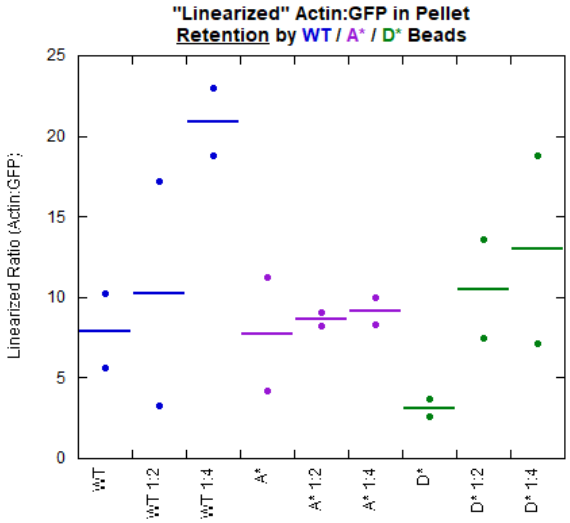

Figure 3-11 – *Spir clustering may affect the retention of actin filaments*

Pulldown of bead-nucleated actin filaments via brief incubation of G-actin with beads conjugated to SpirNT(WT) (*blue*), SpirNT(A*) (*purple*), or SpirNT(D*) (*green*). 400 nM SpirNT alone, 200 nM SpirNT and 200 nM KIND, or 100 nM SpirNT and 300 nM KIND (*Left-to-right for each variant*) were conjugated to beads. The data have been transformed so that the average number of filaments per bead (*solid lines*) is altered by dilution only if pelleted actin and SpirNT concentrations do not share a 1:1 relationship.

CapuCT(I706A) does not nucleate but is still processive

The Spir WH2 domain mutants have enabled us to tease out Spir's unique contributions to synergy. To better understand Capu's contribution to synergy, we turned to the CapuCT(I706A) mutant. CapuCT(I706A) dimerizes but is incapable of actin assembly (Quinlan 2013; Quinlan et al. 2007; Vizcarra et al. 2011), making it an apt tool to isolate and test the role of Spir dimerization by Capu in synergy. In several pilot experiments, we introduced CapuCT(I706A) to SpirNT-beads. Unexpectedly, we observed a synergistic increase in actin assembly (data not shown). If the clustering of Spir on beads mimics its dimerization, these data suggested that CapuCT augments the actin assembly activity of SpirNT-beads through a mechanism other than dimerization and/or that CapuCT(I706A) is capable of polymerizing actin. After confirming that this mutant had no nucleation activity in my hands in the pyrene assay (**Fig. 3-12**), I proceeded to add in the components of the synergy experiment.

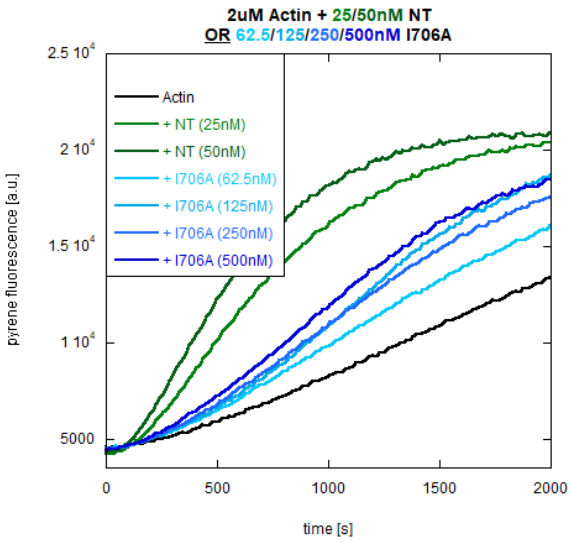

Figure 3-129 – *CapuCT(I706A) does not nucleate actin*

Even at 500 nM (*dark blue line*), CapuCT(I706A) alone does not stimulate actin assembly. A weaker nucleator than wild type CapuCT, SpirNT alone is also shown (*green lines*).

In the presence of profilin, synergy in assembly with SpirNT was evident (**Fig. 3-13**). We also observed that CapuCT(I706A) alone was capable of polymerizing actin in the presence of profilin, albeit with 25-fold weaker activity, based on the concentrations required to obtain specific activity levels (**Fig. 3-14**; compare with **Fig. 3-13**). This result suggested that, although CapuCT(I706A) is essentially incapable of nucleation, it can still enhance the rate of polymerization of spontaneous/existing nuclei. In fact, the lag phase seen in each trace in **Fig. 3-14** is atypical for CapuCT (Bor et al. 2012; Vizcarra et al. 2011) and supports this explanation.

Thus, we hypothesized that the I706A mutation (within the FH2 domain) abolished nucleation but not elongation by CapuCT. To test if CapuCT(I706A) was still capable of processively tracking, elongating, and/or protecting barbed ends, we introduced capping protein to the experiment.

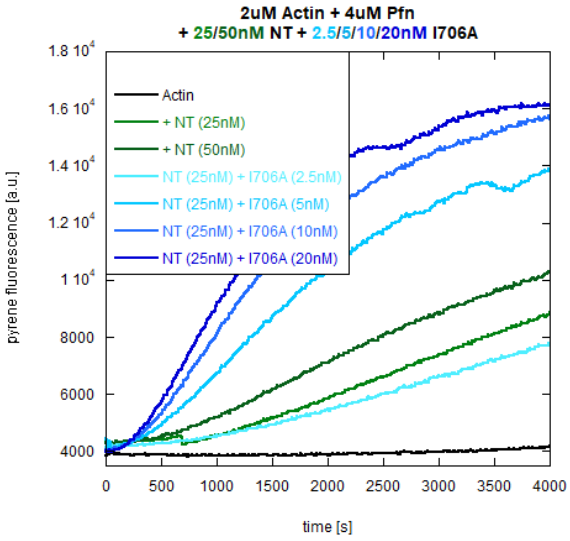

Figure 3-13 – *CapuCT(I706A) synergizes with SpirNT in the presence of profilin*

SpirNT alone is a poor nucleator of actin in the presence of profilin (*green lines*). Actin assembly is increased in a dose-dependent manner by the addition of CapuCT(I706A) (*shades of blue*).

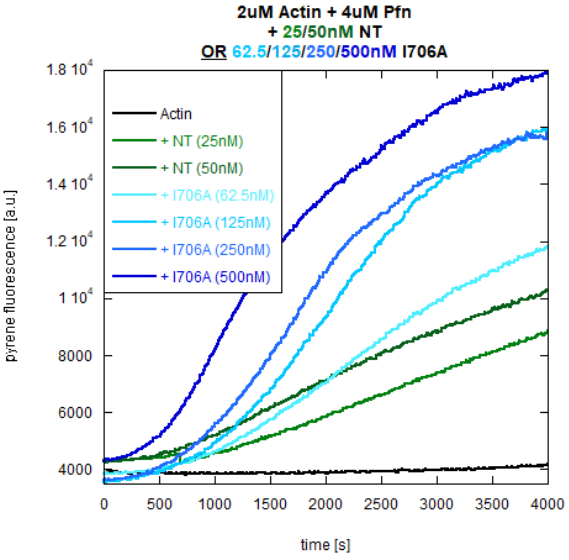

Figure 3-14 – *CapuCT(I706A) weakly assembles actin in the presence of profilin*

At high concentrations (e.g. 500 nM; *dark blue line*), CapuCT(I706A) alone can stimulate actin assembly in the presence of profilin. Notably, and atypical for CapuCT, a lag phase is observed in these conditions, suggesting the impairment, or absence, of nucleation. A poor nucleator in the presence of profilin, SpirNT alone is also shown (*green lines*).

With the same range of CapuCT(I706A) concentrations used when minimal nucleation of PA was observed, a small but obvious change in actin polymerization was apparent in the presence of 2 nM capping protein. Protection of filament capping can be inferred from the steady increase in F-actin signal when 200 nM or greater CapuCT(I706A) was present (**Fig. 3-15**). Strikingly, this effect was still apparent at 25-fold lower concentrations of CapuCT(I706A), and with SpirNT also present (**Fig. 3-16**). Because this effect was weak in both cases, we suspect that CapuCT(I706A) enables, but does not necessarily accelerate, the elongation of filaments in the

presence of profilin and/or capping protein. Furthermore, F-actin plateaus were quickly reached, suggesting that this mutant is easily displaced by capping protein and/or Spir and cannot reciprocally displace either protein to rebind a barbed end. Irreversible displacement by Spir is more likely, given the lack of plateaus observed at the same timescale, but in the absence of Spir (**Fig. 3-15**). However, the concentrations of CapuCT(I706A) used in these two experiments again differ 25-fold. A more careful comparison of this mutant's behavior in each condition is necessary.

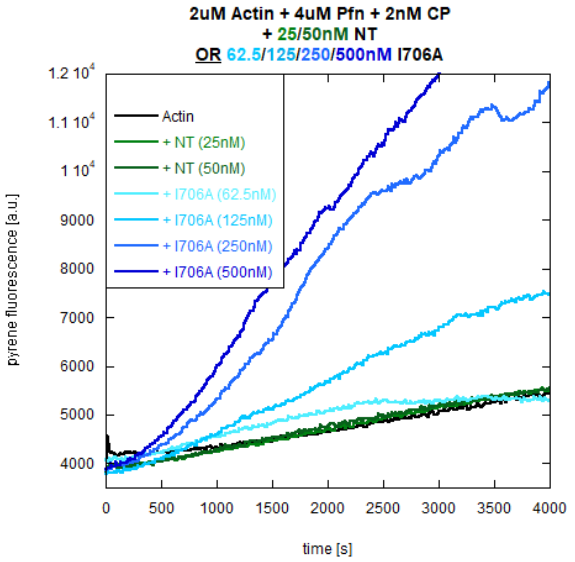

Figure 3-15 – *CapuCT(I706A) weakly assembles actin in the presence of profilin and capping protein*

At high concentrations (e.g. 500 nM; *dark blue line*), CapuCT(I706A) alone can stimulate actin assembly in the presence of profilin and capping protein. Notably, the traces do not plateau, suggesting processive protection and/or elongation of barbed ends by CapuCT. SpirNT alone does not enhance actin assembly in these conditions (*green lines*).

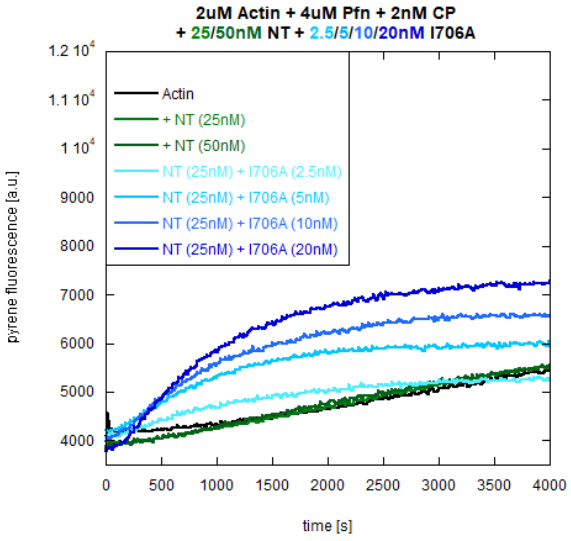

Figure 3-16 – *CapuCT(I706A) synergizes with SpirNT in the presence of profilin and capping protein*

SpirNT alone does not enhance actin assembly in the presence of profilin and capping protein (*green lines*). Actin assembly is increased in a dose-dependent manner by the addition of CapuCT(I706A) (*shades of blue*). Notably, plateaus for each trace are obvious and suggest that CapuCT(I706A) does not efficiently protect barbed ends from capping protein in these conditions.

Further supporting the aforementioned hypotheses; preliminary data from elongation assays by TIRF-M suggested to us that filament growth rates are unaffected by CapuCT(I706A) but that the mutant is likely processive and protects barbed ends from capping protein. There is now

precedent for a formin with native behavior of this sort. Work in the Quinlan lab showed that the Fhod formin antagonizes capping protein and permits, but does not accelerate, the rate of filament elongation in the presence of profilin (Patel et al. 2018). In the presence of profilin and CapuCT(I706A), elongation rates – as measured by bulk, pyrene-actin assembly assays – are unaffected (**Fig. 3-17**). This contrasts with the acceleration of rates seen with wild type CapuCT (**Fig. 3-18**).

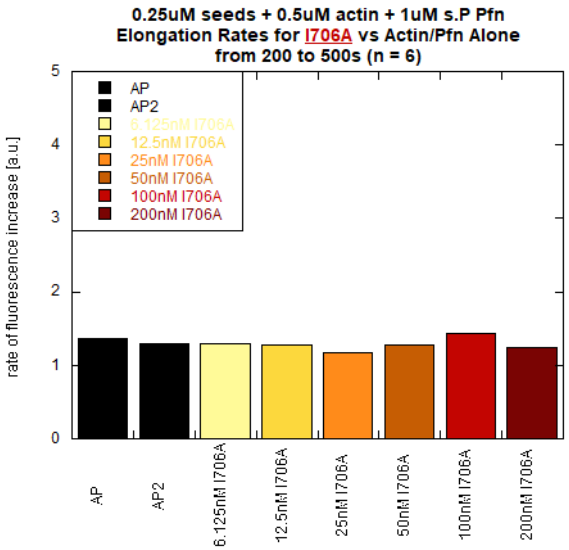

Figure 3-17 – *CapuCT(I706A) does not accelerate filament elongation rates in the presence of profilin*

The rates of increase in F-actin in a pyrene experiment containing seeds, a limiting concentration (500 nM) of G-actin, and profilin reflect the rate of filament elongation. This rate is consistent across experiments without CapuCT (*black bars*) and is unchanged by the presence of even 200 nM CapuCT(I706A) (*rightmost bar; dark red*).

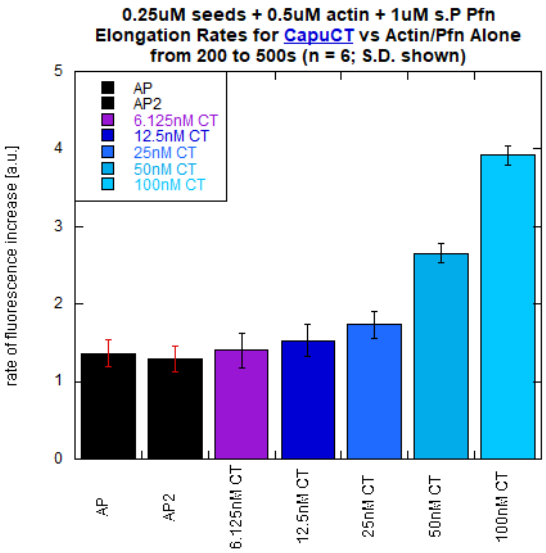

Figure 3-18 – *CapuCT accelerates filament elongation rates in the presence of profilin*

The rates of increase in F-actin in a pyrene experiment containing seeds, a limiting concentration (500 nM) of G-actin, and profilin reflect the rate of filament elongation. This rate is consistent across experiments without CapuCT (*black bars*) and is increased by the addition of CapuCT, in a dose-dependent manner (*purple and blue bars*).

When capping protein was added to these experiments, a saturating concentration of CapuCT(I706A) restored the average rate of growth seen in the absence of capping protein (**Fig. 3-19**) but was incapable of enhancing it, like wild type CapuCT (**Fig. 3-20**). These observations again support the hypothesis that the I706A mutation disrupts nucleation and the

enhancement of elongation by CapuCT, but not its processivity, protection from capping protein, or utilization of PA.

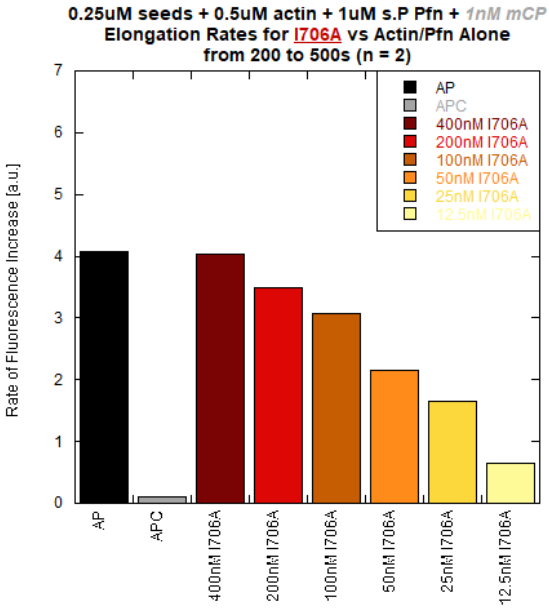

Figure 3-19 – *CapuCT(I706A) rescues filament elongation rates in the presence of profilin and capping protein*

The rates of increase in F-actin in a pyrene experiment containing seeds, a limiting concentration (500 nM) of G-actin, and profilin reflect the rate of filament elongation. In the presence of 1 nM capping protein, effectively no elongation is observed (*gray bar*). The presence of 400 nM CapuCT(I706A) (*dark red bar*) rescues the rate of elongation observed without capping protein (*black bar*), indicating that CapuCT(I706A) can protect barbed ends from capping protein.

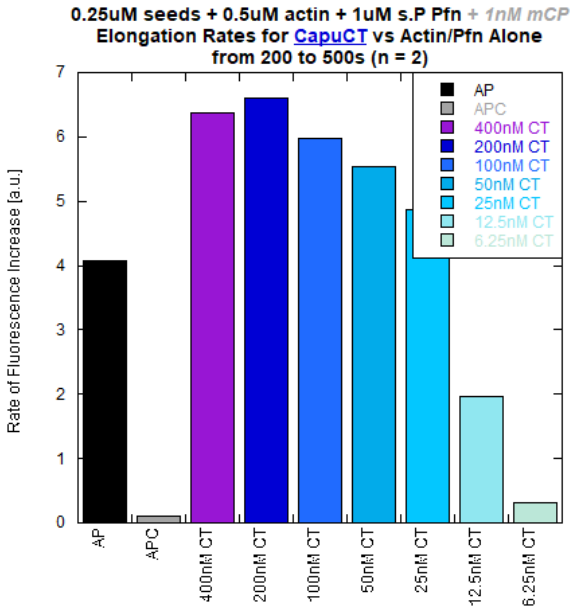

Figure 3-20 – *CapuCT accelerates filament elongation rates in the presence of profilin and capping protein*

The rates of increase in F-actin in a pyrene experiment containing seeds, a limiting concentration (500 nM) of G-actin, and profilin reflect the rate of filament elongation. In the presence of 1 nM capping protein, effectively no elongation is observed (*gray bar*). The addition of CapuCT (*purple and blue bars*) accelerates the rate of elongation above that observed without capping protein present (*black bar*).

Discussion

The role of Spir 490-520aa

In this chapter, we present evidence that the 30 amino acids following 490aa negatively affect nucleation by SpirNT. As previously noted, the same stretch of residues appears to be necessary for MyoV binding. Perhaps the MyoV interaction relieves this additional layer of Spir auto-inhibition in vivo? If this is true, Spir would be activated to nucleate more effectively – possibly, instead of engaging with filament barbed ends – by MyoV proximity. This situation could occur in vivo when MyoV coordinates the movement of one vesicle toward another (**Fig 2-7C'**).

Modulation of Spir nucleation can be simply tested by including MyoV or the 490-520aa peptide in pyrene and bead assays. In the bead experiment, the frequency of capture and retention events can also be measured on SpirNT-beads with and without the 490-520aa domain intact and/or MyoV present. Furthermore, additional, C-terminal residues may alter or intensify any effects observed. The results reported here for SpirNT(1-520), SpirNT(1-490), and their mutants differ strikingly enough to warrant comparison to the slightly longer, known isoform of Spir in flies, containing amino acids 1-586 (isoform "D").

WH2 mutants modulate Spir nucleation

Mutations of WH2 domains A, B, or C variably enhance nucleation by SpirNT, whereas nucleation is abolished when WH2-D or all four WH2 domains are mutated. Notably, the fluorescence plateaus (total F-actin) in pyrene assays begin to drop when concentrations of 200 nM or more SpirNT(B*) (not shown) or SpirNT(C*) (**Fig. 3-7**) are added, consistent with the trend observed for wild type SpirNT. This contrasts with the lack of change in plateau observed in similar assays with high concentrations of SpirNT(A*) (**Fig. 2-8C**), indicating that actin binding by the WH2-A domain is necessary for Spir to sequester actin. Furthermore, changes in plateau

are equivalent for each truncation, suggesting that the 490-520aa domain does not participate in this activity (e.g. **Fig. 3-7**). Perhaps the absence of actin binding by WH2-A discourages formation of the potentially sequestering, so-called SA_4 complex, while WH2-B and -C mutations do not. Further interrogation of these domains is required to test this hypothesis. Structural data (i.e. X-ray crystallographic and/or EM structures) for these mutants, in complex with actin, would offer particularly useful insights into this story.

Because mutating WH2-B, -C, or -D does not impact sequestration and/or capping but mutating WH2-A does, these domains offer a means of tuning Spir nucleation and of switching capping on and off. Various combinations of these mutants, therefore, offer more precise probing of which Spir functions alter synergy with Capu. This approach can be applied to in vitro pyrene and bead assays, as well as in vivo fertility, mesh and streaming experiments. Preliminary data show promise for this approach, as the combination of WH2-A and -C mutations does result in an intermediate nucleator which should also be incapable of capping/sequestering (**Fig. 3-21**).

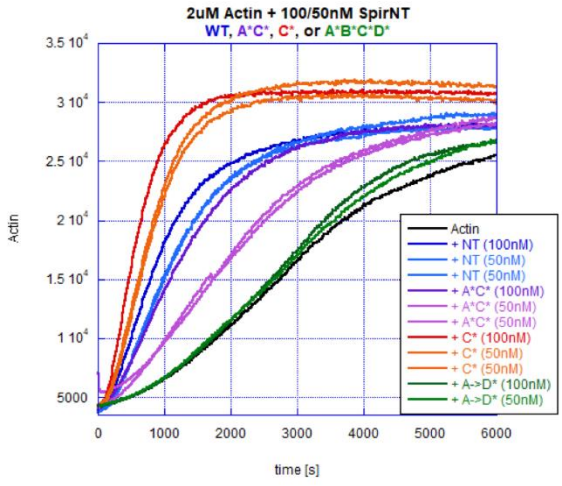

Figure 3-21 – *SpirNT actin assembly can be tuned by multiple WH2 domain mutations*

SpirNT(A*) (*not shown*) and SpirNT(C*) (*orange and red lines*) are stronger nucleators than wild type SpirNT (*blue lines*). While mutation of WH2-D (*not shown*) or all four of Spir's WH2 domains abolishes nucleation (*green lines*), combinations can result in intermediate actin assembly (*e.g. SpirNT(A*C*); purple lines*).

Clustering Spir may tune nucleation, retention, and capture

In conjunction with the development and characterization of various WH2 domain mutant combinations, the bead assay is a powerful method to test capture and retention. However,

measuring these phenomena by TIRF-M is a low-throughput, time-intensive approach. The pulldown experiments introduced in this chapter (**Figs. 3-10** and **3-11**) suffered from numerous limitations but offer an avenue to test retention and capture in higher throughput. This is important, given the number of experimental permutations possible if the aforementioned mutants, truncations, and combinations of each are to be tested. Thus, a discussion of the problems inherent in the pulldown method is warranted. The major sources of error in the capture/retention pulldown experiments, and possible answers to these problems, are detailed below:

1. Inconsistent bead pelleting
    i. Importantly, the pulldown experiments presented in this chapter were performed with smaller, ~100nm diameter beads. These are more challenging to work with than the larger, ~1μm diameter beads, which pellet more quickly/easily.
2. Inconsistent sample loading in gel
    i. This was affected by the inconsistent bead pelleting, but is also a function of protein remaining adhered to beads. The streptavidin-biotin interaction can withstand boiling temperatures. Thus, these gel samples may require additional treatment to better strip the beads of SpirNT and any other conjugated proteins (i.e. GFP/mCherry).
3. Non-specific pulldown of actin catching on beads
    i. When performing 2-color experiments in TIRF (as in Chapter 2), longer actin filaments often became ensnared by beads. Often, the filaments were entangled by clusters of beads. If this occurs in a flow cell, it is likely to occur during centrifugation in a tube, as well. This problem cannot be avoided entirely, but can be mitigated to some extent by brief sonication of beads prior to their introduction to the experiment and by smartly selecting shorter incubation times with actin to preclude the production of very long filaments.
4. “Sticky” GFP/mCherry
    i. Without the presence of some salt and BSA to block them, beads coated in GFP or, to a lesser extent, mCherry were “sticky.” The sides of filaments would often associate with them when visualized by TIRF-M. In fact, control beads (conjugated to only GFP or mCherry) consistently pulled some actin into the pellet in pulldown experiments, which may be due in part to this “stickiness.” Using intrinsically fluorescent beads or alternative fluorophores which demonstrate less of this “sticky” property may address this concern.
5. Imperfect transformation of data
    i. The data for these experiments were simply multiplied by a dilution factor, with the assumption that biotinylated KIND domain would bind beads with kinetics

identical to biotinylated SpirNT. Because the KIND domain is significantly smaller than SpirNT, it is likely that it more quickly accesses and becomes conjugated to beads. Thus, we likely underestimate the density of SpirNT on beads via dilution in this chapter. Notably, this would mean that the trends we observed in **Figs. 3-10** and **3-11** are even farther from our expectation. Perhaps the use of KIND is unnecessary if the concentration of SpirNT on beads can be retroactively well quantified (e.g. by employing a better "bead-stripping" protocol before loading onto a gel). Alternatively, another inert molecule, closer to the size of SpirNT, could be used in place of the KIND domain.

In addition to better refining the dilution and pulldown approaches, testing the role of various mutants and the clustering of Spir on Qdots should not be ruled out. Perhaps obtaining larger Qdots (ideally, better validated and endorsed by other, academic researchers) would similarly make the approach of "smaller beads" a more viable one to test the clustering hypothesis with, while offering a resolution unobtainable by pulldown but required for more detailed measurements (e.g. filament dwell times).

CapuCT(I706A) synergy

We studied CapuCT(I706A) and its effect in the pyrene assay under various conditions because we expected it to demonstrate synergy-promoting activities other than the dimerization of Spir. While we were rewarded with exactly that, we realized that the I706A mutation does not completely abolish CapuCT's actin assembly activities. The data presented here indicate that CapuCT(I706A) is incapable of nucleating actin alone, but that it still synergizes with SpirNT. This mutant was previously reported to synergize with SpirNT. The increase in assembly by SpirNT seen in the presence of CapuCT(I706A) was similar to that of GST-SpirNT (Vizcarra et al. 2011). Thus, the increase in assembly was presumed to be caused by the dimerization of SpirNT, in each case.

However, the observed synergy of CapuCT(I706A) with SpirNT-beads (data not shown) suggests that Capu's contribution to synergy is more complex than the dimerization of Spir. It is

our hypothesis that Spir clustering on membranes/beads effectively dimerizes it, making Spir a better nucleator and increasing its affinity for both pointed and barbed ends. If this is true, dimerization by Capu should have little-to-no effect. Perhaps, instead, Capu enables Spir to utilize PA. Spir's poor nucleation of PA is improved in the pyrene assay, and nucleation of PA by SpirNT-beads in pilot experiments was significantly augmented, in the presence of CapuCT(I706A). In this chapter, we have shown that the FH2 domain mutation, I706A, abolishes CapuCT nucleation and acceleration of elongation. However, the mutant remains processive and protects barbed ends from capping protein. Thus, excluding any effect of dimerization, enhancement of Spir by CapuCT(I706A) is likely mediated by the latter's FH1 domain.

The fruit fly protein, Fhod, antagonizes capping protein and permits, but does not accelerate, the rate of filament elongation in the presence of profilin (Patel et al. 2018). However, this protein still dimerizes and nucleates. Similar to the use of WH2 domain mutations as specific Spir-function-altering modules, Fhod and CapuCT(I706A) offer the potential to tune specific Capu activities and measure their impact on synergy. Strategic hybrids of these proteins (Introducing CapuCT's Spir-binding tail domain to Fhod, or replacing CapuCT's FH2 domain with Fhod's, as examples) offer unique means of both better understanding formin architecture and further interrogating Capu's role in synergy.

Materials and methods

DNA constructs

CapuCT (aa 467-1059) and CapuCT(I706A) constructs were expressed from a modified pET15b vector with an N-terminal hexahistidine tag (Vizcarra et al., 2011). All Spir proteins were expressed from a modified pET20b(+) vector with no affinity tag. A native poly-histidine region within the Spir-KIND domain is sufficient for binding of these constructs to TALON® resin (Clontech). Gibson cloning was employed for the scar-free introduction of Avidity's 45 bp Avitag™ (translated sequence: GLNDIFEAQKIEWHE) to all proteins requiring biotinylation for bead-conjugation. This tag was introduced to the C-terminus of all constructs.

Spir WH2 mutants were either: previously generated, with any "scarring" later removed by Gibson cloning, blunt end ligation, or a similar technique; or generated by the improved "QuikChange" protocol (Liu & Naismith, 2008).

Expression, purification, and biotinylation of proteins

Expression, purification, and biotinylation of proteins were performed as described in Chapter 2.

Pyrene actin assembly assays

Bulk actin assembly assays were carried out as described in Chapter 2.

For the seeded elongation experiments quantified in Figs. 3-17 – 3-20; Actin seeds were prepared by polymerizing 10 µM actin at 25°C for 1 hour in KMEH. The filaments were dispensed in 5 µL aliquots and allowed to re-equilibrate for 1 hour at 25°C. Using a cut pipette tip to prevent shearing, polymerization buffer was added to Mg-actin and then mixed with seeds plus CapuCT. The slope of the pyrene fluorescence trace between 200 and 500 s was considered the elongation rate.

TIRF microscopy assays

Bead assays were performed as described in Chapter 2. For dilution experiments, beads were incubated with the same volume (40 µL) of pre-mixed proteins. Biotin-KIND was used to replace each reduction in biotin-SpirNT (e.g. 2-fold dilution of 400 nM biotin-SpirNT bead incubation = 200 nM biotin-SpirNT + 200 nM biotin-KIND).

Capture and retention bead pulldown assays

For the pulldown experiments quantified in Figs. 3-10 and 3-11, beads were washed, conjugated to SpirNT, and otherwise handled as described in Chapter 2 for the TIRF microscopy assays. Rather than flowing into a chamber to visualize by TIRF, the beads were briefly incubated with actin in a tube as follows:

For capture experiments:

1. Repeat pipette 10 µL of 9.09 µM F-actin (Actin/ME/KMEH) mix into each clear plate well
2. Use a multi-channel pipette to transfer 3.7 µL 9.09 µM actin into each capture tube
3. Wait 10 min
4. Spin for 45 min @ 25,000 G at room temperature
5. Aspirate off and save sups in prepared tubes
6. Wash pellets with 200 µL KMEH(A) if solid enough or spin once more at 100,000 G for 15 min
7. Aspirate off sup and resuspend pellets in 34 µL of 1x KMEH + 1x sample buffer
8. Dispense premixed buffer into each tube, sonicate ~10 s and boil ~5 min
9. Load on a gel or freeze

For retention experiments:

1. Add 20 µL 20 µM actin to 20 µL 2x KMEH
2. Mix a bit and repeat pipette 10 µL 10 µM actin into each clear plate well
3. Add 3.33 µL 10 µM G-actin to each tube; spin 1-2s in microfuge
4. Wait 10 min
5. Spin for 45 min @ 25,000 G at room temperature
6. Aspirate off and save sups in prepared tubes
7. Wash pellets with 200 µL KMEH(A) if solid enough or spin once more at 100,000 G for 15 min
8. Aspirate off sup and resuspend pellets in 33 µL of 1x KMEH + 1x sample buffer
9. Dispense premixed buffer into each tube, sonicate ~10 s and boil ~5 min
10. Load on a gel or freeze

References

Bor, Batbileg, Christina L. Vizcarra, Martin L. Phillips, and Margot E. Quinlan. 2012. "Autoinhibition of the Formin Cappuccino in the Absence of Canonical Autoinhibitory Domains." 23.

Burke, Thomas A., Alyssa J. Harker, Roberto Dominguez, and David R. Kovar. 2017. "The Bacterial Virulence Factors VopL and VopF Nucleate Actin from the Pointed End." *The Journal of Cell Biology* 216(5):1267–76.

Ito, Takuto, Akihiro Narita, Tasuku Hirayama, Masayasu Taki, Shohei Iyoshi, Yukio Yamamoto, Yuichiro Maéda, and Toshiro Oda. 2011. "Human Spire Interacts with the Barbed End of the Actin Filament." *Journal of Molecular Biology* 408:18–25.

Lippert, Lisa G., Jeffrey T. Hallock, Tali Dadosh, Benjamin T. Diroll, Christopher B. Murray, and Yale E. Goldman. 2016. "NeutrAvidin Functionalization of CdSe/CdS Quantum Nanorods and Quantification of Biotin Binding Sites Using Biotin-4-Fluorescein Fluorescence Quenching." *Bioconjugate Chemistry* 27(3):562–68.

Montaville, Pierre, Antoine Jégou, Julien Pernier, Christel Compper, Bérengère Guichard, Binyam Mogessie, Melina Schuh, Guillaume Romet-Lemonne, and Marie-France Carlier. 2014. "Spire and Formin 2 Synergize and Antagonize in Regulating Actin Assembly in Meiosis by a Ping-Pong Mechanism." *PLoS Biology* 12(2):e1001795.

Patel, Aanand A., Zeynep A. Oztug Durer, Aaron P. van Loon, Kathryn V Bremer, and Margot E. Quinlan. 2018. "Drosophila and Human FHOD Family Formin Proteins Nucleate Actin Filaments." *The Journal of Biological Chemistry* 293(2):532–40.

Quinlan, Margot E. 2013. "Direct Interaction between Two Actin Nucleators Is Required in Drosophila Oogenesis." *Development (Cambridge, England)* 140(21):4417–25.

Quinlan, Margot E., John E. Heuser, Eugen Kerkhoff, and R. Dyche Mullins. 2005. "Drosophila Spire Is an Actin Nucleation Factor."

Quinlan, Margot E., Susanne Hilgert, Anaid Bedrossian, R. Dyche Mullins, and Eugen Kerkhoff. 2007. "Regulatory Interactions between Two Actin Nucleators, Spire and Cappuccino." *The Journal of Cell Biology* 179(1):117–28.

Rasson, Amy S., Justin S. Bois, Duy L. Stephen Pham, Haneul Yoo, Margot E. Quinlan, and Correspondence E. to Margot Quinlan. 2015. "Filament Assembly by Spire: Key Residues and Concerted Actin Binding." *Journal of Molecular Biology* 427:824–39.

Vizcarra, Christina L., Barry Kreutz, Avital A. Rodal, Angela V Toms, Jun Lu, Wei Zheng, Margot E. Quinlan, and Michael J. Eck. 2011. "Structure and Function of the Interacting Domains of Spire and Fmn-Family Formins."

Vizcarra, Christina L. and Margot E. Quinlan. 2017. "Actin Filament Assembly by Bacterial Factors VopL/F: Which End Is Up?" *The Journal of Cell Biology* 216(5):1211–13.

Xu, Yingwu, James B. Moseley, Isabelle Sagot, Florence Poy, David Pellman, Bruce L. Goode, and Michael J. Eck. 2004. “Crystal Structures of a Formin Homology-2 Domain Reveal a Tethered Dimer Architecture.” *Cell* 116(5):711–23.

Chapter 4: Development of a Spire-Cappuccino FRET system

Introduction

Spir—Capu binding is transient

In Chapter 2, a bead-based experiment was developed to mimic the geometry seen with Spir localizing to Rab11-positive vesicles in the mouse oocyte (Holubcová, Howard, and Schuh 2013; Kerkhoff et al. 2001). Early localization data in the fly also showed Spir's association with the oocyte cortex and its possible enrichment on vesicles (Quinlan 2013; Quinlan et al. 2007). Forthcoming and higher resolution localization data in the Quinlan lab further support the pattern of vesicle localization. Furthermore, when artificially driven to membranes, Spir's KIND domain was shown to recruit Capu in cultured cells (Quinlan et al. 2007). Genetics experiments indicate that this interaction is required for oogenesis (Quinlan 2013). However, Capu's localization in vivo appears diffuse and distinct from Spir's, suggesting that their interaction is transient. Indeed, we now know that Spir and Capu separate when synergistically assembling actin on beads (**Fig. 2-7B,B'**).

FRET is a sensitive technique

A sensitive method is required to measure when and where necessarily intermittent protein-protein interactions occur. The Förster resonance energy transfer (FRET) phenomenon requires close proximity of fluorescent tags (about 40-50Å) (Akrap, Seidel, and Barisas 2010; Lleres, Swift, and Lamond 2007; Seth et al. 2003). Outside this range, the concomitant reduction and enhancement of donor and acceptor fluorophore emission intensities, respectively, does not occur. Thus, this technique allows for great sensitivity in detecting spatial interactions. With optimized tag placement, only close contacts are observed by FRET. Subtle perturbations in binding efficiency are measurable as a decrease in FRET efficiency.

There are three primary ways of measuring FRET: as a decrease in donor fluorescence, an increase in acceptor fluorescence, or as a decrease in the fluorescence lifetime of the donor. The latter is arguably the most powerful and sensitive approach but requires a unique microscope equipped for fluorescence lifetime imaging microscopy (FLIM). FLIM permits the detection of even very brief binding events. By measuring changes in FRET (by FLIM) in vivo, the points in space and time at which Capu and Spir interact in the oocyte can be sampled. These data would permit us to address the very challenging question of how Spir/Capu localization and interaction change throughout the development of the oocyte.

Visualization of oogenesis stage transitions

FRET is an apt technique to study changes in localization patterns (specifically, points of Spir—Capu interaction) during the various stages of oogenesis. Of particular interest, is the transition of the oocyte from Stage 9 to Stage 10b/11, when mesh disappears and fast streaming begins (Dahlgaard et al. 2007; Quinlan et al. 2007; Theurkauf et al. 1992). The “dumping” of nurse cell contents into the ooplasm closely follows the onset of fast streaming and may further alter Spir/Capu localization/interaction patterns (Bor, Bois, and Quinlan 2015; Dahlgaard et al. 2007; Quinlan 2016). However; historically, visualizing Spir or Capu during these transitions has been impossible. Work is now being done in the Quinlan lab to develop a means of extended, live imaging of the ovary – and potentially individual oocytes – as recently demonstrated with the fruit fly midgut (Martin et al. 2018). A functional FRET system would empower this technique to reveal many unknown facets of Spir—Capu synergy.

Results

Terminal labels fail to FRET

Traditional C/N-terminal labeling of Spir and Capu were predicted to fail based on structural data (Vizcarra et al. 2011), as the termini are farther apart (>10 nm) than the Förster radii of suitable fluorescent protein pairs (Akrap et al. 2010). Our in vitro analyses of these existing fusion proteins confirmed that this was the case: no FRET was observed. Therefore, I developed several new placements of the Spir tag, within predicted loops in the KIND domain (**Fig. 4-1**). These placements were informed by structural data of human Spire1, combined with predictive algorithms which integrated the homologous *Drosophila* Spir sequence, via SWISS-MODEL (Arnold et al. 2006; Biasini et al. 2014; Guex, Peitsch, and Schwede 2009; Kiefer et al. 2009). In this manner, I was able to develop a successful FRET pair, comprised of GFP-tagged Spir and mCherry-tagged Capu (**Fig. 4-2**).

SpirNT-GFP(217-218aa and 275-276aa) demonstrate FRET but also diminished synergy

The homology structure of Spir identified a disordered loop region. Because the modeling software could not ascribe an obvious secondary structure to this region, and because it was near to – but displaced away from – the Fmn-2 binding site, we focused our initial insertions of the GFP tag near this region. At the bottom of the disordered loop, most distal to other secondary structural elements in the Spir homology model, we inserted GFP between Spir residues 275aa and 276aa. When this GFP-SpirNT fusion was added to mCherry-CapuCT, actin polymerization assays unfortunately revealed decreased activity (**Fig. 4-3**). These data suggested that one or both of the fluorescent tag(s) interfered with activity, despite some retention of binding affinity, as evidenced by the FRET signal.

We proceeded to insert GFP into various positions in the SpirNT sequence which were near to its Capu-binding site (**Fig 4-1**; orange tyrosine residue) but not within regions predicted to be

within a secondary structural element. In this way, we identified an insertion point for GFP between SpirNT residues 217-218aa which was also capable of FRET with CapuCT-mCherry. This insertion is just N-terminal to the predicted α-helix which contains the Capu-binding tyrosine residue (Y232). Unfortunately, this insertion also impaired SpirNT's actin assembly with CapuCT in the pyrene assay.

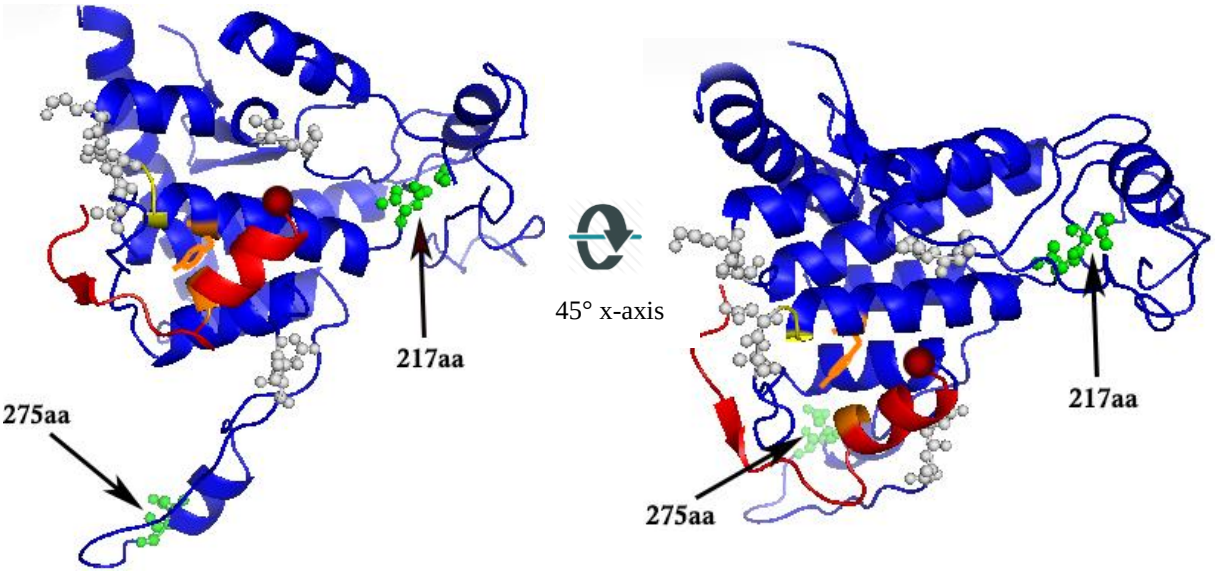

Figure 4-1 – *Successful FRET placements of GFP within Spir*

Homology model of *D.m* Spire (*blue*), based on 3R7G (PDB) co-crystal of Spir1 in complex with Fmn2 (Capu homolog) tail (*red*). Green spheres highlight the residues flanking the two GFP insertion sites that give FRET signals but have attenuated function in pyrene assays. Gray spheres denote the four unsuccessful insertion sites tried. The conserved tyrosine residue, necessary for Spir's ability to bind Capu, is shown in orange, as well as its complementary binding surface on the Fmn2 tail helix. The dark red sphere denotes the C-terminus of Fmn2 tail, where Capu is labeled with mCherry. The two-residue surface highlighted in yellow indicates the C-terminus of the solved Spir1 crystal structure. The residues C-terminal to this yellow patch (including the 275aa site), therefore, fall within extended regions of disorder in the structure, due to uncertainty in modeling.

We suspected that our placement of GFP may have perturbed CapuCT-mCherry binding, or proper folding of the domains in which it was embedded or juxtaposed to. To address these issues, we added apposing linker sequences – as incorporated by Okreglak and Drubin for the ABP, cofilin – on either side of the GFP insertion (Okreglak and Drubin 2007). The addition of a flexible linker should help to displace a fluorophore from the domain it is inserted into and mitigate any interference with proper folding.

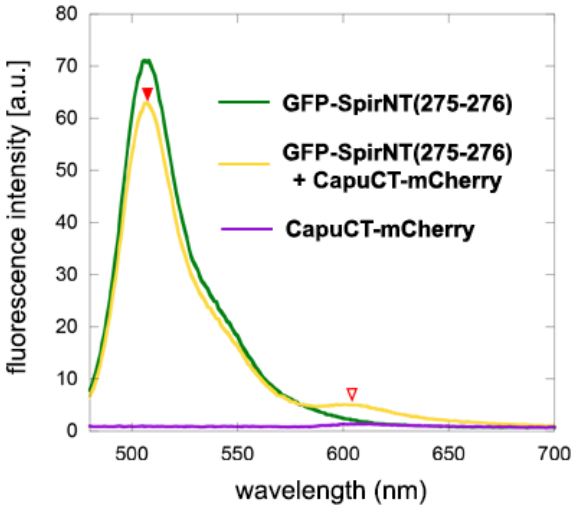

Figure 4-2 – *Emission spectra of GFP-SpirNT(275-276aa) and CapuCT-mCherry*

Emission spectra at excitation, λ = 475nm. In the presence of mCherry (*yellow line*), the fluorescence emission of the GFP tag (*green line*) within Spir's KIND domain is reduced (*solid triangle*), while mCherry's emission (*purple line*) is correspondingly increased (*open triangle*), indicating FRET.

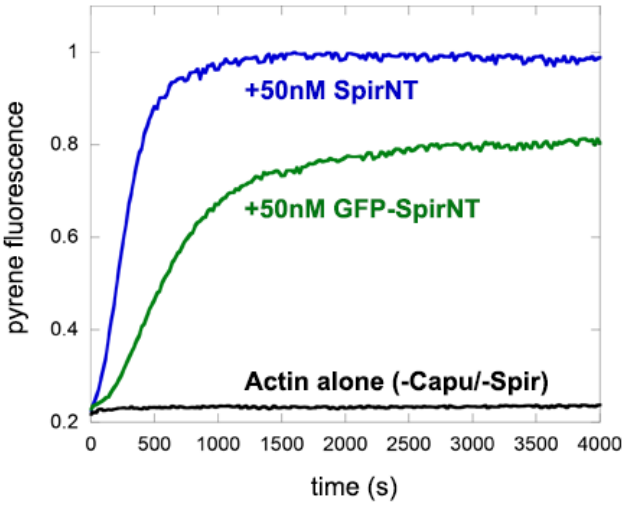

Figure 4-3 – *GFP-SpirNT is impaired in synergistic actin assembly with CapuCT*

In the presence of 4 μM profilin and 2 nM capping protein, spontaneous assembly of 2 μM actin is suppressed (*black line*). Actin assembly by GFP-SpirNT and CapuCT (*green line*) is inhibited relative to wild type SpirNT and CapuCT (*blue line*). Here, GFP-SpirNT(275-276aa) is used but the result is similar for GFP-SpirNT(217-218aa)

Unfortunately, the addition of linkers abolished FRET for both 217-218aa and 275-276aa insertions and failed to improve synergy as measured by pyrene assays. Furthermore, the addition of linkers failed to enable FRET for any of the other GFP insertions they were incorporated for (**Table 4-1**). Despite their reduced activity in biochemical assays, we intended to introduce the constructs with successful FRET to the fly to see if the phenomenon could still be observed in vivo. However, after consultation with multiple fluorescence microscopy experts, it was determined that the degree of FRET observed (**Fig. 4-2**) was insufficient to measure in an in vivo setting. Additionally, I observed that low concentrations of Capu-mCherry could actually increase the light emission of Spir-GFP constructs, while higher concentrations would decrease it. Further confounding, the binding of untagged, control CapuCT to GFP-tagged Spir constructs sometimes altered the fluorescence emission of GFP, precluding meaningful measurements of FRET in vitro.

Table 4-2 – *Locations of GFP insertion within SpirNT*

GFP Placement in SpirNT (aa)	Pyrene Assembly Alone Like WT	Pyrene Synergy with CapuCT Like WT	FRET
100-101	R	ND	No
129-130	Yes	Yes	No
138-139	Yes	Yes	No
138-139+L[a]	ND	ND	No
217-218	Yes	R	Yes[b]
217-218+L[a]	Yes	R	No
238-239	Yes	Yes	No
262-263	R	R	No
262-263+L[a]	R	R	No
275-276	Yes	R	Yes[b]
275-276+L[a]	Yes	R	No

R, reduced. ND, not determined.
[a] L, linker. On both sides of the GFP sequence, the following 12-amino acid linker was added: GHGTGSTGSGSS
[b] As noted in the text, successful FRET pairs still failed to FRET during some experimental repeats and at concentrations that deviated significantly from a 1:2 ratio of GFP-SpirNT:CapuCT-mCherry

Discussion

FRET by Spir and Capu is a high-risk, high-reward opportunity

FRET would be a very valuable tool for probing the Spir—Capu interaction. By measuring changes in FRET (by FLIM) in vivo, the challenging question of how Spir/Capu localization and interaction change throughout the development of the oocyte can be addressed. A FRET pair would also be a very useful tool for screening candidates in vitro for interaction with Spir/Capu.

In addition to their FH1 and FH2 domains, formins typically also bear domains which bind to and inhibit one another. Capu and its homologues do not have canonical, diaphanous inhibitory domains (DID) or diaphanous autoregulatory domains (DAD). However, the presence of Capu's inhibitory and autoregulatory domains (CID and CAD) permit a similar interaction to occur which may prevent nucleation in vivo without activation of some sort (Bor et al. 2012). A direct interaction between Spir and Capu is required for their function,**Error! Bookmark not defined.** and the N-terminal Spir-KIND domain binds the C-terminal Capu-tail with ~100 nM affinity, which should effectively outcompete the tail's interaction with Capu's inhibitory domain (CID) (Bor et al. 2012; Quinlan 2013). However, our understanding of the functional consequences of this interaction remain incomplete.

Additionally, doubly tagging either Spir, Capu, or both, near regions with known or putative autoinhibitory roles (e.g. KIND or 490-520aa, respectively) would allow for the measurement of FRET in regions where they are inactive. Capu is a good candidate for this approach because its autoinhibitory domains are spaced far from one another. A high FRET signal would demarcate where Capu is autoinhibited and a loss of FRET, where Capu is activated. Spir is also a potential candidate for this approach, as it is autoinhibited by the interaction of its termini (Tittel et al. 2015) and we now have evidence of an inhibitory interaction with residues 490-520 (**Chapter 3**).

It's very surprising that the C-terminal, mCherry tag didn't disrupt Capu's activity. It's possible that this placement, and not that of Spir's GFP, is the real problem inhibiting synergy in our in vitro tests of activity, but that the issue only occurs in the presence of Spir and/or GFP. GFP and mCherry can be "sticky" proteins, as I observed when conjugating them to beads. This property could contribute to the undesirable loss of activity seen for several of the **Table 4-1** mutants in pyrene assays. Perhaps alternative fluorophores could be installed in the same positions as for the successful FRET pairs shown in **Table 4-1**, or the insertion of mCherry can be made somewhere else within CapuCT to better preserve folding/function. The development of an extended live-imaging technique in the Quinlan lab would imbue a Spir—Capu FRET pair with significant power/value. Despite the challenges presented here, further investment in developing this FRET system is therefore warranted.

Materials and Methods

DNA constructs

CapuCT-mCherry was expressed from a modified pET15b vector with an N-terminal hexahistidine tag (Vizcarra et al., 2011). All GFP-SpirNT proteins were expressed from a modified pET20b(+) vector with no affinity tag. A native poly-histidine region within the Spir-KIND domain is sufficient for binding of these constructs to TALON® resin (Clontech). Gibson cloning was employed for the scar-free introduction of mEGFP to each of the insertion sites indicated in Table 4-1.

When linkers were added, they were first introduced by Gibson cloning to: 1) Either side of the insertion site within SpirNT, with 10-20 additional bases, each, complementary to the N- and C-terminal mEGFP sequences; or 2) The N- and C-termini of mEGFP, with 10-20 additional bases, each, complementary to either side of the insertion site within SpirNT. The mEGFP – with or without linkers – was amplified by PCR and the SpirNT::pET20b template was linearized from the GFP-insertion site in a separate amplification reaction. The two fragments were then combined by Gibson assembly.

Expression, purification, and biotinylation of proteins

Expression, purification, and biotinylation of proteins were performed as described in Chapter 2.

Pyrene Assays

Pyrene assays were performed as described in Chapter 2 with the conditions indicated in Fig. 4-3.

In vitro FRET tests

Proteins were mixed or not in cold, 1x KMEH. Protein solutions were then added to a cold cuvette, and excited at λ = 475 nm at room temperature using a PTI fluorometer (Photon Technologies International, Lawrenceville, NJ). Emission spectra from λ = 480 nm – 700 nm were obtained and the results of the mixed FRET pair were compared to their individual spectra. In general, 200 nM (final) of each protein was used, whether mixed with its FRET partner or not.

References

Akrap, Nina, Thorsten Seidel, and B. George Barisas. 2010. “Förster Distances for Fluorescence Resonant Energy Transfer between MCherry and Other Visible Fluorescent Proteins.” *Analytical Biochemistry* 402(1):105–6.

Arnold, Konstantin, Lorenza Bordoli, Jürgen Kopp, and Torsten Schwede. 2006. “The SWISS-MODEL Workspace: A Web-Based Environment for Protein Structure Homology Modelling.” *Bioinformatics (Oxford, England)* 22(2):195–201.

Biasini, Marco, Stefan Bienert, Andrew Waterhouse, Konstantin Arnold, Gabriel Studer, Tobias Schmidt, Florian Kiefer, Tiziano Gallo Cassarino, Martino Bertoni, Lorenza Bordoli, and Torsten Schwede. 2014. “SWISS-MODEL: Modelling Protein Tertiary and Quaternary Structure Using Evolutionary Information.” *Nucleic Acids Research* 42(Web Server issue):W252-8.

Bor, Batbileg, Justin S. Bois, and Margot E. Quinlan. 2015. “Regulation of the Formin Cappuccino Is Critical for Polarity of Drosophila Oocytes.” *Cytoskeleton (Hoboken, N.J.)* 72(1):1–15.

Bor, Batbileg, Christina L. Vizcarra, Martin L. Phillips, and Margot E. Quinlan. 2012. “Autoinhibition of the Formin Cappuccino in the Absence of Canonical Autoinhibitory Domains.” 23.

Dahlgaard, Katja, Alexandre A. S. F. Raposo, Teresa Niccoli, and Daniel St Johnston. 2007. “Capu and Spire Assemble a Cytoplasmic Actin Mesh That Maintains Microtubule Organization in the Drosophila Oocyte.” *Developmental Cell* 13(4):539–53.

Guex, Nicolas, Manuel C. Peitsch, and Torsten Schwede. 2009. “Automated Comparative Protein Structure Modeling with SWISS-MODEL and Swiss-PdbViewer: A Historical Perspective.” *Electrophoresis* 30 Suppl 1:S162-73.

Holubcová, Zuzana, Gillian Howard, and Melina Schuh. 2013. “Vesicles Modulate an Actin Network for Asymmetric Spindle Positioning.” *Nature Cell Biology* 15(8):937–47.

Kerkhoff, Eugen, Jeremy C. Simpson, Cornelia B. Leberfinger, Ines M. Otto, Tobias Doerks, Peer Bork, Ulf R. Rapp, Thomas Raabe, and Rainer Pepperkok. 2001. *The Spir Actin Organizers Are Involved in Vesicle Transport Processes*. Vol. 11.

Kiefer, Florian, Konstantin Arnold, Michael Künzli, Lorenza Bordoli, and Torsten Schwede. 2009. “The SWISS-MODEL Repository and Associated Resources.” *Nucleic Acids Research* 37(Database issue):D387-92.

Lleres, David, Samuel Swift, and Angus I. Lamond. 2007. “Detecting Protein-Protein Interactions In Vivo with FRET Using Multiphoton Fluorescence Lifetime Imaging Microscopy (FLIM).” *Current Protocols in Cytometry* (October):1–19.

Martin, Judy Lisette, Erin Nicole Sanders, Paola Moreno-Roman, Leslie Ann Jaramillo Koyama,

Shruthi Balachandra, XinXin Du, and Lucy Erin O'Brien. 2018. “Long-Term Live Imaging of the Drosophila Adult Midgut Reveals Real-Time Dynamics of Division, Differentiation and Loss.” *ELife* 7.

Okreglak, Voytek and David G. Drubin. 2007. “Cofilin Recruitment and Function during Actin-Mediated Endocytosis Dictated by Actin Nucleotide State.” *The Journal of Cell Biology* 178(7):1251–64.

Quinlan, Margot E. 2013. “Direct Interaction between Two Actin Nucleators Is Required in Drosophila Oogenesis.” *Development (Cambridge, England)* 140(21):4417–25.

Quinlan, Margot E. 2016. “Cytoplasmic Streaming in the Drosophila Oocyte.” *Annu. Rev. Cell Dev. Biol* 32:173–95.

Quinlan, Margot E., Susanne Hilgert, Anaid Bedrossian, R. Dyche Mullins, and Eugen Kerkhoff. 2007. “Regulatory Interactions between Two Actin Nucleators, Spire and Cappuccino.” *The Journal of Cell Biology* 179(1):117–28.

Seth, Abhinav, Takanori Otomo, Helen L. Yin, and Michael K. Rosen. 2003. “Rational Design of Genetically Encoded Fluorescence Resonance Energy Transfer-Based Sensors of Cellular Cdc42 Signaling.” *Biochemistry* 42(14):3997–4008.

Theurkauf, W. E., S. Smiley, M. L. Wong, B. M. Alberts, Z. Bryant, H. Ruohola-Baker, and L. Manseau. 1992. “Reorganization of the Cytoskeleton during Drosophila Oogenesis: Implications for Axis Specification and Intercellular Transport.” *Development (Cambridge, England)* 115(4):923–36.

Tittel, Janine, Tobias Welz, Aleksander Czogalla, Susanne Dietrich, Annette Samol-Wolf, Markos Schulte, Petra Schwille, Thomas Weidemann, and Eugen Kerkhoff. 2015. “Membrane Targeting of the Spir·formin Actin Nucleator Complex Requires a Sequential Handshake of Polar Interactions.” *The Journal of Biological Chemistry* 290(10):6428–44.

Vizcarra, Christina L., Barry Kreutz, Avital A. Rodal, Angela V Toms, Jun Lu, Wei Zheng, Margot E. Quinlan, and Michael J. Eck. 2011. “Structure and Function of the Interacting Domains of Spire and Fmn-Family Formins.”

Chapter 5: A biomimetic mesh

Discussion

The bead methodology employed in Chapter 2 has the potential to be developed into a more robust mesh assembly system. Already, our minimal system has shown that Spir binds the barbed ends of existing filaments and the pointed ends of nucleated filaments to create filament—vesicle bridges. Further, this system showed that CapuCT enables the construction of these bridges in the presence of ubiquitous ABPs like profilin and capping protein by processively protecting and accelerating the elongation of barbed ends of Spir-nucleated filaments. Spir mutants which enhanced the nucleation of Spir in pyrene assays – both alone and in synergy conditions with Capu – also demonstrated enhanced nucleation and synergy with Capu on beads. Thus, we clearly discriminated the strengths and weaknesses of the existing models describing Spir—Capu synergy.

The addition of other interactors to this system offers more complex aspects of mesh regulation to be visualized in vitro. Candidates for introduction to this method are numerous. Proteins like Rab11 and MyoV can be directly conjugated to beads and/or complexed with SpirNT on beads, while smaller molecules like depolymerization agents or the Spir(490-520) peptide can be introduced by flow. In the former case, MyoV could be tested for interactions with SpirNT and regulation of SpirNT-bead activity and/or mesh contraction observed, through MyoV's motor activity (i.e. **Fig. 2-7C'**). In the latter case, Spir's ability to nucleate, synergize with CapuCT, or interact with other proteins may be modified in unique ways by the presence of a small molecule inhibitor, peptide, or even microtubules and crosslinkers.

In addition to introducing new components, more precise interrogations of mesh assembly and structure are afforded by the wealth of existing Spir and Capu mutants in the Quinlan lab. In Chapter 3, we show that various Spir functions – including nucleation, sequestration, filament capture, and filament retention – can be targeted and tuned through point mutations within

Spir's four WH2 domains. Furthermore, we show that Spir's amino acids 490-520 offer an additional layer of regulation and predict that MyoV can serve as an activator of SpirNT when these residues are present. Finally, we demonstrated that the CapuCT(I706A) mutant is an excellent tool to further study the role(s) Capu plays in synergy. With both abolished nucleation and acceleration of elongation, while remaining dimeric and processive, this mutant provides potential insights into formin behavior writ large. Modular combinations of Spir WH2 mutants, in conjunction with CapuCT(I706A), offer a long list of permutations and potential for deeper, mechanistic insights into Spir—Capu synergy.

As the bead methodology is further refined to produce a mesh more faithful to the in vivo structure, superior Spir/Capu localization data and structural studies of the mesh will be critical. We note the potential for a functional Spir—Capu FRET system in Chapter 3. A better understanding of when/where Spir and Capu interact in vivo (particularly, in relation to mesh and vesicles) would permit us to further optimize the in vitro mesh assembly system and visualize the more complex aspects of its behavior than could be done in vivo – i.e. single-filament dynamics. Recent advances in super-resolution microscopy and better actin-labeling probes now permit the finer details and nuance of mesh to be visualized. Pairing these technologies with a working FRET system and a more sophisticated bead methodology would leave out of reach very few of the major questions remaining for Spir—Capu synergy.

Several systems have been noted to contain meshes of actin which serve various, essential roles in cell polarity. In the fly and the mouse, direct interactions between Spir and Capu and their homologues crucially regulate mesh, and conserved binding residues indicate that such interactions are important for their roles in other species. A continued interrogation of Spir—Capu synergy offers valuable insights into the curious complexity of actin nucleators across biology.